

Faculty of Biosciences, Fisheries and Economics
Department of Arctic and Marine Biology

Seasonality in mercury bioaccumulation in particulate organic matter and zooplankton in a river-influenced Arctic fjord (Adventfjord, Svalbard).

Nathalie CARRASCO

BIO-3950 Master's thesis in Biology – May 2019



©TopoSvalbard

Supervisors:
Amanda Poste (NIVA)
Anita Evenset (Akvaplan-Niva ; UIT)
Janne E. Søreide (UNIS)
Maeve McGovern (NIVA)



ACKNOWLEDGEMENTS

This project could not have been conducted without the financial support from the Norwegian Research Council (TerrACE 2017-2021: PI Amanda Poste).

I want to thank all my supervisors, Amanda Poste, Anita Evenset and Janne E. Søreide, for their excellent guidance and dedication through the master thesis and for including me in this project. Especially many thanks to Amanda for her availability and her precious advices and comments. Also, special thanks to Maeve McGovern for her patience and help in the field and in the lab, and for teaching me sampling and lab methods. I would also like to thank Bodil Bluhm for her help and her support at several steps of my Master project.

Many thanks to Amalia Keck and Helena Kling Michelsen for their availability and help during my labwork. I would also like to thank the kind personnel at the lab at Akvaplan-niva for showing me how to use equipment.

Many thanks to Miriam Marquardt for running Chlorophyll a analysis at UNIS, Anne Luise Ribeiro, Tina Brytensen, Hans Fredrik Veiteberg Braaten from NIVA lab for running TotHg analysis, Sofi Jonsson from Stockholm University for running MeHg analysis, Michael Arts from Ryerson University in Canada for running fatty acid analysis and the UC Davis Stable Isotope Facility, Davis, in California (USA) for running the stable isotope analysis.

Additionally, I would like to thank UNIS logistics for making fieldwork possible and for all the long days in field. Thanks also to the crew of the Helmer Hanssen and to Jørgen Berge who allowed us to do some sampling during the “AB- 320 Arctic Marine Zooplankton” course at UNIS.

I would also like to thank the whole TerrACE team for help during field and support during this master thesis.

Last, I would like to thank all my friends in France, especially Christian Dudek and Sebastien Astegiano for supporting me in my decisions, and my mother for her cheers during these last two years.

May 2019

ABSTRACT

Methylmercury (MeHg) is of concern because it has the capacity to readily bioaccumulate and biomagnify along trophic levels until humans, exhibiting toxic effects such as neurotoxicity. Increased permafrost melt (that stores large amounts of carbon and mercury (Hg)) and river inputs, are expected to increase the exposure to Hg through uptake and transfer of contaminants through the food web.

The main aim of this study was to determine the impacts of seasonal river inputs on the Hg accumulation in Arctic coastal Particulate Organic Matter (POM) and zooplankton. The study area was Adventfjord located at 78° North by the largest settlement in Svalbard, Longyearbyen. Analysis were carried out for water and zooplankton samples monthly collected in Adventfjord and its main rivers ; Longyearelva, Adventelva and tributaries from April to August 2018. Physicochemical parameters and Hg were paired with the analysis of zooplankton diet and trophic interactions, based on stable isotope and fatty acid analysis in order to describe Hg trophodynamics.

I found that rivers were mainly fed by melt water, and that rainfall were not so important. Seasonal river discharge mainly occurred in June and July and rivers contained 2 fold-higher SPM, 10 fold-higher Hg, and had a 4 fold-higher C :N ratio than Adventfjord waters. However, strong tidal currents and a lack of sill in Adventfjord allowed for a rapid mixing of river inputs throughout the fjord. Although phytoplankton was the most important food source for zooplankton for nearly all sites and study dates, there was some evidence of dietary reliance on allochthonous energy sources during the main river discharge period. Hg- and MeHg-concentrations in zooplankton increased over summer and could be influenced by river inputs, although other processes could also be involved. In contrast to what was expected for a bioaccumulating contaminant, there was no relationship between $\delta^{15}\text{N}$ values in zooplankton and Hg- and MeHg- concentrations. However, « Predators » had the highest concentration in TotHg and MeHg. This study highlights that Adventfjord is a very dynamic system with complex water chemistry and trophic interactions affecting Hg trophodynamics.

Keywords: Zooplankton diet, river inputs, Arctic coastal environment, mercury, terrestrial energy source

TABLE OF CONTENTS

Aknowledgements	ii
Abstract.....	iii
1-INTRODUCTION.....	1
1.1 Arctic coastal ecosystems and climate change	1
1.2 Mercury in the Arctic.....	3
1.3 Arctic pelagig foodweb and diet markers	4
1.4 Study aims	6
2-MATERIALS & METHODS.....	7
2.1 The study area	7
2.2 Sample collection	8
2.3 Sample processing and analysis	10
2.4 Calculations and Statistical analysis	17
3-RESULTS	21
3.1 Physicochemical characterization of river discharge	21
3.2 Physicochemical characterization of Adventfjord.....	24
3.3 Zooplankton data analysis	28
4-DISCUSSION	37
4.1 Seasonal river inputs in Adventfjord	37
4.2 Influence of river inputs on zooplankton diet	40
4.3 Influence of river inputs on Hg concentration in zooplankton	42
5-CONCLUSION	47
6-SUGGESTIONS FOR FURTHER ANALYSIS.....	48
7-REFERENCES.....	49
8-APPENDICES	60

ABBREVIATIONS

AMDEs	Atmospheric Mercury Depletion Events
ALA	Alpha-Linolenic acid
ANOVA	Analysis of variance
[Carbon]	Carbon concentration
CA	Correspondance Analysis
Chl a	Chlorophyll a
DHA	Docosahexaenoic acid
DOC	Dissolved Organic Carbon
DOM	Dissolved Organic Matter
EFAAs	Essential Fatty Acid
EPA	Eicosapentaenoic Acid
FAA	Fatty Acid Analysis
Hg	Mercury
Hg ⁰	Elemental mercury
Hg(II)	Divalent inorganic mercury
Hg ²⁺	Ionic mercury
LIN	Linoleic acid
lm	linear model
MeHg	Methylmercury
MUFA	Monounsaturated Fatty Acid
[Nitrogen]	Nitrogen concentration
Part C	Particulate carbon
Part TotHg	Particulate TotHg
PCA	Principal component analysis
POC	Particulate Organic Carbon
POM	Particulate Organic Matter
PUFA	Polyunsaturated Fatty Acid
RDA	Redundancy Analysis
SFA	Staturated Fatty Acid
SIA	Stable Isotope Analysis
SPM	Suspended Particulate Matter
SPM TotHg	TotHg concentration in SPM
SPM Carbon	Carbon concentration in SPM
TotHg	Total mercury

LIST OF TABLES

Table 1 : Stations coordinates, depth and sampling dates in Adventfjord from April to August 2018

Table 2 : Feeding strategy of taxa/species in size-fractioned samples dominating the biomass. (Jelly plankton included Ctenophore, *B. cucumis* and *M. ovum*). (« Herbivores » : n = 19 ; « Omnivores » : n = 13 ; « Predators » = n = 15)

Table 3 : Fatty acid markers (n=42) analyzed in zooplankton samples (n=24) and included in summary metrics for further statistical analysis.

Table 4 : Physical parameters for surface water in Adventelva and tributary rivers from May to August 2018.

Table 5 : Stable isotopes $\delta^{13}\text{C}$ and $\delta^{15}\text{N}$ (‰), and C :N ratio in surface waters in Adventelva, Longyearlva and tributaries rivers from May to August 2018

Table 6 : Total Hg concentration in water (AqueousTotHg), Particulate Hg concentration (PartTotHg) and Total Hg concentration in SPM (SPMTotHg) in surface waters in Adventelva, Longyearlva and tributaries rivers from May to August 2018

Table 7 : TotHg, MeHg concentrations and MeHg :TotHg ratio (%) in zooplankton samples (mean \pm sd ; ng/g dry weight). Comparison between this study and Ruus et al. 2015 data with samples including copepods *Calanus hyperboreus*, *Calanus glacialis*, *Calanus finmarchicus*; krill/euphausiids; amphipods.

LIST OF FIGURES

Figure 1 : Map of Svalbard. Isfjorden indicated in the red circle and Adventfjord indicated with red point.

Figure 2 : Adventfjord and Adventelva catchment with sampling locations indicated.

Figure 3 : Mean daily water level, air temperature ($^{\circ}\text{C}$), and total daily precipitation (mm) data from 15/06/2018 to 15/09/2018. (Blue box = sampling dates ; Arrows and dashed blue lines = peaks of precipitation.)

Figure 4: Boxplots of (A) Chl a concentration ($\mu\text{g/L}$), (B) C :N ratio, (C) $\delta^{13}\text{C}$ acidified (‰) and $\delta^{15}\text{N}$ (‰) in POM sampled at the 3 stations in Adventfjord (AF1, AF2 and ISA), at 2 depth (surface and 15m) from April to August 2018. The horizontal band inside the boxes marks the median, the lower and upper lines of the boxes represent the first and the third quartiles, respectively. The extended whiskers are the most extreme data points (while the individual points represent outliers).

Figure 5 : Boxplots of (A) SPM concentration, (B) TotHg concentration in SPM, (C) Particulate TotHg concentration, (D) Aqueous TotHg concentration in POM from water samples (fjord : $n=28$; river : $n=8$) taken at the surface and 15m deep in the 3 stations (AF1, AF2, ISA) from April to August 2018 ; and in water samples from Adventelva and Longyearlva (« River ») from May to August 2018. Data presented on a log10 scale. The horizontal band inside the boxes marks the median, the lower and upper lines of the boxes represent the first and the third quartiles, respectively. The extended whiskers are the most extreme data points (while the individual points represent outliers).

Figure 6 : Principal Component Analysis (PCA) of physicochemical parameters (response variables shown as black vectors) measured in water samples (surface and 15m) (shown as points ; $n=28$) taken at the 3 stations (AF1, AF2, ISA) from April to August 2018. The two first components explained 80% of the total variance. CNratio : C :N ratio as a molar ratio ; PartTotHg : Particulate TotHg concentration (ng/L) ; SPM : SPM concentration (mg/L) ; AqueousTotHg : aqueous TotHg (ng/L) ; Month of sampling are indicated by colors; Stations and sampling depth are indicated by shapes.

Figure 7: (A & B) Salinity (psu) and (C & D) Temperature ($^{\circ}\text{C}$) data from CTD data in inner fjord (AF1) and outerfjord (ISA) in April and July 2018.

Figure 8: Biplot for $\delta^{13}\text{C}$ and $\delta^{15}\text{N}$ (mean and sd) in POM and zooplankton samples (« Herbivores », « Omnivores », and « Predators ») collected at the 3 stations in Adventfjord from April to August 2018.

Figure 9 : Boxplots of $\delta^{13}\text{C}$ and $\delta^{15}\text{N}$ (‰) in zooplankton samples collected at the 3 stations in Adventfjord (AF1, AF2 and ISA) from April to August 2018. The horizontal band inside the boxes marks the median, the lower and upper lines of the boxes represent the first and the third quartiles, respectively. The extended whiskers are the most extreme data points (while the individual points represent outliers).

Figure 10: Biplots of (A) $\delta^{13}\text{C}_{\text{Zooplankton}} - \delta^{13}\text{C}_{\text{POM}}$ and (B) $\delta^{15}\text{N}_{\text{Zooplankton}} - \delta^{15}\text{N}_{\text{POM}}$ (mean ; sd) in zooplankton samples with « Dominant species », sampled in the 3 stations from April to August 2018 (Fish larvae, n=2 ; Chaetognatha, n=2 ; Ephausiacea, n=3 ; *O. similis*, n=3 ; *C. limacina*, n=5 ; Jelly plankton, n=10 ; *L. helicina*, n=2 ; *Calanus* spp., n=13 ; Amphipod, n=1 ; Decapod zoea, n=1 ; Cirripedia nauplii, n=3).

Figure 11 : CA biplot of data based on all 42 fatty acid analyzed in zooplankton samples taken at the 3 stations (AF1, AF2, ISA) from April to August 2018. The analyzed samples were dominated by Cirripedia nauplii in May and *Calanus* spp. in the other samples (n=15). The two axis explained 75% of the total variance. Only the summary metrics which were passively added to the CA are shown (ΣSFA ; ΣMUFA ; ΣPUFA ; $\Sigma\text{MUFA}\geq 18$; $\Sigma\text{MUFA}>18$; $\Sigma\text{C18 PUFA}$; $\Sigma\text{C20 PUFA}$; $\Sigma\text{C22 PUFA}$; $\Sigma\text{EPA \& DHA}$; $\Sigma\text{n-6}$; $\Sigma\text{n-3}$; $\Sigma\text{Odd chain}$; n-3/n-6).

Figure 12: CA biplot of data based on all 42 fatty acid analyzed in zooplankton samples taken at the 3 stations (AF1, AF2, ISA) from April to August 2018. The samples were dominated by *Calanus* spp (n=12). The two axis explained 79% of the total variance. Only the summary metrics which were passively added to the CA are shown : sums and ratio (ΣSFA ; ΣMUFA ; ΣPUFA ; $\Sigma\text{MUFA}\geq 18$; $\Sigma\text{MUFA}>18$; $\Sigma\text{C18 PUFA}$; $\Sigma\text{C20 PUFA}$; $\Sigma\text{C22 PUFA}$; $\Sigma\text{EPA \& DHA}$; $\Sigma\text{n-6}$; $\Sigma\text{n-3}$; $\Sigma\text{Odd chain}$; n-3/n-6).

Figure 13: Boxplots of (A) TotHg, (B) MeHg concentrations and (C) MeHg :TotHg ratio in zooplankton from samples collected at the 3 stations from April to August 2018. (TotHg : n= 28 ; MeHg : n = 45 ; MeHg :TotHg: n=28). The horizontal band inside the boxes marks the median, the lower and upper lines of the boxes represent the first and the third quartiles, respectively. The extended whiskers are the most extreme data points (while the individual points represent outliers).

Figure 14: Principal Component Analysis (PCA) of Aqueous TotHg concentration in the fjord water, Stable isotopes $\delta^{13}\text{C}$ and $\delta^{15}\text{N}$, Fatty Acid diet markers, Carbon and Nitrogen concentration and TotHg and MeHg concentrations (response variables shown as black vectors) measured in « Herbivores » (n=15; shown as points) taken in the 3 stations (AF1, AF2, ISA) from April to August 2018. The two first components explained 71% of the total variance. AqueousTotHg : aqueous TotHg (ng/l) ; $d^{13}\text{C}_{\text{corr}}$: $\delta^{13}\text{C}_{\text{Zooplankton}} - \delta^{13}\text{C}_{\text{POM}}$ (‰) ; $d^{15}\text{N}_{\text{corr}}$: $\delta^{15}\text{N}_{\text{Zooplankton}} - \delta^{15}\text{N}_{\text{POM}}$ (‰) ; Carbon and Nitrogen concentration (ug/mg). Month of sampling are indicated by colors; Stations are indicated by shapes.

Figure 15: Principal Component Analysis (PCA) of Aqueous TotHg concentration in the fjord water, Stable isotopes $\delta^{13}\text{C}$ and $\delta^{15}\text{N}$, Carbon and Nitrogen concentration and TotHg and MeHg concentration (response variables shown as black vectors) measured in zooplankton samples (n= 30 ; shown as points) taken in the 3 stations from April to August 2018. The two first components explained 85% of the total variance. AqueousTotHg : aqueous TotHg (ng/L) ; $d^{13}\text{C}_{\text{corr}}$: $\delta^{13}\text{C}_{\text{Zooplankton}} - \delta^{13}\text{C}_{\text{POM}}$ (‰) ; $d^{15}\text{N}_{\text{corr}}$: $\delta^{15}\text{N}_{\text{Zooplankton}} - \delta^{15}\text{N}_{\text{POM}}$ (‰) ; Carbon and Nitrogen concentration (ug/mg). Month of sampling are indicated by colors; Stations are indicated by shapes.

1-INTRODUCTION

Multiple stressors such as climate change and land-use changes related to increasing human activity in northern regions are expected to alter water, nutrients and contaminants fluxes in land-ocean interactions. This thesis focuses on seasonal river inputs to Adventfjord in Svalbard, and their effects on mercury (Hg) contamination of coastal ecosystems.

1.1 ARCTIC COASTAL ECOSYSTEMS AND CLIMATE CHANGE

Arctic coastal biogeochemistry is impacted by river inputs and estuarine gradients are associated with river plumes (Holmes et al. 2012; McClelland et al 2012). The Arctic ocean, in terms of volume, receives the highest input of freshwater and organic matter worldwide (Lobbes et al. 2000; Opsahl et al. 1999). Although it only represents ~1% of global ocean volume, the Arctic Ocean receives more than 10% of global river discharge (Gordeev et al. 1996; Holmes et al 2012; McClelland et al. 2012). Arctic rivers transport and discharge high amounts of organic matter (mainly soil and terrestrial plants derived matter) in both the dissolved or particulate phases, as well as terrestrial nutrients and contaminants such as Hg into the Arctic Ocean (Heiskanen et al. 1996; Lobbes et al. 2000).

The composition of dissolved and particulate material inputs from rivers to the coastal ocean depends on the season and on the water flow paths through the catchment (land cover, soil type, and topography). In catchments, dominated by permafrost, flow paths are constrained to the seasonally thawed portion of the soil profile (organic rich surface active layer), and deep groundwater contributions are relatively small (Frey et al. 2009 ; MacLean et al. 1999).

There is also a large seasonal variation in the amount of freshwater discharged in Arctic Ocean. With the progressive increase of air temperature, freshwater discharge increases from late spring until reaching maximum values during the summer period, and transporting over 90% of the annual delivery to the Arctic Ocean during this relatively short period (3–4 months) (Gordeev et al. 1996).

Rivers are an important terrestrial carbon source to coastal marine ecosystems. The six largest arctic rivers (Yenisey, Lena, Ob', Mackenzie, Yukon and Kolyma) export an average of 3055×10^9 g of Particulate Organic Carbon (POC). POC export is substantially lower than

Dissolved Organic Carbon (DOC) export (McClelland et al. 2016), which is the most abundant form of carbon in Arctic rivers. The Arctic Ocean receives about 25 Tg of terrigenous DOC each year (Benner et al. 2004; Opsahl et al. 1999). DOC lability (availability of bacterial uptake and remineralization) appears to be seasonal and closely linked to its chemical composition and source. During the spring freshet, DOC comes from fresh litter and surface soil horizons enriched in mineral nutrient and is highly labile. By contrast, the DOC exported by rivers during late summer are biologically recalcitrant in nature (Holmes et al. 2008; Mann et al. 2012).

Rivers are also an important source of Hg to marine ecosystems. Global Hg discharge from rivers to oceans are estimated to $5500 \pm 2700 \text{ Mg year}^{-1}$ (Amos et al. 2014). Among Arctic rivers, the Mackenzie River is the largest source of Total Mercury (TotHg) ($\sim 2200 \text{ kg year}^{-1}$) and a substantial source of Methylmercury (MeHg) ($\sim 15 \text{ kg year}^{-1}$) to the Beaufort Sea (Leitch et al. 2007). Hg discharge in coastal areas from river is closely linked to river flow, meaning that higher freshwater discharge during melting season increases the amount of Hg inputs (Leitch et al. 2007). Hg cycle is also linked to the organic carbon cycle through transport of organic-matter associated mercury (Coquery et al. 1995). Most of the Hg in aquatic systems is present as Hg(II) and strongly binds to POC (Morel et al. 1998). A large fraction (around >80%) of the Hg in rivers is in the particulate phase (Emmerton et al. 2013; Schuster et al. 2011) and is rapidly deposited to benthic sediments. Dissolved Hg consist in divalent inorganic mercury (Hg(II)) complexes with DOC (Zhang et al. 2015).

In the context of climate change, the increase of temperature, the changes in the timing of ice break and ice formation, the increase of precipitation (snow or rain), the melt of glaciers and permafrost inducing the increase of river discharge, all will affect carbon cycle and Hg dynamics (Jørgenson et al. 2006; Peterson et al. 2002 ; Waussmann et al. 2011). Large amounts of mercury and carbon accumulated and stored in soils, permafrost and glaciers should be released in rivers and ultimately in coastal waters, affecting the global carbon cycle, food chain structure and MeHg production (Frey et al. 2009; Peterson et al. 2002; Schuster et al. 2011).

1.2 MERCURY IN THE ARCTIC

Hg is a source of concern in the Arctic. This global contaminant cycles through air, water and soil (Nriagu et al. 1988). Natural Hg sources include volcanic eruptions, forest fires, while major anthropogenic sources of mercury to the atmosphere include coal, peat, wood burning and waste incineration (Steffen et al. 2005). Gaseous elemental Hg (Hg(0)) is the main type of Hg in the atmosphere in which it settles for a long time (between 6 to 12 months), and can thus be distributed over a large geographical area (Morel et al. 1998).

Anthropogenic Hg introduction to the Arctic originates from long-range transport rather than point source emissions (Durnford et al 2010; Steffen et al. 2008). In polar regions, Atmospheric Mercury Depletion Events (AMDEs) are an annual recurring spring time phenomenon (Douglas et al. 2012; Kirk et al 2012; Lu et al. 2001; Steffen et al. 2008) that consists in the oxidation of Hg(0) (Lindberg et al. 2002) to change mercury vapor into a water-soluble form Hg(II), and is then deposited on earth through rainfall or snow over the land and the ocean (Douglas et al. 2008; Morel et al. 1998).

Once deposited, Hg either penetrates aquatic environments (rivers discharge and ocean currents) or remains in soils, multi-year snow-pack, ice found on glaciers and ice sheet. Hg deposited onto the soil surface binds with organic matter in the active layer and, over time, sedimentation increases soil depth until it freezes to form permafrost. (Schuster et al. 2018). Current estimates suggest that Northern Hemisphere permafrost regions contain $1,656 \pm 962$ Gg Hg, of which 793 ± 461 Gg Hg is frozen in permafrost, which makes it a globally significant pool (Ariya et al. 2004; Macdonald et al 2010; Olsen et al., 2018; Schuster et al. 2018). During melting events, Hg(II) leaves the snow-pack, glacier and permafrost in the meltwater until reaching rivers and being discharged in arctic estuaries (Dommergue et al. 2003 ; Emmerton et al. 2013; Olsen et al., 2018; Schuster et al. 2011).

Several chemical processes can occur after Hg(II) deposition, including production of MeHg. Hg methylation is primarily carried out by sulfate-reducing bacteria in the anoxic zone of sediments (Gagnon et al. 1996; Morel et al. 1998). Other MeHg sources in coastal ecosystems include : snow-pack melt water (St Louis et al. 2005), river discharge (Emmerton et al. 2013; Leitch et al. 2007), MeHg production in the water column (Lehnherr, et al. 2011; Morel et al. 1998), and in stratified surface waters near the river mouth (Schartup et al. 2015) and

atmospheric MeHg deposit on ocean surface waters and adjacent terrestrial ecosystems (Baya et al. 2015). Aqueous concentration of methylmercury in estuaries depends on its rate of production (sources) and degradation (eg photochemical degradation) (DiMento et al. 2017; Poste et al. 2019; Sellers et al. 1996)

MeHg is of concern because of its capacity to readily bioaccumulate and biomagnify along trophic levels up until humans, exhibiting toxic effects such as neurotoxicity (Clarkson et al. 2003; Kuhnlein et al. 2000; Morel et al. 1998). Northern population relying on traditional foods for living (such as marine mammals) are particularly at risk from Hg exposure (Dewailly et al. 2001). Dietary exposure is the main pathway by which higher trophic level species are exposed to MeHg (Hall et al. 1997). It bioaccumulates more than inorganic Hg(II). Indeed, approximately four times as much MeHg is assimilated at the base of the food web by phytoplankton compared with inorganic Hg (Douglas et al. 2012; Mason et al. 1996). Thus, in higher trophic level species, Hg concentration depends on the Hg and MeHg bioavailability at the bottom of the food chain, species-specific processes controlling bioaccumulation, and food web length and structure (Kirk et al 2012).

1.3 ARCTIC PELAGIC FOOD WEB AND DIET BIOMARKERS

High latitude marine coastal ecosystems are characterized by a strong seasonality in light regime and ice cover (Rysgaard et al. 1996). Good conditions for primary production only occur few months during the year. In seasonally ice-covered fjords, before the ice break up, and as soon as enough light is available, growth of the algal community associated with sea ice occurs. In later spring, pelagic phytoplankton blooms are then usually observed along the ice edge when light and nutrients become available in spring and summer (Rysgaard et al. 1996; Rysgaard et al. 1999). During melting events in summer, primary production is lower due to nutrient depletion (Juul-Pedersen et al. 2015; Rysgaard et al. 1999) but also because of reduced light availability due to high turbidity from freshwater influx in coastal areas (Rysgaard et al. 1996). When autochthonous carbon source (i.e. phytoplankton) is less available, coastal pelagic organisms could rely on allochthonous carbon source discharged from river inputs. Several studies showed that terrestrial sources of organic matter is an alternative food source for omnivorous organisms (Dunton et al. 2006 ; Dunton et al. 2012), through the microbial loop,

whereby DOM is utilized by bacteria, which are grazed on by ciliates, heterotrophic nanoflagellates and rotifers, and then transferred to larger zooplankton (Rysgaard et al. 2006).

In pelagic food webs, phytoplankton are the major providers of high nutritional quality food and metabolic energy. (Dalsgaard et al. 2003; Parsons 1963). To cope with this seasonal food availability, pelagic marine organisms rapidly convert phytoplankton into lipid stores (Sargent et al. 1988) which can then be used as sources of metabolic energy in period of food shortage (i.e. during the polar night) (Falk-Petersen et al. 1990). These high-energy lipids are rapidly transferred to upper trophic levels in large amounts (Falk-Petersen et al. 1990). Polyunsaturated fatty acid (PUFAs), produced by algae and known as essential fatty acid (EFAs), are high quality food for marine invertebrates and higher trophic levels, and are needed to regulate physiological processes, survival, reproductive success and immunological responses (Arts et al. 2009; Brett et al. 1997).

Marine algae are the only known organisms able to biosynthesize de novo PUFAs such as linoleic acid (LIN) (18:2 n -6), alpha-Linolenic acid (ALA) (18:3n-3), Eicosapentaenoic acid (EPA) (20:5n-3) and Docosahexaenoic acid (DHA) (22:6n-3). Although fatty acid (FA) composition in marine algae can be influenced by abiotic factors (such as light, nutrient availability and temperature) (Harrison et al. 1990; Thompson et al. 1992), it is mainly determined by taxonomy. Because these PUFAs are only produced by algae, but well conserved and found in all organisms, they can be used as trophic markers. A high proportion of PUFAs will usually indicate herbivorous feeding (Dalsgaard et al. 2003). Other FA can be used as markers for dietary reliance on other food sources including ciliates (Saturates Fatty Acid; SFA), bacteria (characterized by odd-numbered, iso- and anteiso-branched SFA), heterotrophic flagellates (SFA and Monounsaturated Fatty Acid; MUFA), detritus (SFA, mainly 18:0), and terrestrial matter (such as 24:0 and 22:0, 18:2(n-6) and 18:3(n-3)) (Arts et al. 2009; Dalsgaard, et al. 2003; Mayzaud (2013); Saliot et al. 1991; Sørense (2008)). Because the only use and interpretation of FA as dietary markers can be bias (fatty acid selection and modification during food uptake, biosynthesis de novo, confounding of biomarkers) (Budge et al. 2006), it remains useful to cross results obtained with other methods such as stable isotope analysis.

Stable carbon (^{13}C) and nitrogen (^{15}N) isotopes are widely used in marine sciences to identify trophic structures and energy pathways in food webs (McConnaughey et al. 1979; Post 2002)

Isotope values are expressed as δ , the difference of heavy to light isotope ratio (i.e. $^{15}\text{N}:^{14}\text{N}$ or $^{13}\text{C}:^{12}\text{C}$), relative to standards (Fry 2006). $\delta^{15}\text{N}$ can be used to estimate trophic position of an organism, since fractionation during trophic transfer typically leads to an increase of 3-4‰ in $\delta^{15}\text{N}$ of consumers compared to their diet (Peterson et al. 1987; Post 2002). $\delta^{13}\text{C}$ is often used to identify main carbon sources in an organisms' diet. $\delta^{13}\text{C}$ values stay relatively similar from one trophic level to the next (approximately 1‰) but can differ strongly between different primary carbon sources (Peterson 1987; Post et al. 2002). This contrast in $\delta^{13}\text{C}$ between carbon sources is due to differences in fractionation during carbon uptake between primary producers. Stable isotope analyses are also used in ecotoxicological studies (especially ^{15}N) to highlight contaminant biomagnification processes in food webs. (Jardine et al. 2006)

1.4 STUDY AIMS

The aim of this study was to understand whether seasonal river inputs in Adventfjord could affect Particulate Organic Matter (POM) composition, zooplankton diet and mercury bioaccumulation in a coastal marine food web. To answer this question, the 3 main objectives were:

1-To describe seasonality in river inputs of particles, organic matter and Hg to Adventfjord (Svalbard) during the spring and summer, to assess their influence on POM composition in the fjord and to determine whether there is a gradient from inner to outer fjord.

2-To describe seasonal zooplankton diet and to assess whether zooplankton utilize terrestrial energy source during the main river discharge period, especially in the inner fjord.

3-To assess the influence of river inputs on zooplankton TotHg- and MeHg- concentrations and determine whether there is a gradient from inner to outer fjord in zooplankton contamination.

2 MATERIALS & METHODS

2.1 THE STUDY AREA

The current study was carried out in Adventfjord, one of the southern arms of Isfjorden, Svalbard (Figure 1). It is 8.3 km long and 3.4 km wide and is located between 78°13 and 78°17N and 15°25 and 15°46E. The central basin of the fjord has no significant sill and is between 60 to 100 m deep, and the depth increases downfjord (Zajaczkowski et al. 2010). The lack of sill promotes good water circulation in Adventfjord with a high degree of exchange with outer Isfjord. The water masses in Isfjord and thus the outer area of Adventfjord are influenced both by the West Spitsbergen Current (relatively warm Atlantic water) (Zajaczkowski et al. 2010) and the South Cape Current (relatively cold Arctic water).

The inner part of Adventfjord experiences significant freshwater input from two rivers (Adventelva and Longyearelva) (Zajaczkowski et al. 2010), which transport meltwater from the glaciers (Zajaczkowski et al. 2007; Zajaczkowski 2008 ; Zajaczkowski et al. 2010), and runoff from rain and snowmelt.

There is not much quantitative data available on riverine inputs to Adventfjord, but during summer 2001, the discharge in Adventelva flow reached a maximum of $3.6 \text{ m}^3 \text{ s}^{-1}$ (Zajaczkowski 2008), and the concentration of suspended solids in the river waters varied between 132 and 486 mg dm^{-3} . During the same period, Longyearelva discharged less water (average $2.04 \text{ m}^3 \text{ s}^{-1}$) but with a slightly higher concentration of suspended solids (between 149 and 592 mg dm^{-3}) (Zajaczkowski et al. 2004). During the spring tide, the range of semidiurnal tides is 159 cm (Zajaczkowski et al. 2007 ; Zajaczkowski et al. 2010).



Figure 1 :Map of Svalbard. Isfjorden indicated in the red circle and Adventfjord indicated with red point.

2.2 SAMPLE COLLECTION

2.2.1 Water sampling

Surface water was collected using carboys (5 L) from Adventelva on a monthly basis from May to August 2018, and additional water samples were also collected from Longyearelva (from June to August) and several tributaries of Adventelva (Todalselva, Bolterelva, Endalselva, Foxelva) in June and August (Figure 2). Rivers were sampled on : 17.05.18, 19.06.18, 5.08.18 and 16.08.18. Hourly water level data in Adventelva was provided by sensor-based measurements from NIVA's river monitoring station (78°2N, 15°8E), and included data from 19/06/18 to 15/09/18. Hourly data were converted to mean daily data (24 hours). Data on precipitation and air temperature were obtained from yr.no for the Svalbard Airport meteorological station.

Seawater in Adventfjord was collected monthly using a Niskin sampler from April to August 2018 at the 3 stations (AF1, AF2 and ISA) at 2 depths: just below surface and at 15m. Seawater was transferred from the sampler either directly into sample bottles for further analysis or into carboys (20 L). A CTD was deployed at each station from the surface to 5 m above the bottom for salinity and temperature measurements (Figure 2).

For TotHg analysis, river and fjord water was poured directly into a 250mL FLPE bottle using trac-metal clean sampling techniques and stored in dark and cold (~4°C) conditions in the field and then frozen at -20°C, until they were sent to Oslo for analysis. Water sampled in carboys were kept in cold and dark until filtration at the University Centre in Svalbard as soon as possible after water collection. Some extra water was collected in rivers and fjord in a bucket for immediate physical parameter analysis : Thermo Fisher Eutech TN-100 turbidimeter, and a Hanna Instruments HI98195 multisensor (pH, salinity, temperature).

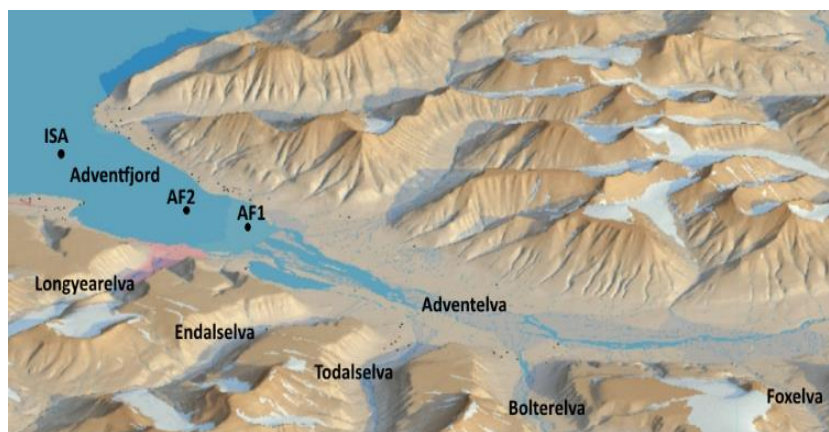


Figure 2 : Adventfjord and Adventelva catchment with sampling locations indicated.

2.2.2 Zooplankton sampling

Zooplankton samples were collected monthly from April to August 2018 from the 3 fjord stations (Table 1 ; Figure 2) . In order to collect sufficient sample material for planned analyses, we carried out vertical hauls from 5 m above bottom to surface with two WP2 nets (opening 0.25m²) with different mesh sizes : 60 µm and 200 µm) and a larger and coarser WP3 net (opening 1 m² ; mesh size 1000 µm). All net haul material was pooled and macrozooplankton (Chaetognatha, Jelly plankton, Euphausiacea, and *C. limacina*) were hand-picked before the remaining samples from each station were size-fractionated using sequential Nitex mesh screens with mesh sizes of 1000 µm, 500 µm, 200 µm, and 50 µm.

Subsamples of size fractionated zooplankton samples were removed for identification (fixed with 4% formalin-seawater solution buffered with hexamine in 30 mL Falcon tubes). For stable isotope and Hg analysis subsamples of size fractionated zooplankton samples were placed in 20 mL polyethylene vial and stored at -20°C and for FA analysis placed in cryovials and stored at -80°C until analyses. Hand-picked macrozooplankton samples were frozen separately in 20 mL polyethylene vial and stored at -20°C for stable isotope and Hg analysis, and at -80°C for FA analysis.

Table 1 Stations coordinates, depth and sampling dates in Adventfjord from April to August 2018

Station	Latitude (N)	Longitude (E)	Station depth	Sampling depth (Seawater samples)	Sampling depth (Zooplankton samples)	Sampling dates
AF2	78 14.22	15 41.50	20 m	0 m 15 m	Bottom to surface	5.04.2018* 14.05.2018 18.06.2018 19.07.2018 17.08.2018 *AF2 was not sampled in April
AF1	78 14.792	15 39.443	45 m	0 m 15 m	Bottom to surface	
ISA	78 15.57	15 31.30	120 m	0 m 15 m	Bottom to surface	

2.3 SAMPLE PROCESSING AND ANALYSIS

2.3.1 Suspended Particulate Matter (SPM)

Water samples from fjord and rivers were filtered on to pre-dried and pre-weighed 47 mm Whatman® glass microfiber filters (GF/F grade), and 47 mm Whatman® QMA quartz filters (QMA filter) (filters had been dried in an oven at 60°C for 1 hour) and were stored in petridish at -20 °C.

Gravimetric analysis of SPM was carried out at the University Centre in Svalbard. Samples (n=37) were dried in an oven at 60°C until weight had stabilized (approximately 4 hours), and each filter was then weighted using a microbalance. SPM concentration (mg/L) was calculated based on the difference in mass of the filter before and after filtration and the volume of water filtered.

2.3.2 Chlorophyll a (Chl a)

Water samples from fjord were filtered onto 25mm GF/F filters for Chl a analysis which were then stored in aluminium foil in freezer at -80°C.

Chl a was analysed at the University Centre in Svalbard (n= 28). Chl a on filters was extracted with 10 mL of 100% methanol in the dark at 4°C for 20-24 hrs (Holm-Hansen and Riemann 1978), and fluorescence was determined using 10-AU-005-CE Fluorometer (Turner, USA).

After measuring total Chl a, non-degraded Chl a was degraded by the addition of 5% HCl, and fluorescence measurements were repeated.

2.3.3 $\delta^{13}\text{C}$, $\delta^{15}\text{N}$ and C and N content in POM and zooplankton

Water samples from fjord and river were filtered onto pre-combusted 25mm Whatman® GF/F filters, wrapped in aluminium foil and frozen at -20°C until analysis for stable isotopes of carbon ($\delta^{13}\text{C}$) and nitrogen ($\delta^{15}\text{N}$) and in parallel determination of particulate C (PartC) and N (PartN).

Prior to analysis, both POM filters (River $n = 14$; Fjord $n = 28$) and zooplankton samples ($n = 59$) were freeze-dried for 24-48 hours. Zooplankton samples were homogenized using an agate mortar and pestle. A sub-sample was then weighted to the nearest $1\ \mu\text{g}$ using a Metler Toledo balance and packed in aluminium capsules. For every 10th zooplankton sample a replicate sample was weighed out. POM on filters were also packed in aluminium capsules.

Because $\delta^{15}\text{N}$ measurements can be influenced by carbonate (Bodin et al. 2007), we analyzed two parallel filters for POM, one unacidified to provide data on $\delta^{15}\text{N}$, and particulate nitrogen and carbon content and one acidified to provide data on $\delta^{13}\text{C}$ and POC content. Filters were acidified by placing inside a dessicator with a beaker of 100 ml 1M HCl for 24 hours. They were then dried in an oven at 60°C for 48 hours before being packed in tin capsules for analysis. For zooplankton, unacidified samples were analyzed for ^{13}C and ^{15}N isotopes and carbon and nitrogen content. For a subset of zooplankton samples ($n= 16$), I analyzed parallel acidified samples to test for effects on $\delta^{13}\text{C}$ values. Zooplankton sub-samples were acidified by adding 2-3 drops of 1M HCl and then were dried in the oven at 60°C for 48 hours. C :N molar ratios were calculated from C and N content data from unacidified samples.

Stable Isotope Analysis were carried out for zooplankton size-fractioned samples and POM, at the Stable Isotope Facility, University of California Davis (UC Davis Stable Isotope Facility, Davis, California, USA). Briefly, ^{13}C and ^{15}N isotopes for POM filters were analysed using an Elementar Vario EL Cube or Micro Cube elemental analyser (Elementar analysensysteme GmbH, Hanau, Germany) interfaced to a PDZ Europa 20-20 isotope ratio mass spectrometer (Sercon Ltd., Cheshire, UK). ^{13}C and ^{15}N isotopes for zooplankton were analyzed using an PDZ

Europa ANCA-GSL elemental analyser interfaced to a PDZ Europa 20-20 continuous flow isotope ratio mass spectrometer (IRMS), (Sercon Ltd., Cheshire, UK). Long term standard deviation for these instruments is ± 0.2 ‰ for ^{13}C and ± 0.3 ‰ for ^{15}N .

$\delta^{13}\text{C}$ and $\delta^{15}\text{N}$ values were determined by :

$$\delta X = [R_{\text{sample}}/R_{\text{standard}} - 1] \times 1000 \quad (\text{Equation 1})$$

expressed in units of per thousand (‰) and where X is « Carbon » or « Nitrogen », and R is one of the following ratios $^{13}\text{C}/^{12}\text{C}$ or $^{15}\text{N}/^{14}\text{N}$. The reference material, which are international 'standard' are Pee Dee Belemnite limestone for carbon and atmospheric N_2 for nitrogen.

2.3.4 Zooplankton Identification

I estimated the relative contribution of different zooplankton taxa to the biomass of size fractionated samples by pairing sample identification through microscopy with previously reported taxon-specific estimates of dry weights for individuals of Arctic zooplankton (Blachowiak-Samolyk et al. 2008 and references therein).

Each size-fractionated sample was washed for 2 hours to remove formalin and was then analyzed using a Leica stereomicroscope under 10 to 40 times magnification. Individuals were identified, measured and counted. In size-fractionated samples containing few organisms (< 200), all individuals were identified. In size-fractionated samples containing abundant zooplankton, the sample was diluted in 100 ml of seawater and 2 mL sub-samples were analyzed, until 200 individuals had been counted. The rest of the size-fractionated sample was then screened to look for « rare » species. To distinguish between the morphologically similar *C. glacialis* and *C. finmarchicus* from formalin-preserved samples, I used size classes derived for each developmental stage (copepodites CIII–CVI) from prosome length frequency analyses for the study region (Daase et al. 2007), which were readjusted after considering molecular-based studies (Gabrielsen et al. 2012, Choquet et al. 2018, Renaud et al. 2018).

Relative proportion of species or taxa in each size fraction sample, was calculated based on the estimation of dry weight of individuals provided by Katarzyna Dmoch from IOPAS - Institute of Oceanology Polish Academy of Science and Janne Søreide (*Table Appendix A1*). However, it should be noted that these data reflect relative abundance and biomass, rather than absolute

abundances and biomass, since these samples are non-quantitative subsamples from net hauls where the water volume that has passed through the net is not known.

Since there were no significant variability in $\delta^{13}\text{C}$ and $\delta^{15}\text{N}$ and Hg data between zooplankton samples collected at the 3 stations on the same date (no spatial variability) (*Figure Appendix A1*), and not all size-fraction were available for each month, and because some taxa were dominating the biomass of several size-fractioned samples at a same sampling date (e.g *Calanus* spp.), zooplankton samples were sorted by feeding category for further data analysis.

Although zooplankton can change diet and feeding strategy along a year according to several factors such as developmental stage, the season and food availability (Paffenhöfer et al. 1988), for the purpose of this study, a zooplankton sample belonged to one of these categories when taxa/species mainly using this feeding strategy represented more than 85% of the biomass of the sample (Table 2). A sample was represented by a « Dominant species », when a species/taxa represented more than 85% of the biomass of the sample.

Table 2 Feeding strategy of taxa/species in size-fractioned samples dominating the biomass. (Jelly plankton included Ctenophore, *B. cucumis* and *M. ovum*). (« Herbivores » : n = 19 ; « Omnivores » : n = 13 ; « Predators » = n = 15)

Dominant Species / Taxa	Feeding strategy	References
<i>C. limacina</i> (n = 5)	Predator	Hermans et al. 1992 Falk-Petersen et al. 2001
Fish larvae (n = 2)	Predator	Walkusz et al. 2011
Chaetognatha (n = 2)	Predator	Pearre et al. 1981 Samemoto et al. 1987)
Amhipod (n = 1)	Predator	Auel et al. 2002
Jelly plankton (n = 10)	Predator	Falk-Petersen et al. 2002 Haddock et al. 2007
<i>O. similis</i> (n = 3)	Omnivore	Lischka et al. 2007
Decapod zoea (n = 1)	Omnivore	Jones et al. 1997
Euphausiacea (n = 3)	Omnivore	Foster et al. 2012
<i>L. helicina</i> (n = 2)	Omnivore	Gilmer et al. 1991 Gannefors et al. 2005 Falk-Petersen et al. 2001
<i>Calanus</i> spp. (n = 13)	Herbivore	Søreide et al. 2008
Cirripedia nauplii (n = 3)	Herbivore	Turner et al. 2001

2.3.5 Fatty Acid (FA) Analysis in zooplankton

FA analysis were carried out for a subset of zooplankton size-fractionated samples (n=24) at the Ryerson University in Toronto (Ontario,Canada) by Michael Arts. In brief, total lipid were extracted with 4 mL of 2:1 chloroform:methanol. 18 ug of Tricosanoic acid (23:0) was added to each tube as an internal standard (23:0) for determining methylation efficiency (mean ~80%). The extracts were then dried with non-reactive nitrogen gas. For the methylation of Fatty Acid, 2 mL of hexanes was added to each of the tubes after which 2 x 100 µL of the lipid solution was removed from each tube and placed in cast tin cups. After evaporation of the solvent, tubes were placed on a heating block for 90 min at 90°C. A Shimadzu GC-2010 plus, with an AOC-20i/s auto sampler and twin auto injectors, with Shimadzu LabSolutions software, was used to quantify FA. Column temperature was set to hold at 140°C for 5 min, ramping up to 240°C at 2°C/min for 50 min, and then holding at 240°C for the final 10 min. Fatty acid in the samples were identified and quantified by referencing them to the retention times of FA and using a series of calibration standards (GLC 463, GLC 68E, and 23:0, NuChek Prep., Waterville, MN, USA), respectively.

42 fatty acid markers were analyzed and were included in summary metrics for further statistical analysis (Table 3).

Table 3 Fatty acid markers (n=42) analyzed in zooplankton samples (n=24) and included in summary metrics for further statistical analysis.

Diet marker summary metrics:	Fatty Acid included:
Σ PUFA	18:2n-6c; 18:3n-6; 18:3n-3; 18:2n-6t; 18:2n-6c; 18:3n-6; 18:3n-3; 18:2n-6t; 20:3n-6; 20:3n-3; 20:4n-6; 20:5n-3; 20:3n-6; 20:3n-3; 20:4n-6; 20:5n-3; 22:3n-3; 22:2n-6; 22:4n-6; 22:5n-3; 22:6n-3;
Σ C18 PUFA	18:2n-6c; 18:3n-6; 18:3n-3; 18:2n-6t; 18:2n-6c; 18:3n-6; 18:3n-3; 18:2n-6t;
Σ C20 PUFA	20:3n-6; 20:3n-3; 20:4n-6; 20:5n-3; 20:3n-6; 20:3n-3; 20:4n-6; 20:5n-3
Σ C22 PUFA	22:3n-3; 22:2n-6; 22:4n-6; 22:5n-3; 22:6n-3
Σ EPA & DHA	20:5n-3; 22:6n-3
Σ n-6	18:2n-6c; 18 :3n-6; 18:2n-6t; 20:2n-6; 20:3n-6; 20:4n-6; 22:2n-6; 22:4n-6
Σ n-3	18:3n-3; 18:4n-3; 22:3n-3; 20:3n-3; 20:5n-3;
Σ MUFA	14:1n-5; 15:1n-5; 16:1n-7c; 16:1n-7t; 17:1n-7; 18:1n-9c; 18:1n-9t; 18:1n-12c; 18:1n-7c; 18:1n-7t; 19:1n-12; 20:1n-15; 20:1n-9; 20:1n-11; 22:1n-11; 22:1n-9; 24:1n-9
Σ MUFA \geq 18	18:1n-9c; 18:1n-9t; 18:1n-12c; 18:1n-7c; 18:1n-7t; 19:1n-12; 20:1n-15; 20:1n-9; 20:1n-11; 22:1n-11; 22:1n-9; 24:1n-9
Σ MUFA > 18	19:1n-12; 20:1n-15; 20:1n-9; 20:1n-11; 22:1n-11; 22:1n-9; 24:1n-9
Σ SFA	14:0; 15:0;16:0; 17:0; 18:0; 19:0; 20:0; 22:0; 24:0;
Σ Odd chain	15:0; 15:1n-5; 17:0; 17:1n-7; 19:0; 19:1n-12;

2.3.6 Total Mercury (TotHg) analysis in water, POM and zooplankton

TotHg analysis in river and fjord water (Aqueous TotHg) was carried out at NIVA. TotHg in water was determined through oxidation, purge and trap and cold vapor atomic fluorescence spectrometry (CVAFS) based on USEPA method 1631. In the current study, Aqueous TotHg is reported ng/L.

For TotHg analysis in POM, fjord and river water samples were filtered onto pre-combusted QMA filters, and were then stored in aluminium foil in freezer at -20°C.

TotHg analysis were carried out for POM (Rivers n = 12 ; Fjord n = 28) and zooplankton (n=35) using a Direct Mercury Analyzer (DMA-80) at Akvaplan-niva in Tromsø. This technique is based on sample combustion, concentration of mercury by amalgamation with gold, and cold vapor atomic absorption spectrometry (Cizdziel et al 2010). Prior to analysis, POM filters were freeze dried for 24-48 hours and were cut into strips and put into analytical boats for TotHg analysis. When biomass was sufficient, a sub-sample (around 10 mg) of homogenized zooplankton samples (taken from the same samples than for Stable Isotope analysis) were put in analytical boats for analysis.

Quality assurance measures included 3 blanks (0,04 g ± 0,03 for zooplankton samples ; 0,03 g ± 0,02 for POM samples) and 3 blank analytical boats (0,01 g ± 0 for zooplankton samples ; 0,02 g ± 0 for POM samples) to prevent from contamination, and analysis of reference materials (CRM-DORM-4, fish, CRM-DORM-4; National Research Council Canada) (n=2) to assess precision. CRMs were always within the certified concentration range 416 ng/g ± 28. In the current study, TotHg concentration in zooplankton is reported ng/g d.w basis, Particulate TotHg (PartTotHg) is reported ng/L and TotHg concentration in SPM (SPMTotHg) is reported ng/g basis.

2.3.7 Methyl Mercury (MeHg) analysis in zooplankton

MeHg analysis was carried out for zooplankton (n=56). When biomass was sufficient, a sub-sample of homogenized zooplankton samples (taken from the same samples than for Stable Isotope analysis) was analyzed.

MeHg analysis in zooplankton was carried out at Stockholm University (SU), Sweden. The procedure for preparation and analysis of MeHg was based on the method described in Braaten et al (2014) and Hintelmann & Nguyen (2005), however with minor adjustments. Briefly, MeHg was extracted via digestion using nitric acid (30%) (Fisher Scientific®) in a 60°C bath for 16-17 hours. After acid digestion, the samples were analysed using a 2700 Methyl Mercury Auto-Analysis System (Tekran, Canada). Quality assurance measures included method blanks (0.01± 0.002 ng/L), to discover contamination, and analysis of certified reference materials

(CRM-DORM-4, n=6; National Research Council Canada and TORT-2, n=3; National Research Council Canada), matrix spikes (n=6 ; recoveries ranged from 85 to 100 %) and sample duplicates (n=6 ; relative % difference from 1.5 to 35%). CRMs were always within the certified concentration range. MeHg concentration in zooplankton in the current study are reported on a ng/g d.w. basis

2.4 CALCULATIONS AND STATISTICAL ANALYSIS

All the statistics analysis were run in R version 3.5.2 2 (R Core Team 2017) using RStudio and the following R packages : FactomineR, Factoextra, Vegan, ggplot2 and OCE package

2.4.1 Baseline variability in Stable Isotope Analysis

To remove the strong seasonal variability in $\delta^{13}\text{C}$ and $\delta^{15}\text{N}$ of POM in the study, the differences in $\delta^{13}\text{C}$ and $\delta^{15}\text{N}$ between zooplankton and « marine » POM were calculated on a month-by-month basis (data for POM were for deep water from the outermost station and assumed to primarily consist of phytoplankton). This allowed to assess whether there was a consistent, or seasonally and/or taxonomically variable difference between POM and zooplankton in $\delta^{13}\text{C}$ and $\delta^{15}\text{N}$ values ; and to get a more accurate picture of the main dietary carbon sources and trophic level of zooplankton in a seasonally dynamic system.

The following calculation were used :

$$\delta^{13}\text{C}_{zooplankton} - \delta^{13}\text{C}_{POM} \quad (\text{Equation 2})$$

$$\delta^{15}\text{N}_{zooplankton} - \delta^{15}\text{N}_{POM} \quad (\text{Equation 3})$$

2.4.2 Inorganic Carbonate and Lipid correction in Stable Isotope data

Inorganic carbonate and lipid content may bias $\delta^{13}\text{C}$ values and thus some acid and lipid correction should be done.

Paired T-tests were performed between acidified and non-acidified POM and zooplankton samples respectively. There was a significant difference between acidified and non-acidified POM samples (Paired t-test, $p < 0.001$) ; so $\delta^{13}\text{C}$ values from acidified samples and $\delta^{15}\text{N}$ from non acidified samples were used for the analysis of fjord and rivers POM samples.

Since there was no significant difference between acidified and non acidified zooplankton samples, data from non acidified samples were used for futher data analysis.

Lipid correction in zooplankton samples was necessary to reduce the variability of carbon isotopic signature due to seasonal fluctuation and inter specific variability in lipid concentration (Hobson et al. 1992). Previous studies have found that lipid normalization in zooplankton based on C :N ratio (used as a proxy of lipid content)) can be challenging due to species-specificity, spatio-temporal differences (Logan et al. 2008, Matthews et al. 2005). However in this study, because we had measurements of lipid content in a subset of samples ($n=24$), we were able to directly assess the relationship between C :N ratio and lipid content, and found a significant positive relationship between these parameters ($R^2=0.6$, $p < 0.01$), suggesting that for our samples, C :N ratio can be used as a proxy for lipid content (*Figure Appendix A2*)

$\delta^{13}\text{C}$ values in zooplankton were lipid-corrected by applying the model using C :N ratio in Pomerleau et al. 2014 :

$$\Delta^{13}\text{C} = (0.206 * \text{C} : \text{N}) + 2,02 \quad (\text{Equation 4})$$

($r^2= 0,28$; $p\text{-value}=0,01$; Model efficiency : 0,87) (Pomerleau et al 2014)

$$\delta^{13}\text{CLEA} = \delta^{13}\text{C}_{\text{bulk}} + \Delta^{13}\text{C} \quad (\text{Equation 5})$$

with $\delta^{13}\text{CLEA}$ meaning $\delta^{13}\text{C}$ lipid-extracted- acidified.

2.4.3 Univariate Analysis

To assess if the data deviated from normal distribution, the Shapiro-Wilk normality test was performed on water data, POM data and zooplankton data. Several variables of the datasets did not show a normal distribution.

In order to determine whether there were significant differences in physicochemical parameters, stable isotope and Hg in POM and zooplankton between months, stations and feeding category, I used Kruskal-Wallis tests. This non-parametric approach was selected due to the non-normal distribution of several of the parameters. In addition, pairwise comparisons using Wilcoxon rank sum tests was used to do a multicomparison among months, stations and feeding category and test the significance of differences between pairs of results.

Spearman's rank correlation was used to examine correlation between the different physicochemical water parameters in Adventfjord, and correlation between TotHg and MeHg concentration in zooplankton with dietary markers ($\delta^{15}\text{N}$, $\delta^{13}\text{C}$ and FA).

To investigate the potential relationship between water physicochemical parameters, dietary markers and Hg concentration in POM and zooplankton, linear regression models (lm) were used. To respect the assumptions of normal distribution and homogeneity, data were Log10 transformed.

2.4.4 Multivariate Analysis

To visualize the similarities and differences in zooplankton FA profiles across months, Correspondance Analysis (CA) were conducted. The analysis included all 42 FA analyzed in zooplankton samples dominated by *Calanus* spp. and Cirripedia nauplii (n= 15) taken at the 3 stations (AF1, AF2, ISA) from April to August 2018. Similarly, a second CA was conducted including only zooplankton samples dominated by *Calanus* spp. (n=12) and taken at the 3 stations from April to August.

To explore correlations, similarities and differences between physicochemical parameters from the 3 stations in Adventfjord across months (from April to August 2018) (n = 28), a Principal component analysis (PCA) was conducted. A redundancy analysis (RDA) was also used in

order to determine the amount of variance in the data set that could be explained by the explanatory variables station, month (sampling date) and depth.

Similarly, a PCA was used to characterize relationships between AqueousTotHg, dietary markers ($\delta^{13}\text{C}$, $\delta^{15}\text{N}$, FA composition), and TotHg- and MeHg- concentrations in « Herbivores » (n=15) and a RDA was used to determine the amount of variance in the zooplankton data set that was attributable to station, and month.

Finally, a PCA was used to characterize relationships between zooplankton taxonomy, dietary markers ($\delta^{13}\text{C}$, $\delta^{15}\text{N}$), Aqueous TotHg and TotHg- and MeHg- concentrations in zooplankton samples with « Dominant species » (n = 30) and a RDA was used to determine the amount of variance in the zooplankton data set that was attributable to station, month and feeding strategy. Each RDA was followed by an analysis of variance (ANOVA) to investigate if the amount of variance explained was significant.

3-RESULTS

3.1 PHYSICOCHEMICAL CHARACTERIZATION OF RIVER DISCHARGE

The water level in Adventelva, (provided by sensor-based measurements from NIVA’s river monitoring station) was higher between 19/06/18 and 31/07/18 (during the main melting period), after which it progressively decreased (Figure 3). This seasonal pattern was closely aligned with air temperature (as measured at the Longyearbyen airport), and there was a significant positive relationship between air temperature and water level ($R^2 = 0.5$; $p < 0.01$) (Figure Appendix A3). Rainfall peaks had little impact on the water level compared to air temperature (Figure 3).

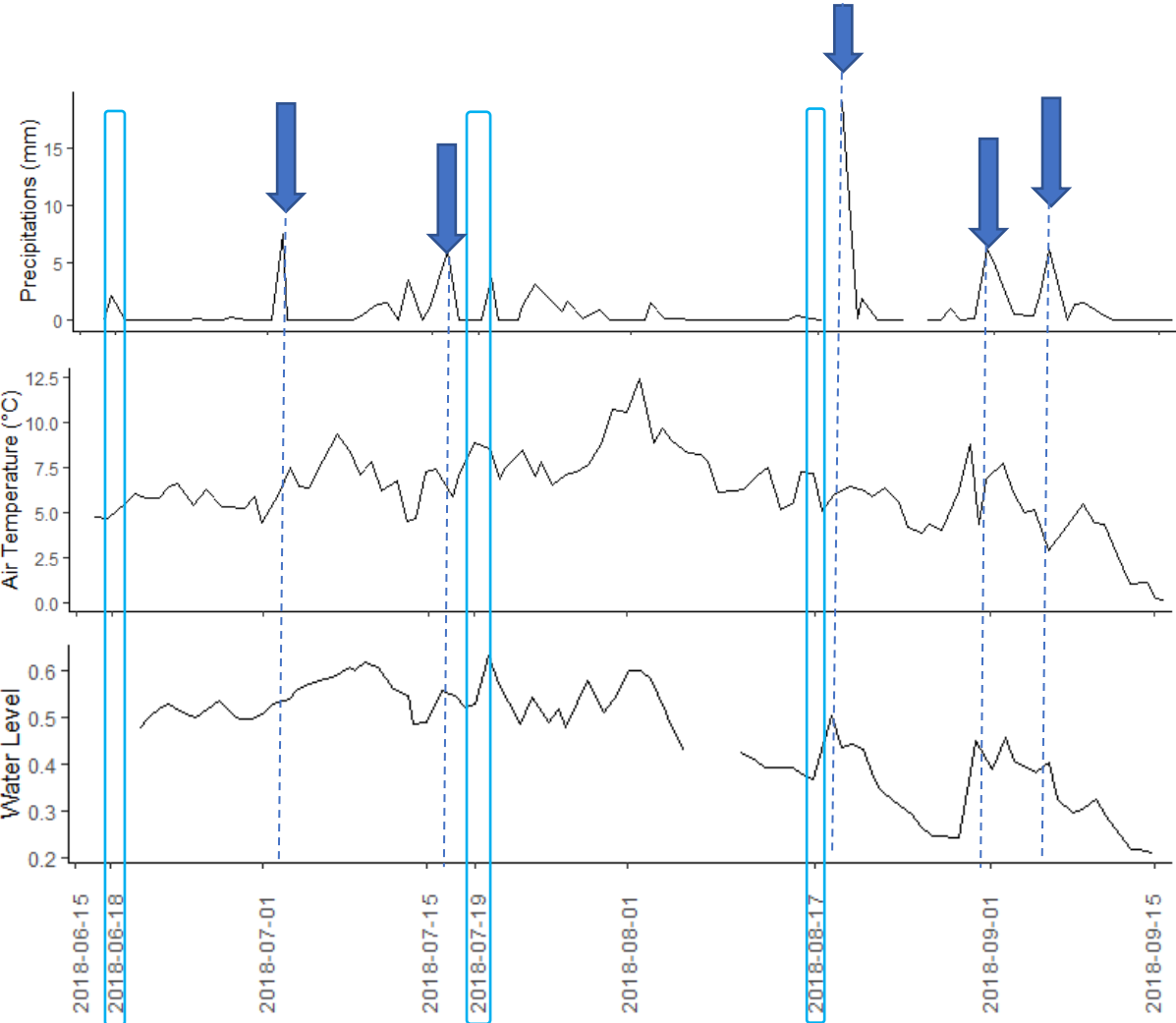


Figure 3 Mean daily water level, air temperature (°C), and total daily precipitation (mm) data from 15/06/2018 to 15/09/2018. (Blue box = sampling dates ; Arrows and dashed blue lines = peaks of precipitation.)

The water temperature, Turbidity and SPM concentrations increased during the summer season. Turbidity values ranged from 37 to 98 NTU in June and from 292 to 694 NTU in August, and SPM concentrations ranged from 42 to 137 mg/L in June and from 204 to 669 mg/L in August (Table 4).

Table 4 Physical parameters for surface water in Adventelva and tributary rivers from May to August 2018.

Rivers		Month	Turbidity (NTU)	SPM (mg/L)	Salinity (PSU)	Temperature (°C)	pH
Adventelva	n = 1	May	1	147	0.5	6	7.4
Adventelva	n = 1	June	98	137	0.3	9	7.4
Adventelva	n = 1	August	262	204	0.4	13	6.9
TRIBUTARIES							
Todalselva	n = 1	June	37	42	0.1	8	7
Bolterelva	n = 1	June	62	71	0.1	7	7
Todalselva	n = 1	August	402	295	0.1	11	7
Bolterelva	n = 1	August	694	-	0.1	11	6.9
Endalselva	n = 1	August	664	669	0.1	12	7
Foxelva	n = 1	August	445	361	0.1	11	7.1

$\delta^{13}\text{C}$ values in POM ranged from -27.9 to -26.3 ‰ in June and from -26.9 to -25.4 ‰ in August. These relatively high values compared to what would be expected for soil derived organic matter, could be explained by a lack of acidification during samples processing. $\delta^{15}\text{N}$ values ranged from 2.3 to 4.0 in June and from 2.7 to 3.4 in August. The C :N molar ratio decreased in tributaries between June and August. Adventelva had its highest ratio in June (180.4) and Longyearelva in August (117.0) (Table 5).

Table 5 Stable isotopes $\delta^{13}\text{C}$ and $\delta^{15}\text{N}$ (‰), and C :N ratio in surface waters in Adventelva, Longyareelva and tributaries rivers from May to August 2018

Station		Month	$\delta^{13}\text{C}$	$\delta^{15}\text{N}$	C:N ratio
Adventelva	n = 1	May	-26.5	1.5	116.5
Adventelva	n = 1	June	-26.3	2.9	180.4
Adventelva	n = 1	July	-	1.3	36.9
Adventelva	n = 1	August	-25.4	3.3	72.6
Longyareelva	n = 1	June	-26.8	2.3	33.1
Longyareelva	n = 1	July	-26.8	3.3	61.1
Longyareelva	n = 1	August	-26.5	3.0	117.0
TRIBUTARIES					
Endalselva	n = 1	June	-26.7	2.6	108.1
Todaselva	n = 1	June	-27.9	3.1	496.3
Bolterelva	n = 1	June	-26.5	4.0	48.9
Endalselva	n = 1	August	-26.9	3.0	44.5
Todaselva	n = 1	August	-26.7	2.7	73.2
Bolterelva	n = 1	August	-26.8	3.3	30.3
Foxelva	n = 1	August	-26.3	3.4	58.1

Adventelva had the highest AqueousTotHg concentration value in June (2.3 ng/L) compared to May and August. The concentration of Particulate TotHg in the water (PartTotHg) increased during the summer period. Bolterelva and Endalselva had higher PartTotHg concentration (27 ng/L) than Adventelva in August and Longyareelva had the highest value in June (16 ng/L). A significant positive relationship between PartTotHg and SPM concentrations, suggest that these two parameters are linked ($R^2 = 0.9$; $p < 0.01$) (*Figure Appendix A4*). The Hg concentration in the particles (SPMTotHg, i.e. how Hg-rich the particles are) were higher in Adventelva than in Longyareelva and tributaries over the study period (Table 6).

Table 6 Total Hg concentration in water (AqueousTotHg), Particulate Hg concentration (PartTotHg) and Total Hg concentration in SPM (SPMTotHg) in surface waters in Adventelva, Longyearelva and tributaries rivers from May to August 2018

River		Month	AqueousTotHg (ng/L)	PartTotHg (ng/L)	SPMTotHg (ng/g)
Adventelva	n = 1	May	0.8	9	63
Adventelva	n = 1	June	2.3	7	50
Adventelva	n = 1	August	1.6	13	62
Longyearelva	n = 1	June	1.0	16	21
Longyearelva	n = 1	July	1.3	15	-
Longyearelva	n = 1	August	1.9	15	-
TRIBUTARIES					
Todalselva	n = 1	June	1.0	2	35
Bolterelva	n = 1	June	1.3	3	43
Todalselva	n = 1	August	1.6	14	47
Bolterelva	n = 1	August	0.9	27	-
Endalselva	n = 1	August	0.6	27	41
Foxelva	n = 1	August	1.1	17	46

3.2 PHYSICOCHEMICAL CHARACTERIZATION OF ADVENTFJORD

3.2.1 POM composition

Chl a concentration in POM ranged from 0.1 to 3.0 ug/l, with the lowest values in all stations in April and the highest value in surface water in outer fjord in June. (Figure 4A). C :N molar ratios ranged from 4.5 to 41.0 , and were highest in surface water from the inner fjord in July, and lowest in May and August (all stations) and in the outer fjord (May–August) (Figure 4B). $\delta^{13}\text{C}$ values in POM ranged from -33.5 to -22.8 ‰ and were seasonally variable, with highest values in May (Kruskal-Wallis $p < 0.01$; Pairwise Wilcoxon $p = 0.02$) and lowest values in the outer fjord in April. (Figure 4C). $\delta^{15}\text{N}$ values in POM ranged from 2.87 to 6.8 ‰ and showed a decrease throughout the study period (Kruskal-Wallis ; $p = 0.02$). (Figure 4D). There were no significant variability between stations sampled the same day for all these parameters, except for $\delta^{13}\text{C}$ values in April (Kruskal-Wallis ; $p < 0.05$)

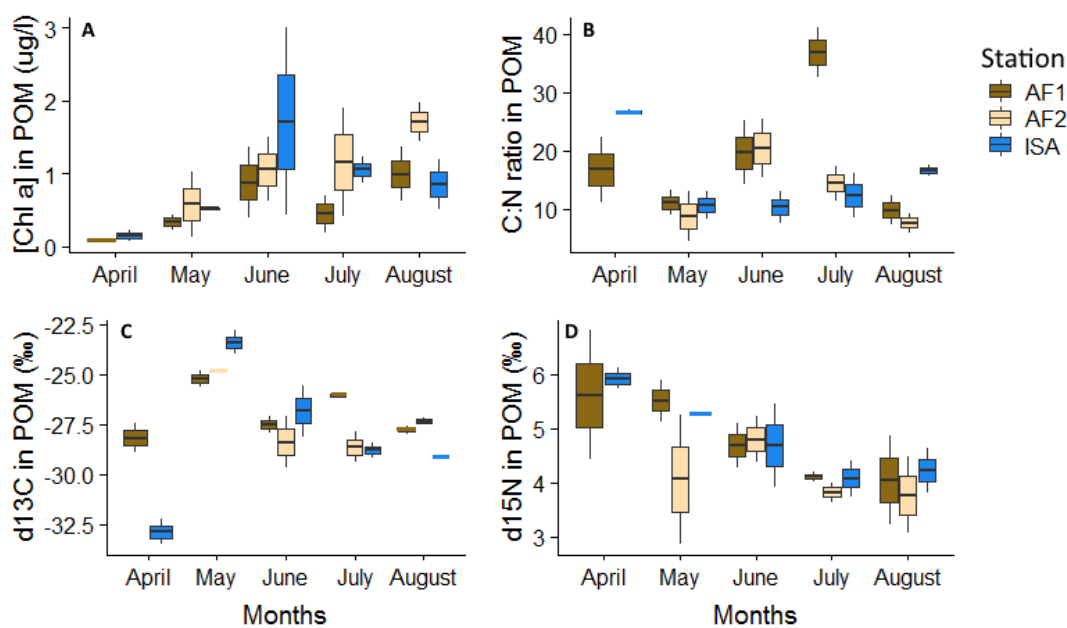


Figure 4 Boxplots of (A) Chl a concentration ($\mu\text{g/L}$), (B) C :N ratio, (C) $\delta^{13}\text{C}$ acidified (‰) and $\delta^{15}\text{N}$ (‰) in POM sampled at the 3 stations in Adventfjord (AF1, AF2 and ISA), at 2 depth (surface and 15m) from April to August 2018. The horizontal band inside the boxes marks the median, the lower and upper lines of the boxes represent the first and the third quartiles, respectively. The extended whiskers are the most extreme data points (while the individual points represent outliers).

3.2.2 SPM, and TotHg analysis in POM

Overall, rivers had higher SPM, Particulate TotHg and Aqueous TotHg concentrations than Adventfjord stations during the study period (Figure 5).

SPM concentration in Adventfjord water had the highest values in the inner fjord in July (Figure 5A). TotHg concentration in SPM (SPMTotHg) were highest in inner fjord in June and July and lowest in the outer fjord in June (Figure 5B). Values were also highest in surface waters in June (Figure Appendix A5). Particulate TotHg (PartTotHg) concentrations were highest in the inner fjord in July and lowest in the outer fjord in June and July and at all stations in April, May and August (Figure 5C). Values were also highest in surface waters in June and in July (Figure Appendix A5). There was a significant positive relationship between Particulate carbon and PartTotHg concentrations in Adventfjord surface waters ($R^2 = 0.8$; $p < 0.01$) (Figure Appendix A6). Aqueous TotHg concentration were highest at all stations from June to August (Figure 5D). Values were also highest in surface waters in June, July and August (Figure Appendix A5).

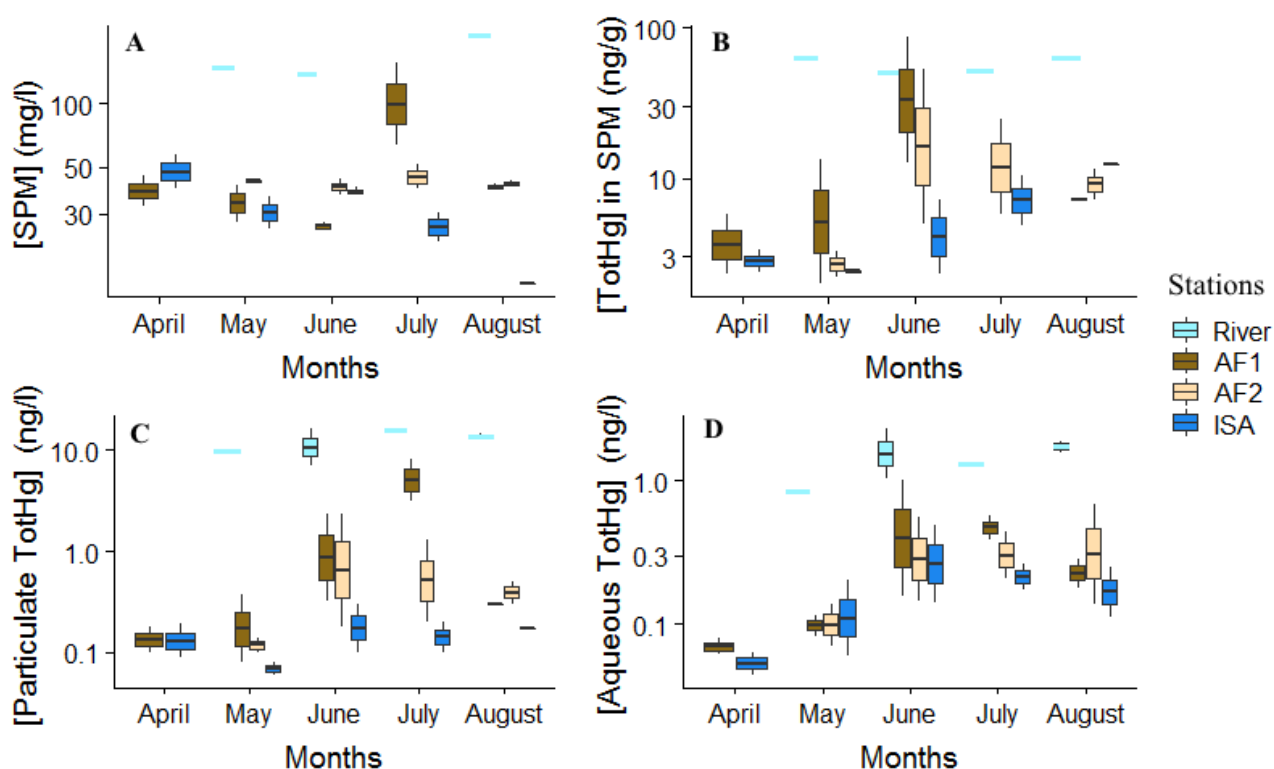


Figure 5 : Boxplots of (A) SPM concentration, (B) TotHg concentration in SPM, (C) Particulate TotHg concentration, (D) Aqueous TotHg concentration in POM from water samples (fjord : $n=28$; river : $n=8$) taken at the surface and 15m deep in the 3 stations (AF1, AF2, ISA) from April to August 2018 ; and in water samples from Adventelva and Longyearelva (« River ») from May to August 2018. Data presented on a log₁₀ scale. The horizontal band inside the boxes marks the median, the lower and upper lines of the boxes represent the first and the third quartiles, respectively. The extended whiskers are the most extreme data points (while the individual points represent outliers).

Surface waters from inner and middle fjord were characterized by low salinity and high TotHg values over the summer period compared to deep waters and outer fjord (Figure 6). The inner fjord had a thin layer of freshwater at the surface in July, whereas it was not the case in outer fjord (Figure 7). In July, inner fjord, both surface and deep waters, were characterized by high C:N ratio and PartTotHg values (Figure 6). Turbidity and Particulate carbon were positively correlated with Particulate TotHg and Aqueous TotHg concentrations. (*Table Appendix A2*).

A redundancy analysis (RDA) revealed that Depth and Station were the main explanatory variables, explaining 14 % (10 % and 4% respectively) of the variance in the dataset (RDA, Anova test, $p < 0.01$), whereas Month did not explain any variability in the dataset (RDA, Anova test, $p > 0.1$).

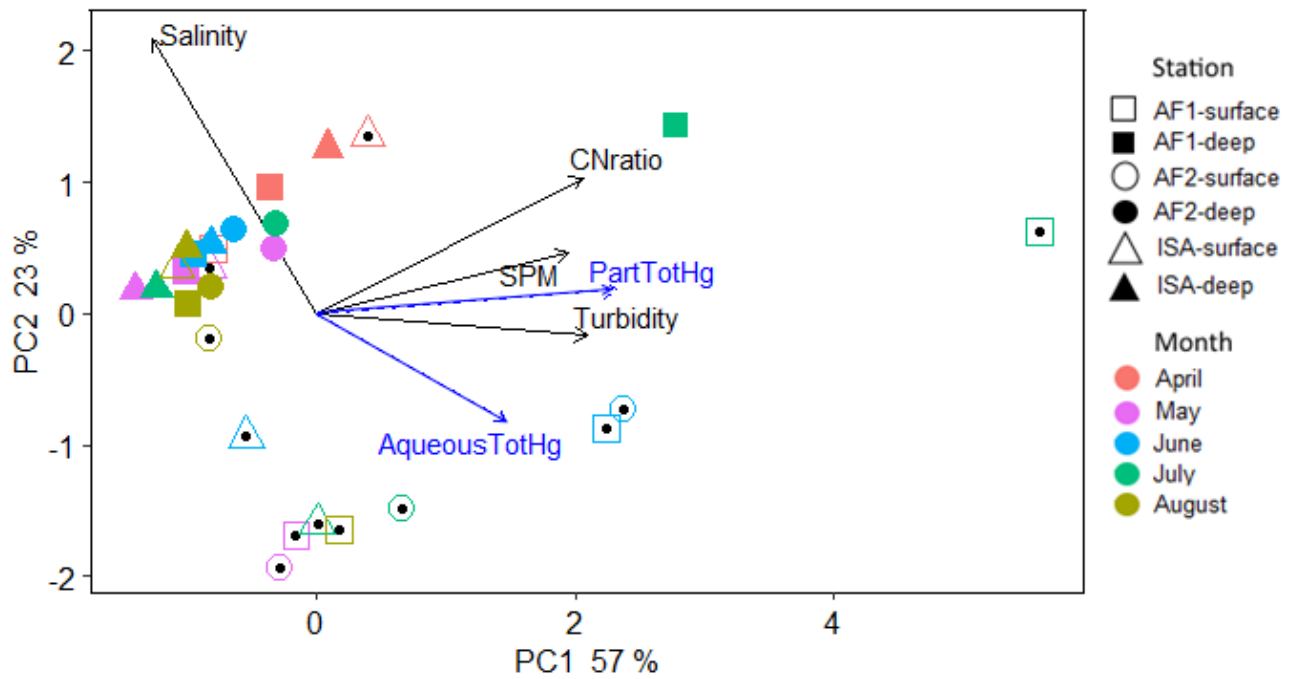


Figure 6 : Principal Component Analysis (PCA) of physicochemical parameters (response variables shown as black vectors) measured in water samples (surface and 15m) (shown as points ; n=28) taken at the 3 stations (AF1, AF2, ISA) from April to August 2018. The two first components explained 80% of the total variance. CNratio : C :N ratio as a molar ratio ; PartTotHg : Particulate TotHg concentration (ng/L) ; SPM : SPM concentration (mg/L) ; AqueousTotHg : aqueous TotHg (ng/L) ; Month of sampling are indicated by colors; Stations and sampling depth are indicated by shapes.

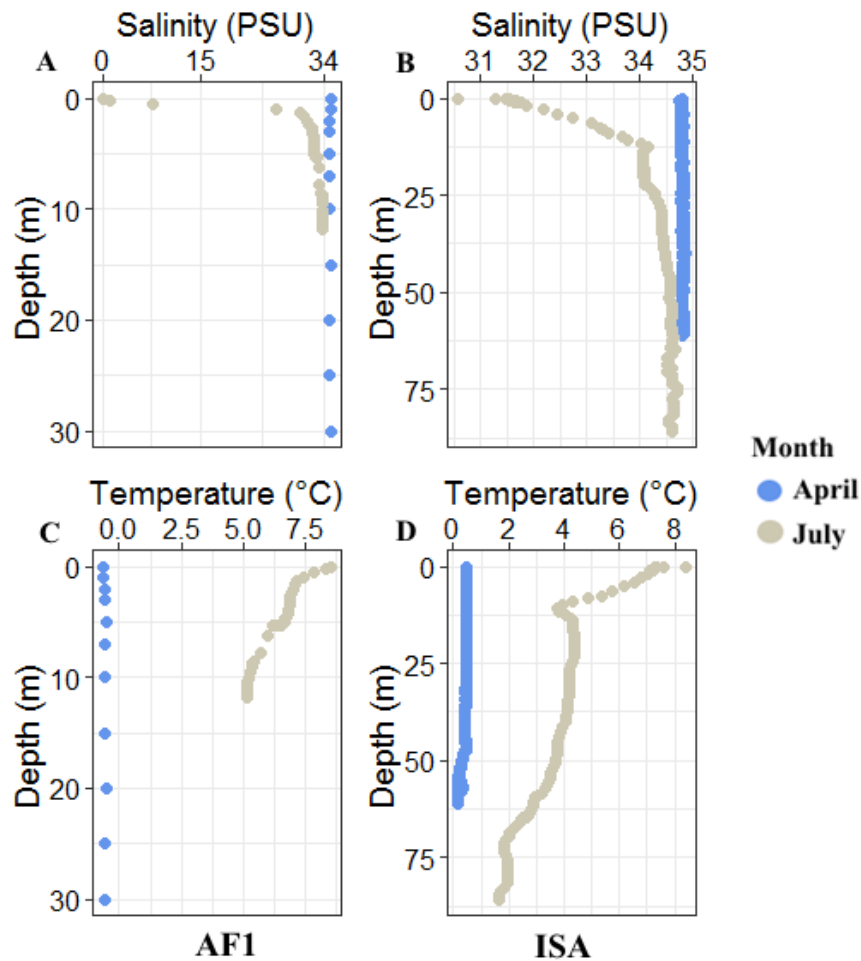


Figure 7: (A & B) Salinity (psu) and (C & D) Temperature (°C) data from CTD data in inner fjord (AF1) and outerfjord (ISA) in April and July 2018.

3.3 ZOOPLANKTON DATA ANALYSIS

3.3.1 Zooplankton diet

In April, *Oithona similis* and *Calanus* spp. dominated the biomass of zooplankton samples. In May, Cirripedia nauplii and Decapod zoea (benthic organisms) were dominant. *Calanus* spp. dominated the biomass of zooplankton samples in June, July and August. Macrozooplankton (Chaetognatha, Euphausiacea, *Clione limacina*, *Limacina helicina*, Fish larvae, Amphipod, Ctenophora) were mainly found in samples in July and August. Jelly plankton included the ctenophores *Mertensia ovum* and *Beroë cucumis*, and unidentified cnidarians (Tables Appendix A3, A4, A5 & A6).

There was no significant differences in $\delta^{13}\text{C}$ and $\delta^{15}\text{N}$ values between zooplankton samples from stations sampled on the same date (Kruskal-Wallis ; $p > 0.05$). Over the study period, zooplankton had higher $\delta^{13}\text{C}$ and $\delta^{15}\text{N}$ values than POM and followed the same seasonal variability (Figure 8).

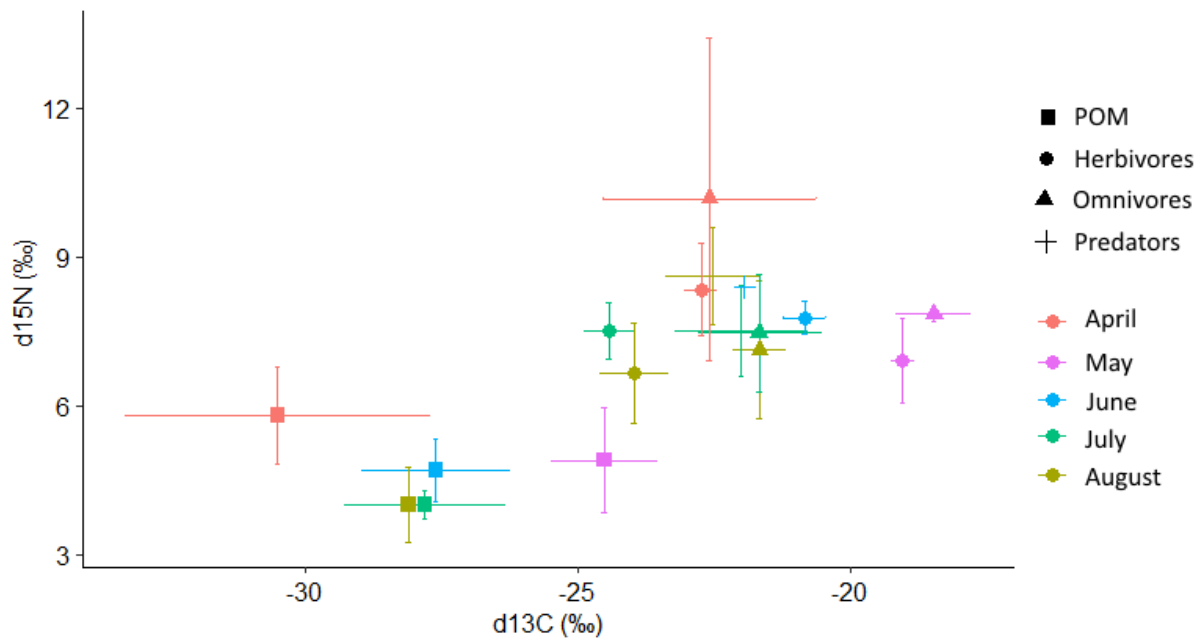


Figure 8: Biplot for $\delta^{13}\text{C}$ and $\delta^{15}\text{N}$ (mean and sd) in POM and zooplankton samples (« Herbivores », « Omnivores », and « Predators ») collected at the 3 stations in Adventfjord from April to August 2018.

$\delta^{13}\text{C}$ values in zooplankton samples ranged from -24.9 to -17.8 ‰ with significantly higher values in May than in April, July and August (Kruskal-Wallis $p < 0.01$; Pairwise Wilcoxon $p < 0.01$). There was a significant difference in $\delta^{13}\text{C}$ values between feeding category in July and in August with lower values in « Herbivores » than « Omnivores » and « Predators » (Kruskal-Wallis $p < 0.01$). There was no seasonal variability in « Predators » $\delta^{13}\text{C}$ values.

$\delta^{15}\text{N}$ values in zooplankton samples ranged from 5.82 to 12.31 ‰ but there was no significant seasonal variability. And there was no significant difference between feeding category across month (Figure 9).

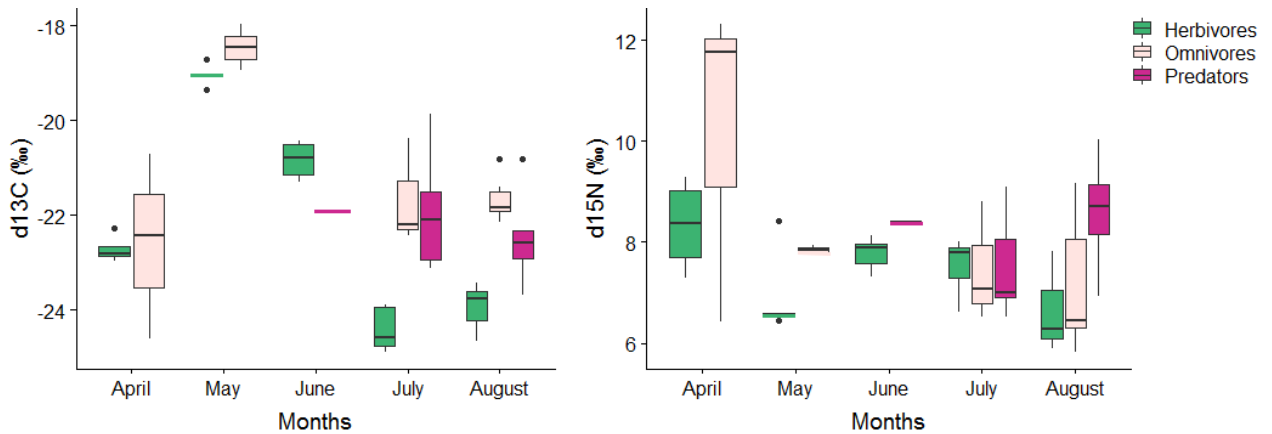


Figure 9 : Boxplots of $\delta^{13}\text{C}$ and $\delta^{15}\text{N}$ (‰) in zooplankton samples collected at the 3 stations in Adventfjord (AF1, AF2 and ISA) from April to August 2018. The horizontal band inside the boxes marks the median, the lower and upper lines of the boxes represent the first and the third quartiles, respectively. The extended whiskers are the most extreme data points (while the individual points represent outliers).

$\delta^{13}\text{C}_{\text{zooplankton}} - \delta^{13}\text{C}_{\text{POM}}$ values ranged from 3.2 to 12.4 ‰ with the highest values in April and the lowest in May (Kruskal-Wallis $p < 0.01$; Pairwise Wilcoxon $p < 0.01$). There was a significant difference in $\delta^{13}\text{C}_{\text{zooplankton}} - \delta^{13}\text{C}_{\text{POM}}$ values between feeding category in July and in August with lower values in « Herbivores » than « Omnivores » and « Predators » (Kruskal-Wallis $p < 0.01$). $\delta^{15}\text{N}_{\text{zooplankton}} - \delta^{15}\text{N}_{\text{POM}}$ values ranged from 0.3 to 6.2 ‰ with the highest values in July and August and the lowest in May (Kruskal-Wallis $p < 0.01$; Pairwise Wilcoxon $p < 0.01$). There was no significant difference in $\delta^{15}\text{N}_{\text{zooplankton}} - \delta^{15}\text{N}_{\text{POM}}$ between feeding category across month (Figure Appendix A7).

Over the study period, samples dominated by *O. similis* and amphipod had the highest $\delta^{13}\text{C}_{\text{zooplankton}} - \delta^{13}\text{C}_{\text{POM}}$ values, and samples dominated by cirripedia nauplii and decapod zoea the lowest ones (Figure 10A). Fish larvae and Chaetognatha had the highest $\delta^{15}\text{N}_{\text{zooplankton}} - \delta^{15}\text{N}_{\text{POM}}$ values, and samples dominated by cirripedia nauplii and decapod zoea the lowest ones (Figure 10B).

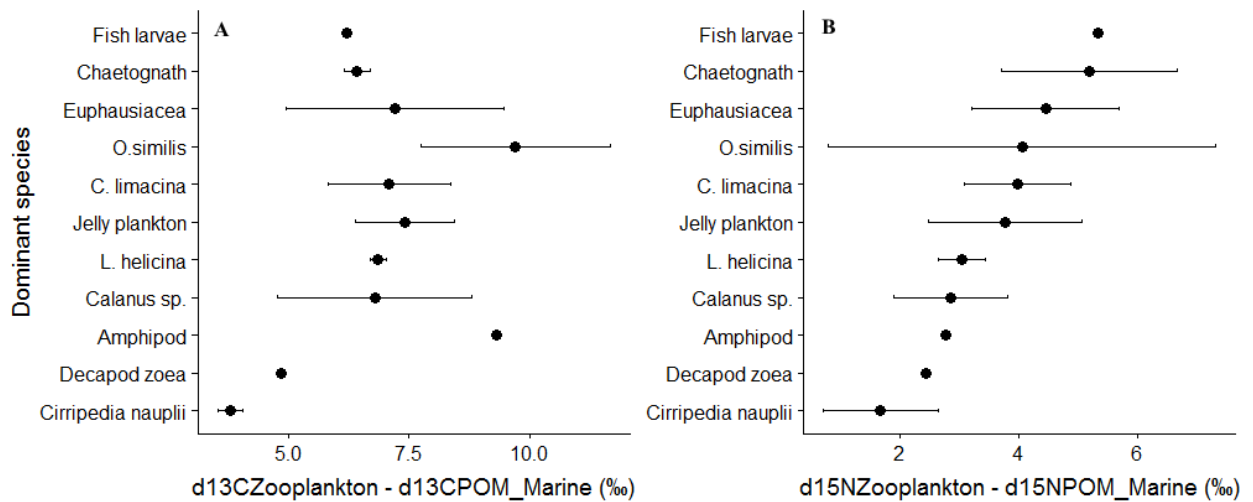


Figure 10 : Biplots of (A) $\delta^{13}\text{C}_{\text{Zooplankton}} - \delta^{13}\text{C}_{\text{POM}}$ and (B) $\delta^{15}\text{N}_{\text{Zooplankton}} - \delta^{15}\text{N}_{\text{POM}}$ (mean ; sd) in zooplankton samples with « Dominant species », sampled in the 3 stations from April to August 2018 (Fish larvae, n=2 ; Chaetognatha, n=2 ; Euphausiacea, n=3 ; *O. similis*, n=3 ; *C. limacina*, n=5 ; Jelly plankton, n=10 ; *L. helicina*, n=2 ; *Calanus* spp., n=13 ; Amphipod, n=1 ; Decapod zoea, n=1 ; Cirripedia nauplii, n=3).

FA analysis highlighted taxonomic specificity and seasonal variability in FA composition among « Herbivores » (Figure 11). Cirripedia nauplii (dominant in May samples) were characterized by a high n-3/n-6 ratio and $\sum\text{C20}$ PUFA content, and *Calanus* spp. (dominant in April, June, July and August samples) had a strong variability in their FA maker content across month. The RDA revealed Month as a significant explanatory variable, explaining 80 % of the variance in the data set (RDA, Anova test, $p < 0.01$).

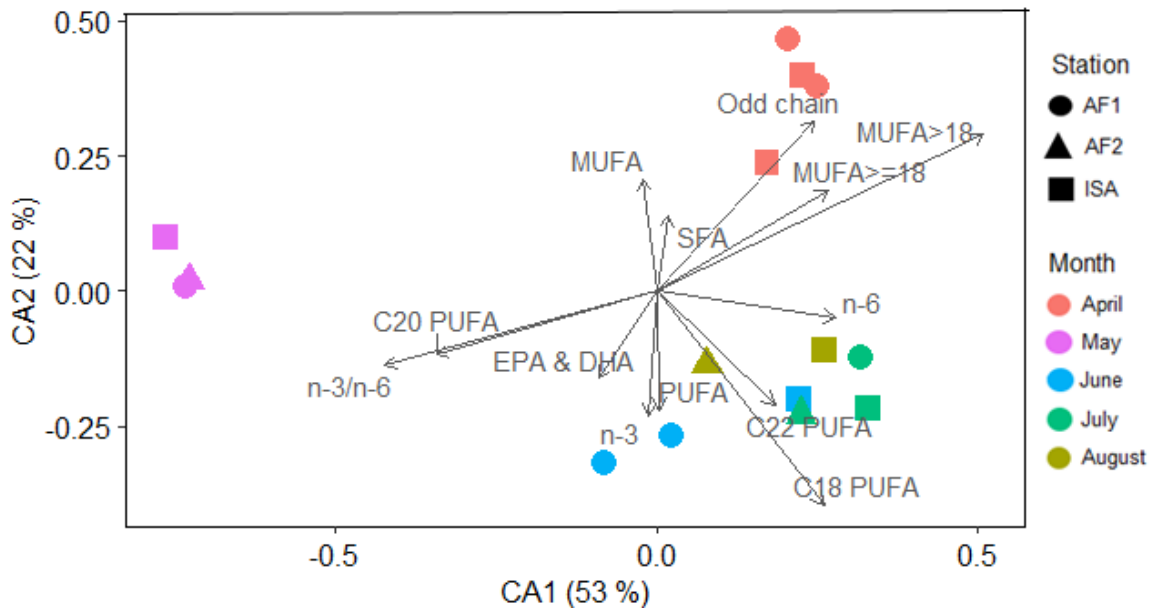


Figure 11 : CA biplot of data based on all 42 fatty acid analyzed in zooplankton samples taken at the 3 stations (AF1, AF2, ISA) from April to August 2018. The analyzed samples were dominated by Cirripedia nauplii in May and *Calanus* spp. in the other samples (n=15). The two axis explained 75% of the total variance. Only the summary metrics which were passively added to the CA are shown (\sum SFA ; \sum MUFA ; \sum PUFA ; \sum MUFA \geq 18 ; \sum MUFA>18 ; \sum C18 PUFA ; \sum C20 PUFA ; \sum C22 PUFA ; \sum EPA & DHA ; \sum n-6 ; \sum n-3 ; \sum Odd chain ; n-3/n-6).

Samples dominated by *Calanus* spp. had a strong seasonal variability in their FA composition (Figure 12). Samples from April were dominated by flagellates, ciliates and detritus diet markers (\sum SFA; \sum MUFA ; \sum MUFA \geq 18 ; \sum MUFA>18) and bacteria diet marker (\sum Odd chain). In June, samples showed a higher variability, with samples from inner and middle fjord dominated by \sum C20 PUFA ; \sum C22 PUFA ; \sum EPA & DHA and n-3/n-6, and the sample taken outer fjord more dominated by \sum C18 PUFA. Finally, July and August samples were dominated by \sum PUFA, \sum n-3 and \sum C18 PUFA. This suggest that marine phytoplankton biomarkers were dominant in *Calanus* spp. lipid profiles from June to August. The RDA revealed Month as the only significant explanatory variable, explaining 72 % of the variance in the data set (RDA, Anova test, $p < 0.01$), whereas Station did not explain any variability in the dataset (RDA, Anova test, $p > 0.1$)

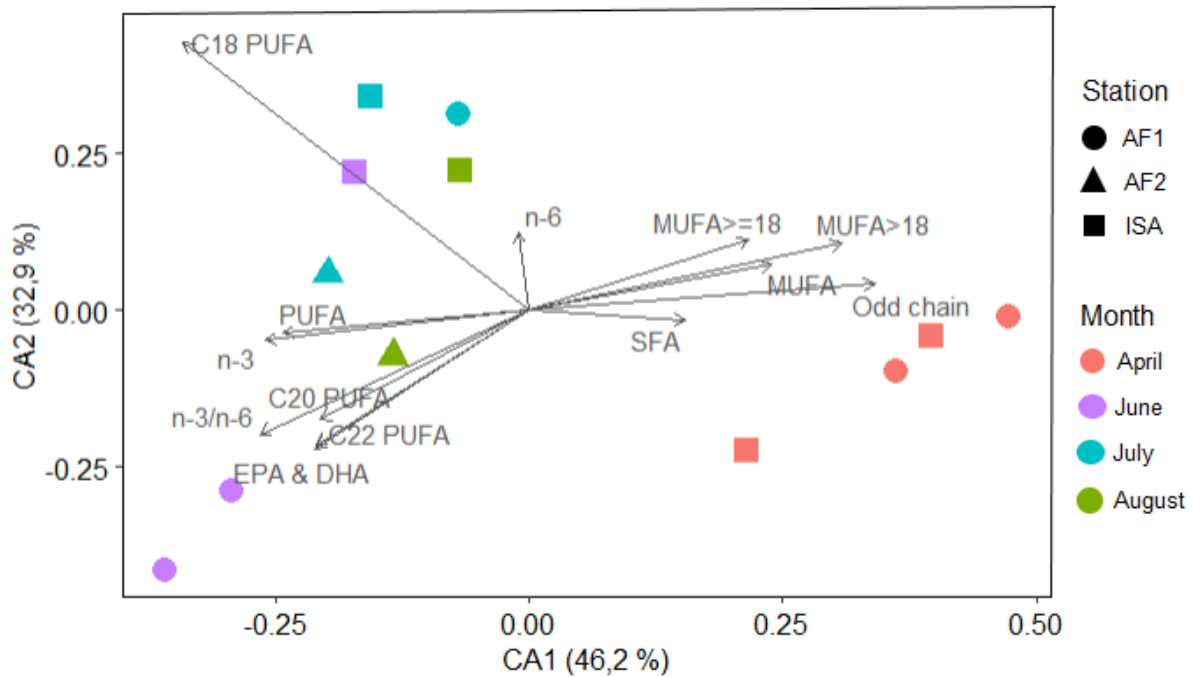


Figure 12 : CA biplot of data based on all 42 fatty acid analyzed in zooplankton samples taken at the 3 stations (AF1, AF2, ISA) from April to August 2018. The samples were dominated by *Calanus* spp (n=12). The two axis explained 79% of the total variance. Only the summary metrics which were passively added to the CA are shown : sums and ratio (\sum SFA ; \sum MUFA ; \sum PUFA ; \sum MUFA \geq 18 ; \sum MUFA>18 ; \sum C18 PUFA ; \sum C20 PUFA ; \sum C22 PUFA ; \sum EPA & DHA ; \sum n-6 ; \sum n-3 ; \sum Odd chain ; n-3/n-6).

3.3.2 Total Mercury (TotHg) and Methyl Mercury (MeHg) concentration in zooplankton

There was no significant variation between stations in TotHg-, MeHg- concentrations and MeHg :TotHg ratio in zooplankton samples taken on the same date (Kruskal-Wallis $p > 0.1$).

TotHg concentration in zooplankton samples ranged from 1.3 to 15.1 ng/g, with the lowest values in April (Kruskal-Wallis $p < 0.01$; Pairwise Wilcoxon $p < 0.01$). There were significant differences in TotHg concentration between feeding category with higher values in « Herbivores » in April and August (Kruskal-Wallis $p < 0.05$) and « Omnivores » and « Predators » had a large variability between samples in August (Figure 13A).

MeHg concentration in zooplankton samples ranged from 0,01 to 14.8 ng/g, with the lowest values in April and May, and highest values in July and August (Kruskal-Wallis $p < 0.01$; Pairwise Wilcoxon $p < 0.01$). There were significant differences in MeHg concentration between feeding category with higher values in « Herbivores » in April and higher values in

« Predators » in August (Kruskal-Wallis $p < 0.05$). « Omnivores » and « Predators » had a large variability between samples in July and August (Figure 13B).

MeHg :TotHg ratio (in %) in zooplankton samples ranged from 0.5 to 45.4 % with the lowest values in April and May, and highest values in July and August (Kruskal-Wallis $p < 0.01$; Pairwise Wilcoxon $p < 0.01$) (Figure 13C).

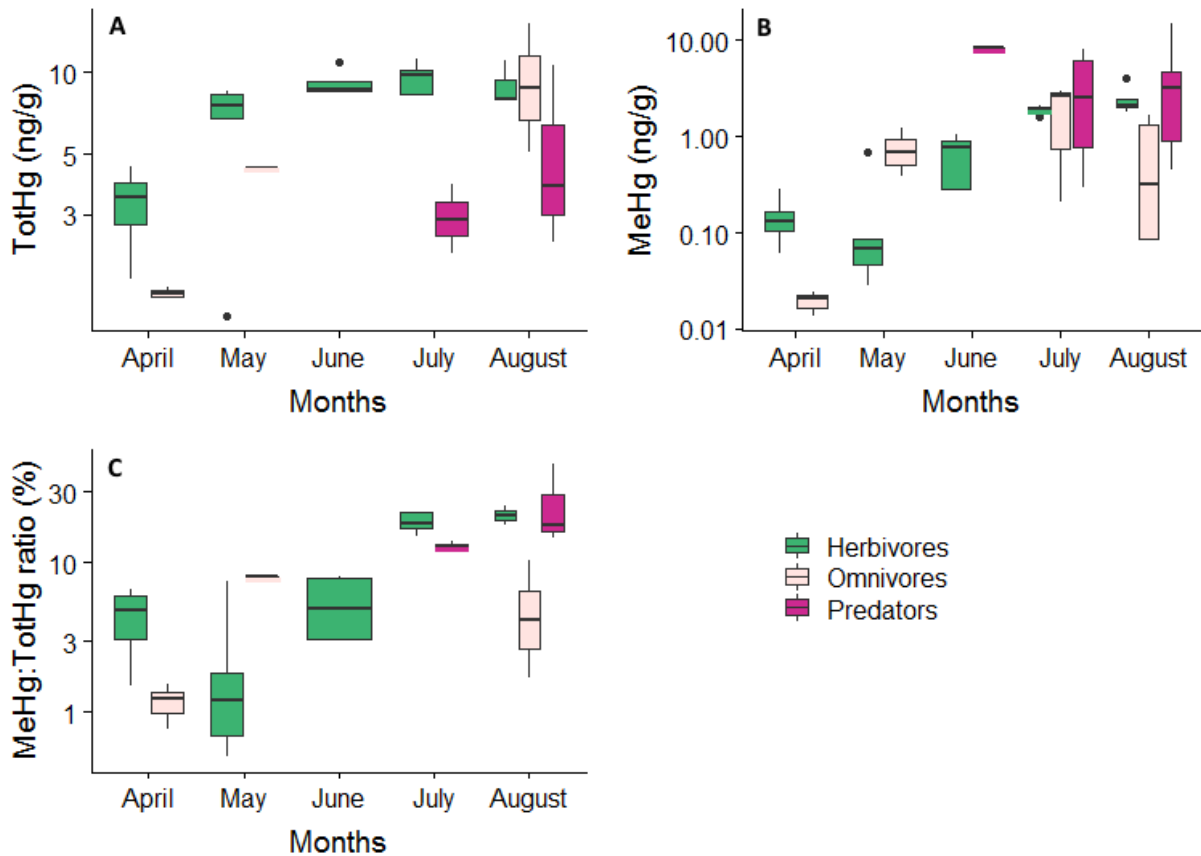


Figure 13 : Boxplots of (A) TotHg, (B) MeHg concentrations and (C) MeHg :TotHg ratio in zooplankton from samples collected at the 3 stations from April to August 2018. (TotHg : $n = 28$; MeHg : $n = 45$; MeHg :TotHg: $n = 28$). The horizontal band inside the boxes marks the median, the lower and upper lines of the boxes represent the first and the third quartiles, respectively. The extended whiskers are the most extreme data points (while the individual points represent outliers).

There were a strong seasonality in diet markers ($\delta^{15}\text{N}_{\text{zooplankton}} - \delta^{15}\text{N}_{\text{POM}}$ and $\delta^{13}\text{C}_{\text{zooplankton}} - \delta^{13}\text{C}_{\text{POM}}$ values and FA) and MeHg- and TotHg- concentrations in « Herbivores » (Figure 14). Sums of PUFAs, Carbon and Nitrogen concentration were positively correlated with TotHg concentration in « Herbivores ». And TotHg was negatively correlated with the sums of MUFA

and SFA (Table Appendix A7). The positive linear relationship between PUFA and TotHg concentration in « Herbivores » samples from April to August at the 3 stations ($R^2 = 0.6$; $p < 0,01$), suggest that these two variables are linked. (Figure Appendix A8). Aqueous TotHg and sum of PUFAs were also positively correlated with MeHg concentration in « Herbivores » and sum of MUFAs were negatively correlated MeHg (Table Appendix A7).

The RDA revealed Month as the only significant explanatory variable, explaining 38 % of the variance in the data set (RDA, Anova test, $p < 0.05$), whereas Station did not explain any variability in the dataset (RDA, Anova test, $p > 0.1$)

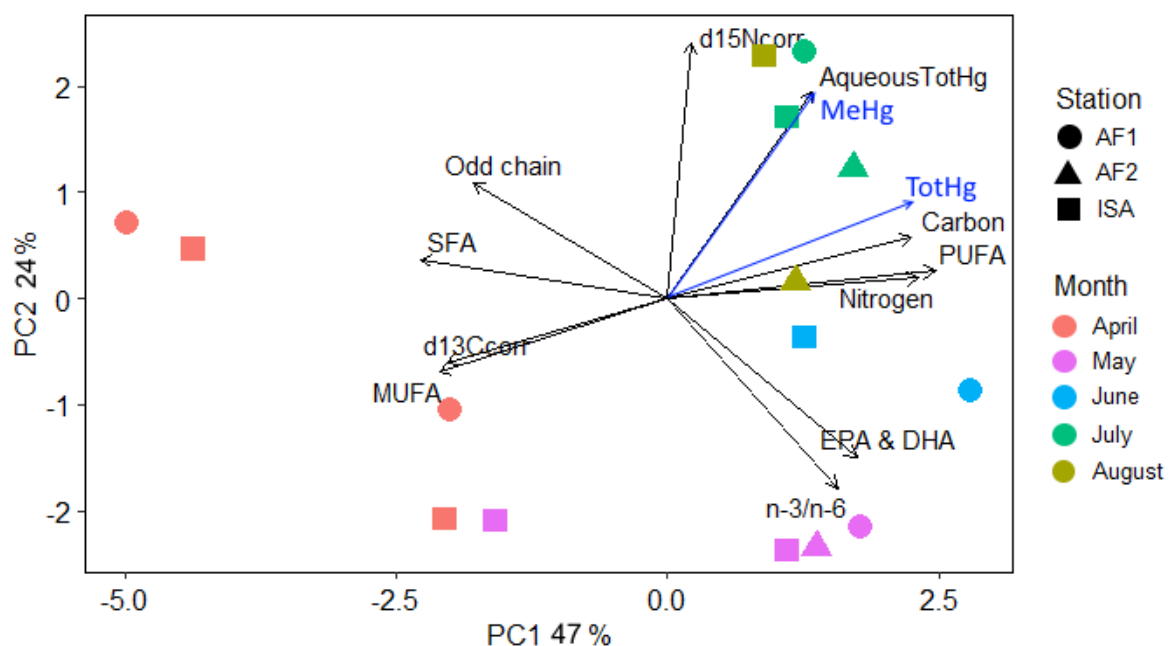


Figure 14 : Principal Component Analysis (PCA) of Aqueous TotHg concentration in the fjord water, Stable isotopes $\delta^{13}\text{C}$ and $\delta^{15}\text{N}$, Fatty Acid diet markers, Carbon and Nitrogen concentration and TotHg and MeHg concentrations (response variables shown as black vectors) measured in « Herbivores » ($n=15$; shown as points) taken in the 3 stations (AF1, AF2, ISA) from April to August 2018. The two first components explained 71% of the total variance. AqueousTotHg : aqueous TotHg (ng/l) ; $d^{13}\text{C}_{\text{corr}}$: $\delta^{13}\text{C}_{\text{zooplankton}} - \delta^{13}\text{C}_{\text{POM}}$ (‰) ; $d^{15}\text{N}_{\text{corr}}$: $\delta^{15}\text{N}_{\text{zooplankton}} - \delta^{15}\text{N}_{\text{POM}}$ (‰) ; Carbon and Nitrogen concentration (ug/mg). Month of sampling are indicated by colors; Stations are indicated by shapes.

There was a strong seasonal and taxonomic variability in diet markers and Hg concentrations in zooplankton samples (Figure 15). The first axis (PC 1) showed the seasonal variability with summer samples characterized by higher MeHg and TotHg concentrations and lower $\delta^{13}\text{C}_{\text{zooplankton}} - \delta^{13}\text{C}_{\text{POM}}$ values, and the second axis 2 (PC2) showed variability across trophic

levels. Samples dominated by Cirripedia nauplii were characterized by lower MeHg concentration than Fish larvae and samples dominated by *O. similis* were characterized by lower TotHg concentration than *Calanus* spp. (Figure 15). Aqueous TotHg, Carbon and Nitrogen concentrations in zooplankton were positively correlated with TotHg- and MeHg-concentrations in zooplanktons (Table Appendix A8). There was a positive linear relationship between Aqueous TotHg and MeHg concentration in zooplankton ($R^2 = 0.6$; $p < 0.01$) (Figure Appendix A9) and a negative linear relationship between $\delta^{13}\text{C}_{\text{zooplankton}} - \delta^{13}\text{C}_{\text{POM}}$ and TotHg concentration in zooplankton samples in July ($R^2 = 0.9$, $p < 0.01$) (Figure Appendix A10).

The RDA revealed that Month and Feeding Category were the main explanatory variable, explaining 72 % (55 and 17% respectively) of the variance in the data set (RDA, Anova test, $p < 0.01$), whereas Station did not explain any variability (RDA, Anova test, $p > 0.1$). In contrast to what would be expected, there was no linear relationship between $\delta^{15}\text{N}$ and TotHg- or MeHg-concentrations in zooplankton, over the study period or even by month (Table Appendix A9), but as shown in the PCA (Figure 15), « Predators » such as Fish larvea and *C. limacina* had the highest mean in TotHg and MeHg concentrations respectively over the study period (10,7 and 9,5 ng/g respectively) (Table Appendix A10).

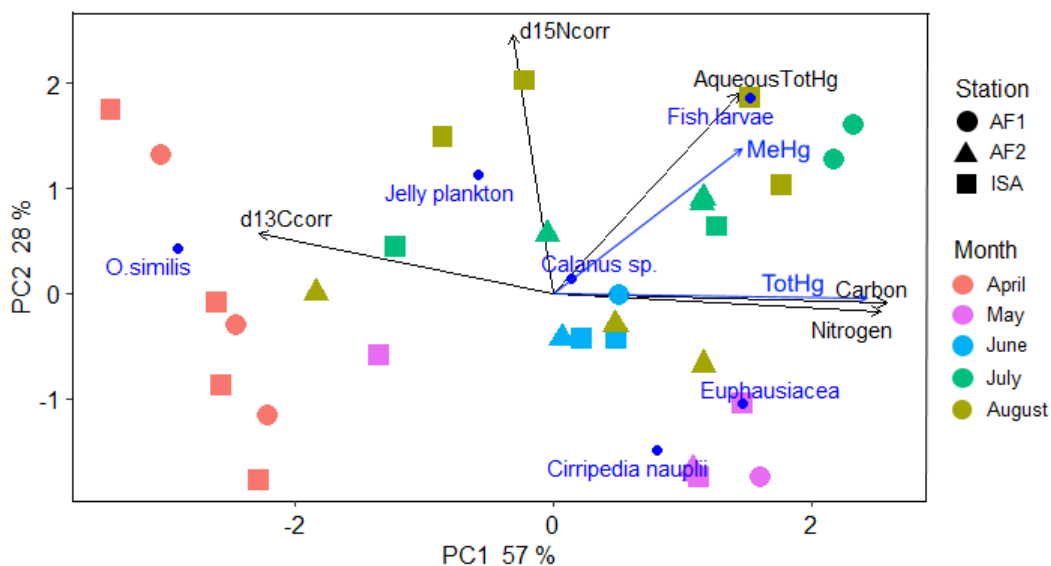


Figure 15 : Principal Component Analysis (PCA) of Aqueous TotHg concentration in the fjord water, Stable isotopes $\delta^{13}\text{C}$ and $\delta^{15}\text{N}$, Carbon and Nitrogen concentration and TotHg and MeHg concentration (response variables shown as black vectors) measured in zooplankton samples ($n = 30$; shown as points) taken in the 3 stations from April to August 2018. The two first components explained 85% of the total variance. AqueousTotHg : aqueous TotHg (ng/L) ; $d^{13}\text{C}_{\text{corr}}$: $\delta^{13}\text{C}_{\text{zooplankton}} - \delta^{13}\text{C}_{\text{POM}}$ (‰) ; $d^{15}\text{N}_{\text{corr}}$: $\delta^{15}\text{N}_{\text{zooplankton}} - \delta^{15}\text{N}_{\text{POM}}$ (‰) ; Carbon and Nitrogen concentration (ug/mg). Month of sampling are indicated by colors; Stations are indicated by shapes.

4-DISCUSSION

4.1. SEASONAL RIVER INPUTS IN ADVENTFJORD

In this study, Adventelva water level was more linked to air temperature than to rainfall events, suggesting that during summer, rivers were mainly fed by snow, glaciers and permafrost melting water. These results are consistent with other studies that have identified winter precipitation and spring and summer air temperature as important drivers of summer river discharge (Peterson et al. 2002 ; Ye et al. 2004). With a mean annual precipitation (1971- 2000) measured at the airport weather station in Svalbard of 196 mm, rainfall are not so important in this Arctic desert area, but this could change with expected heavy rainfall occurring even midwinter with climate change (Hanssen-Bauer et al. 2019).

During the summer (in June and July), Adventelva and Longyarelva contained 2 fold-higher SPM, 10 fold-higher Hg and C :N ratio 4 fold-higher than Adventfjord waters. This suggest that Adventelva was an important source of TotHg, Carbon and SPM for Adventfjord. The positive linear relationships between SPM and Particulate TotHg in river water samples, and the positive linear relationship between Particulate TotHg and Particulate carbon concentrations in surface water in Advenfjord are consistent with observations from several other Arctic river systems, where Hg inputs are strongly linked to inputs of suspended sediments and Particulate Carbon (Balogh et al. 1998 ; Coquery et al. 1995).

Although seasonality, is a driver of river water chemistry, the variability in PartTotHg concentration between Adventelva, Longyarelva and tributaries across months, could possibly be explained by the geomorphology of the catchment, with Longyarelva and tributaries rivers having higher SPM and PartTotHg concentrations and a steeper slope than Adventelva (*Figure Appendix A11*). Leitch et al. (2007), observed that tributaries draining mountainous terrain to the west of the Mackenzie river had a higher Particulate TotHg concentration than those on the flatter east side.

The peak river discharge occurred in June and July, with highest concentration in SPM, TotHg and Particulate Carbon and lower salinity in inner Adventfjord surface waters. This is consistent with observations from other studies where dissolved and particulate Hg concentration were much higher during the spring and summer season than the rest of the year (Leitch et al. 2007 ; Schuster et al. 2011).

Although deep waters were less impacted by river inputs, probably because of the freshwater layer at the surface creating a stratification (Fisher et al. 2012), deep water in the inner fjord had a little increase in Particulate TotHg and SPM concentrations in July. This may be explained by the fact that the innermost fjord station was very shallow (< 20 m), and likely strongly influenced by turbulent resuspension of sediments (Zajączkowski et al. 2007).

Climate change perspective

In the context of climate change, the increase in air temperatures should produce a shift toward earlier onset of spring runoff (Tan et al. 2011). Also storms and rainfall are expected to increase (Hanssen-Bauer et al. 2019), leading to larger surface runoff with mobilization of large amounts of carbon and Hg stored in Arctic soils (Schuster et al. 2011). In addition to MeHg directly discharged in fjord by rivers, inputs of large amounts of inorganic Hg and DOC, may exacerbate the production of bioavailable MeHg (Schartup et al. 2015, Schuster et al. 2011).

Influence of river inputs on POM composition

POM composition in Adventfjord changed across months and was impacted by river inputs. The low Chl a concentration and the high $\delta^{15}\text{N}$ values in POM samples from April in Adventfjord suggest that heterotrophs (ciliates, flagellates), detritus and bacteria may have been an important component of the POM at that time. Degradation of organic material by bacteria can lead to increased $\delta^{15}\text{N}$ of POM, since consumers are enriched in $\delta^{15}\text{N}$ relative to their diet (Hoch et al 1996 ; Søreide et al. 2006) and pelagic-POM from detritus-rich waters also tends to be enriched in $\delta^{15}\text{N}$ (Søreide et al. 2006). Low C :N ratios are typically observed where phytoplankton contribution to the POM is high, and where N is not limiting (Bates et al. 2005 ; Søreide et al. 2006). In contrast, high C :N ratios are typical of systems strongly influenced by inputs of terrestrial organic matter (Bates et al 2005 ; Søreide et al. 2006). Also, higher $\delta^{13}\text{C}$ values have been observed during the peak bloom phase (Tamelander et al. 2009). In this study, the highest $\delta^{13}\text{C}$ values were measured in May. This, together with an increase in Chl a concentration and a low C :N ratio, suggest that phytoplankton bloom occurred at this time. The highest C :N ratios, observed in inner fjord in June and July, suggest a greater contribution of terrestrial particulates to the POM during the peak river discharge.

The relatively high concentration of Chl a in all sampled stations from June to August (ranging from 0.2 to 3.0 $\mu\text{g/l}$), suggest that phytoplankton was present in the fjord during the whole study period, likely due to advection processes occurring in Adventfjord (Kubiszyn et al. 2017). The decrease of $\delta^{13}\text{C}$ and $\delta^{15}\text{N}$ values from May to August (with the lowest values : -29,4‰ and 3,6 ‰ in July and -29,2‰ and 3,1 ‰ in August) can partly be explained by a terrestrial carbon source and nitrogen depleted POM from river inputs (Kuzyk et al. 2010). The variability in $\delta^{13}\text{C}$ and $\delta^{15}\text{N}$ values could also be explained by the fact that differences in phytoplankton taxonomy, growth and cell size can lead to strong changes in $\delta^{13}\text{C}$ values across months (Fry et al. 1991 ; Post 2002 ; Tamelander et al 2009).

Defining carbon source in POM based in $\delta^{13}\text{C}$ only, is challenging because of the relative narrow range in $\delta^{13}\text{C}$ values (Raymond et al. 2007) due to many sources with potentially overlapping and seasonally variable $\delta^{13}\text{C}$ values. In this study, there also was a narrow range between the two endpoints, with the river $\delta^{13}\text{C}$ values ranging from -26,49‰ to -25,38‰ and the outer fjord $\delta^{13}\text{C}$ values ranging between -24,89‰ and -22,88‰.

Therefore, combining stable isotope data with other parameters such as the C:N ratio and the Chl a concentration, is important to get a more accurate picture of the system.

Although there was a gradient in C:N ratio in POM from inner to outer fjord , there was no significant differences between stations for Chl a, $\delta^{13}\text{C}$ and $\delta^{15}\text{N}$ data. This suggests that Adventfjord is a dynamic system, with water currents, tides and advection processes, moving phytoplankton and terrestrial derived river inputs from one part to another part of the fjord, and mixing marine and terrigenous organic matter.

Limitations

Results from this study only reflect monthly snapshots of conditions in the river and the fjord. Indeed, as previously mentioned, although precipitation did not affect much river water level, it may cause variability in river and fjord water composition from one day to the next. For examples, the heavy rainfall that occurred the day after our sampling in August (19/08/19 : 19 mm), led to an extensive river plume covering the whole of Adventfjord, which was very different from our visual observations on the day of sampling, where the plume only covered a limited extent of the fjord. Observations in the Minnesota river suggested that river

composition in mercury and particulates displayed a large variability in response to snowmelt and precipitation runoff (Balogh 1998).

4.2 INFLUENCE OF RIVER INPUTS ON ZOOPLANKTON DIET

When studying an ecosystem with several carbon sources (e.g. marine vs. terrestrial), it is important to take into account the strong variability in $\delta^{13}\text{C}$ and $\delta^{15}\text{N}$ at the base of the food web. Without a reliable estimation of baseline $\delta^{13}\text{C}$ and $\delta^{15}\text{N}$ in each system, it would not be possible to determine if the $\delta^{13}\text{C}$ and $\delta^{15}\text{N}$ values in organism reflect changes in carbon flow and changes in foodweb structure or just variation of the baseline. Furthermore, the high temporal variation in $\delta^{13}\text{C}$ and $\delta^{15}\text{N}$ of primary producers and detrital energy sources may also complicate the study of isotopic signatures of consumers (Post 2002).

The lack of spatial gradient in zooplankton $\delta^{13}\text{C}$ and $\delta^{15}\text{N}$ values across the fjord can be explained by the fact that this system is dynamic, with water currents, tides and advection processes, moving zooplankton from one part to another part of the fjord.

Zooplankton samples followed the same seasonal trajectory as $\delta^{13}\text{C}$ values as POM, with highest values in May during the phytoplankton bloom and lowest values in July and August during and after the peak river discharge. This suggest that seasonal variability in $\delta^{13}\text{C}$ values in zooplankton was not caused by a real shift in zooplankton diet, but more by the seasonal variability in the baseline. The highest $\delta^{13}\text{C}$ values in zooplankton samples in May, could partly be explained by the fact that that these samples are dominated by Cirripedia nauplii, which may reflect benthic $\delta^{13}\text{C}$ isotopic values, which are known to be higher than in pelagic organisms (France 1995 ; Lavoie et al. 2010).

Zooplankton from all stations were enriched in $\delta^{13}\text{C}$ and $\delta^{15}\text{N}$ relative to POM for all months. It is well known that the consumers are enriched in $\delta^{15}\text{N}$ by relatively to the prey (Post 2002 ; Minagawa et al. 1984). The enrichment in $\delta^{13}\text{C}$ can be explained by the fact that POM is a mix of detritus, phytoplankton, heterotrophs, and bacteria (Rau et al. 1990), while many zooplankton taxa are selective feeders (DeMott et al. 1988 ; Paffenhöfer et al. 1988). Thus

POM composition does not necessarily reflect zooplankton diet (Del Giorgio et al. 1996). In marine systems, zooplankton are enriched in $\delta^{13}\text{C}$ compared to POM (Del Giorgio et al. 1996 ; Fry et al. 1991) because they preferably feed on higher $\delta^{13}\text{C}$ sources such as phytoplankton (which often has $\delta^{13}\text{C}$ values of approximately -20‰ – Post. 2002) (Del Giorgio et al. 1996 ; Fry et al. 1991 ; Post. 2002 ; Sørense et al. 2006).

The higher $\delta^{13}\text{C}$ values in zooplankton compared to marine POM (that we assume to be mainly phytoplankton derived) from May to August, suggest that « Herbivores » and « Omnivores » selectively fed on phytoplankton rather than on other carbon sources, even during periods of high river discharge. In addition to stable isotope data, Fatty Acid diet markers analysis supported the previous statement, also suggesting that « Herbivores » mainly fed on phytoplankton from May to August and relied on heterotrophs (bacteria, ciliates, flagellates) and detritus in April. On the other hand, the temporal variability in zooplankton samples $\delta^{13}\text{C}$ values, with lower values in July and August, suggest that zooplankton may have included some terrestrial carbon source in their diet during the summer. This may especially be the case for « Herbivores », which had the lowest $\delta^{13}\text{C}_{\text{zooplankton}} - \delta^{13}\text{C}_{\text{POM}}$ values and lowest $\delta^{13}\text{C}$ values in July and August, that have been associated with terrigenous organic carbon (Schell et al. 1998). « Herbivores » samples in June, July and August were dominated by *Calanus* spp. Although, Calanoid copepods are known to be selective suspension feeders, in freshwater systems they have been found to include terrestrial energy sources in their diet where phytoplankton availability is low relative to allochthonous particles (Poste et al. 2019, Berggren et al. 2014).

Limitations of diet markers

Some challenges can be met when using stable isotope data to assess diet. Firstly, each organism's tissues have a different turnover and a different fractionation factors, and thus different isotope values (Hobson et al. 1992 ; MacNeil et al. 2006). For example, lipid rich tissues have a faster turnover rate (Graeve et al. 2005 ; Tieszen et al. 1983). Furthermore, individual organisms can have different enrichment in stable isotope, depending on their age (Overman et al. 2001) or metabolism (Gaye-Siessegger et al. 2004 ; Focken et al. 1998).

In this study, samples dominated by « Omnivores » and « Predators » did not show any significant differences in $\delta^{13}\text{C}$ values between months. This could be explained by the fact that

these are longer-lived animals with longer tissue turnover times, which may lead to tissue $\delta^{13}\text{C}$ values that do not reflect their current diet. Although the intensive feeding and growth during the spring bloom may lead to rapid tissue turnover and thus a rapid incorporation of phytoplankton carbon (and a shift to $\delta^{13}\text{C}$ values that reflect phytoplankton) in « Herbivores », « Omnivores » and « Carnivores » are likely to incorporate POM signatures more slowly due to lower tissue turnover (Søreide et al. 2006). Overall, the $\delta^{13}\text{C}$ values ranged from from -24,6‰ to -18,0‰ and from -23,7‰ to -19,9‰ for « Omnivores » and « Predators », respectively. This may suggest that phytoplankton were also a major food source for these species (via prey), as it has been shown that higher $\delta^{13}\text{C}$ values are associated with a marine carbon source (Schell et al. 1992) .

The use of summary metrics in the analysis of zooplankton FA profiles can also be challenging. Although it's an easy way to get an overview and assess zooplankton diet according to general diet markers, some food source could be misread and left besides. In this study, this is the case for terrestrial diet markers which include SFA>C20, 18:2(n-6) and 18:3(n-3) (Budge et al. 1998 ; Dalsgaard J. et al. 2003), and that were mixed with other SFAs and PUFAs in the Correspondance Analysis. Zooplankton samples dominated by « Herbivores » from June to August (n=8), had on average 3,6% of fatty acid diet marker representing terrestrial carbon source, which is consistent (although it is a small prorportion) with stable isotope analysis, suggesting that zooplankton included some allochtonous carbon source during the strong river discharge period.

4.3 INFLUENCE OF RIVER INPUTS ON HG CONCENTRATION IN ZOOPLANKTON

TotHg and MeHg concentrations in zooplankton were much lower in Adventfjord than values found in pan-arctic coastal and open marine systems such as the Laptev sea, the Hudson Bay, the southern Beaufort sea, the Chukchi sea, or the Northern Baffin Bay, with TotHg concentrations in zooplankton ranging from 7,0 to 226 ng/g and MeHg ranging from 3,0 to 24 ng/g in summer (Foster et al. 2012 ; Pomerleau et al. 2016 ; Loseto et al. 2009 ; *Table Appendix A11*). This can be explained by the fact that the riverine inputs to Adventfjord are low as all rivers in the area are relatively small. On the other hand, Hg-concentrations were comparable

to those measured by Ruus et al. (2015) (Table 7), where TotHg concentrations ranged from 4,7 to 6,9 ng/g and MeHg concentrations from 2,3 to 4,4 ng/g during their study period from May to October 2007. Although Kongsfjorden is a glacier-influenced fjord, this system may share more characteristics with Adventfjord than more open coastal systems previously mentioned.

Table 7 TotHg, MeHg concentrations and MeHg :TotHg ratio (%) in zooplankton samples (mean \pm sd ; ng/g dry weight). Comparison between this study and Ruus et al. 2015 data with samples including copepods *Calanus hyperboreus*, *Calanus glacialis*, *Calanus finmarchicus*; krill/euphausiids; amphipods.

		April	May	June	July	August	October
Kongsfjord (Ruus et al. 2015)	[TotHg] (ng/g)	-	6.9 \pm 2.1	-	7.5 \pm 2.5	-	4.7 \pm 0.6
	[MeHg] (ng/g)	-	2.3 \pm 1.4	-	4.4 \pm 2.5	-	3.6 \pm 0.8
	MeHg:TotHg ratio (%)	-	39 \pm 13	-	59 \pm 23	-	78 \pm 19
Adventfjord (This study) With samples dominated by <i>Calanus</i> spp and Krill)		n=3	n=1	n=3	n=4	n=5	-
	[TotHg] (ng/g)	3.3 \pm 1.2	4.42	9.7 \pm 1.7	9.4 \pm 1.0	9.51 \pm 2.19	-
	[MeHg] (ng/g)	0.2 \pm 0.1	0.4	0.7 \pm 0.4	1.4 \pm 0.8	2.0 \pm 1.4	-
	MeHg:TotHg ratio (%)	4.5 \pm 2.3	8	0.06 \pm 0.04	18.4 \pm 3.3	20.9 \pm 3.1	-

Influence of river inputs and diet on Hg concentration in zooplankton

Diet is the most important pathway for Hg and MeHg uptake by zooplankton (Lawson et al 1998 ; Lee et al. 2017). The positive linear relationship between PUFAs and TotHg concentration in « Herbivores » highlights the same seasonal variation of both variables. In addition, the increase in TotHg concentration in zooplankton from the phytoplankton bloom in May, suggest that phytoplankton is an important source for TotHg. According to Pućko et al.

(2014) and Lee et al. (2017) physiological processes can contribute to an increase of TotHg concentration in metabolically active phytoplankton cells during bloom events. Evidence exist for both passive and active uptake of Hg in phytoplankton with Hg binding organic compounds, such as DOC, that are actively acquired by phytoplankton cells (Pickhardt et al 2007).

Results from this study suggested that seasonal variations in diet quality or food availability may cause variations in TotHg and MeHg concentrations in zooplankton. The lower TotHg and MeHg concentrations in zooplankton samples collected in April, in which *O. similis* and *Calanus* spp. were dominant, could be explained by life cycle. According to Pučko et al. (2014), TotHg concentration could be controlled by physiological factors such as egg laying and grazing activity (decrease and increase in TotHg concentration respectively). This lower TotHg and MeHg concentration in April zooplankton samples, could also be explained by lower Hg-concentrations in their food at this time. Indeed, there were relatively lower Particulate TotHg concentration in April than during the river discharge period in June and July in Adventfjord.

Several results from this study in Adventfjord suggest that river inputs enhanced TotHg and MeHg concentrations in zooplankton:

- The increase in TotHg and MeHg concentrations in zooplankton during the summer period
- The positive linear relationship between MeHg concentration in zooplankton and Aqueous TotHg concentration in water
- The negative linear relationship between $\delta^{13}\text{C}$ and TotHg concentration in zooplankton sampled in July

This is consistent with results from Pomerleau et al. (2016) that showed higher Hg concentration and lower $\delta^{13}\text{C}$ values in zooplankton from the southeastern Beaufort Sea compared to marine influenced areas. The Beaufort Sea is largely influenced by river inputs from the Mackenzie River. Also, several studies in boreal lakes have described how terrestrial inputs can enhance TotHg and MeHg concentration in water and in zooplankton that included terrestrial carbon sources in their diet (Poste et al. 2019, Wu et al. 2019). These processes could also occur in Arctic fjord estuaries during river discharge events like in Adventfjord. Ingestion of microbial food-web derived energy, which adds a trophic linkage within the food web, can increase Hg bioaccumulation in microzooplankton, mesozooplankton and macrozooplankton (Kainz et al. 2004 ; Pomerleau et al. 2016).

Because, TotHg and MeHg concentrations in « Predators » were only available in July and August, the seasonal variability in Hg concentration for this feeding category could not be explored.

Other factors influencing Hg concentration in zooplankton

Other factors such as the age of zooplankton could also explain the increase in TotHg and MeHg concentrations in zooplankton over the study period, due to bioaccumulation when zooplankton are getting older. In this study, *Calanus* spp. developmental stages in samples changed across the study period with a much higher proportion of CV stages in July and August than during the previous months (e.g CIV stages were dominant in June) (Figure Appendix A12).

In order to determine if river inputs have a real influence on seasonal Hg concentration in zooplankton, a non river influenced area should be used as a « control ». In this study, the outer fjord was expected to be less river influenced, creating a spatial gradient across the fjord, with the outer station used as a « control ». But because of this dynamic system with water currents, tides and advection processes, Adventfjord was a more homogeneous river influenced area than expected.

There were large differences in TotHg and MeHg concentrations between taxonomic groups and species, and samples dominated by « Predators » showed the largest variability. According to Foster et al. (2012), although predators exposure to contaminant is assumed to be relatively constant with time because of a lower seasonality in their diet compared to herbivores for example, differences in life cycle and age, period of fasting, and seasonal differences in diet among taxa, may affect contaminant concentration and induce a strong variability among predators. In this study, taxonomic group variability was mainly driven by the predator *C. limacina* which showed a 3 times higher MeHg concentration than Fish larvae, and a MeHg :TotHg ratio that was more than two times higher than that in *Calanus* spp. in August samples. These data are consistent with observations from other studies (Foster et al. 2012 ; Loseto et al. 2009 ; Pomerleau et al. 2016). This can be explained by the fact that until summer, *C. limacina* larvae grow to adult stage by utilising its storage lipids, and in July/August, lipids are depleted to about 10% dry mass due to maturation and reproduction (Böer et al. 2005). Therefore, this fasting period could enhance MeHg concentrations in *C. limacina* during the summer period, although food is available.

In contrast to what would be expected for a biomagnifying contaminant, there was no linear relationships between MeHg or TotHg concentration in zooplankton and $\delta^{15}\text{N}$ values over all the study period or even within month. Several previous studies have shown biomagnification processes occurring along marine zooplankton foodwebs (Foster et al. 2012 ; Fox et al. 2017 ; Pommerleau et al. 2016 ; Pućko et al. 2014,). However in this study, « Predators » such as Fish larvae and *C. limacina* had the highest TotHg- and MeHg- mean concentrations respectively over the study period. This lack of correlation between Hg and $\delta^{15}\text{N}$ values in Adventfjord may be explained by the fact that the fjord is a very dynamic system (strong seasonality in baseline values and different tissue turnover times for zooplankton at different trophic levels) and it makes it difficult to characterize trophic interactions and quantify Hg bioaccumulation/biomagnification using stable isotope.

5. CONCLUSION

This study highlighted the seasonal variability in Adventfjord physicochemistry, and in zooplankton diet and Hg and MeHg concentrations.

Results suggested that rivers were mainly fed by melt water, and that rainfall were not so important in this Arctic desert area (although this could change with climate changes). TotHg, SPM concentrations and C :N ratios in rivers were significantly higher than in Adventfjord, and river inputs had impact in inner fjord during the main river discharge period in June and July. However, strong tidal currents and a lack of sill in Adventfjord allowed for a rapid mixing of river inputs throughout the fjord. Zooplankton communities were relatively homogenous through the fjord. Determination of zooplankton diet was challenging due to the seasonal variability in baseline $\delta^{13}\text{C}$ and $\delta^{15}\text{N}$. River inputs appear to have affected zooplankton diet, with some evidences of terrestrial energy source included in zooplankton diet during the main river discharge period. However, phytoplankton was the most important food source for zooplankton for nearly all sites and study dates. Hg- and MeHg-concentrations in zooplankton increased over summer. Several explanations were suggested such as river inputs, or zooplankton getting older and accumulating over the summer. The lack of correlation between $\delta^{15}\text{N}$ values and Hg-concentrations in zooplankton was explained by the fact that Adventfjord is a very dynamic system in which it seems difficult to characterize trophic interactions and quantify Hg bioaccumulation/biomagnification using stable isotope.

Although river discharge is limited because the rivers are relatively small compared to larger pan-Arctic coastal systems, river inputs had some influence on Adventfjord water chemistry and biota. Because very little work has been done on small river systems, more studies should be done in the future, since they domiante much of the pan-Arctic coastline.

6. SUGGESTIONS FOR FURTHER STUDIES

The present study has revealed that river inputs have a significant impact on the Adventfjord system. However, a deeper understanding of mechanisms underlying elevated levels of TotHg and MeHg could be obtained with some additional analyses. Dissolved Organic Carbon (DOC) and flow cytometry analysis could help understanding seasonal microbial loop processes occurring in Adventfjord. And paired with seasonal river discharge, would maybe help to predict MeHg production in the water column. FA analysis from more samples (including « Omnivores » and « Predators »), could maybe help to describe seasonal trophic interactions.

Dissolved TotHg and MeHg concentrations in water samples would be useful to calculate Bioconcentration and Bioaccumulation Factors (BAF) for zooplankton samples. These paired with MeHg concentration in POM, could help to get a better understanding of the seasonal Hg concentration in zooplankton.

Some adjustment could be taken into account in future similar studies. The use of Hydrogen and Oxygen stable isotopes would allow to assess river water source (glaciers melt water vs rainfall).

Because Adventfjord is a very dynamic system, with physicochemical conditions changing very quickly (from one day to another because of different weather conditions), several samplings each month would give a more accurate picture of the system. Studying stable isotope and Hg in zooplankton species, instead of size fractionated or bulk samples, would maybe increase the understanding of complex trophic interactions occurring in this dynamic system.

7. REFERENCES

- Amos H. M., Jacob D. J., Kocman D., Horowitz H. M., Zhang Y., Dutkiewicz S., Horvat M., Corbitt E. S., Krabbenhoft D. P., Sunderland E. M. (2014) Global Biogeochemical Implications of Mercury Discharges from Rivers and Sediment Burial. *Environmental Science & Technology*, Vol 48 (16), 9514–9522.
- Arts M. T., Brett M. T., Kainz M. J. (2009) Lipid in aquatic ecosystems.
- Auel H., Harjes M., da Rocha R., Stübing D., Hagen W. (2002) Lipid biomarkers indicate different ecological niches and trophic relationships of the Arctic hyperiid amphipods *Themisto abyssorum* and *T. libellula*. *Polar Biology*, Vol. 25 (5), 374–383.
- Balogh S. J., Meyer M. L., Johnson D. K. (1998) Transport of Mercury in Three Contrasting River Basins. *Environmental Science & Technology*, Vol 32 (4), 456–462.
- Bates N. R., Hansell D. A., Moran S. B., Codispoti L. A. (2005) « Seasonal and spatial distribution of particulate organic matter (POM) in the Chukchi and Beaufort Seas » *Deep-Sea Research II*, Vol. 52, 3324–3343.
- Baya, P. A., M. Gosselin, I. Lehnerr, V. L. St. Louis, and H. Hintelmann (2015), Determination of monomethylmercury and dimethylmercury in the Arctic marine boundary layer, *Environmental Science & Technology*, Vol. 49(1), 223–232.
- Benner R., Benitez-Nelson B., Kaiser K., Amon R. M. W. (2004) Export of young terrigenous dissolved organic carbon from rivers to the Arctic Ocean. *Geophysical Research Letters*, Vol. 31, L05305.
- Berggren M., Ziegler S.E., St-Gelais N.F., Beisner B.E., del Giorgio P.A. (2014) Contrasting patterns of allochthony among three major groups of crustacean zooplankton in boreal and temperate lakes. *Ecology*, Vol. 95, 1947-1959.
- Blachowiak-Samolyk K., Søreide J.E., Kwasniewski S., Sundfjord A., Hop H., Falk-Petersen S., Hegseth E. N. (2008) Hydrodynamic control of mesozooplankton abundance and biomass in northern Svalbard waters (79-81°N). *Deep-Sea Research II*, Vol. 55, 2210-2224.
- Bodin N., Le Loc'h F., Hily C. (2017) Effect of lipid removal on carbon and nitrogen stable isotope ratios in crustacean tissues. *Journal of Experimental Marine Biology and Ecology*, Vol. 341 (2), 168-175.
- Böer M., Gannefors C., Kattner G., Graeve M., Hop H., Falk-Petersen S. (2005) The Arctic pteropod *Clione limacina*: seasonal lipid dynamics and life-strategy. *Marine Biology*, Volume 147 (3), 707–717.
- Braaten H., Harman C., Øverjordet I., Larssen T. (2014) Effects of sample preparation on methylmercury concentrations in Arctic organisms. *International Journal of Environmental Analytical Chemistry*, Vol. 94 (9), 1-11.
- Brett M.T., Müller-Navarra D.C. (1997) The role of highly unsaturated fatty acids in aquatic foodweb processes. *Freshwater Biology*, Vol. 38, 483 – 499.

Budge S. M., Parrish C. C (1998) Lipid biogeochemistry of plankton, settling matter and sediments in Trinity Bay, Newfoundland. II. Fatty acids. *Organic Geochemistry*, Vol. 29 (5–7), 1547-1559.

Budge S. M., Iverson S. J. and Koopman H. N. (2006) Studying trophic ecology in marine ecosystems using fatty acids: a primer on analysis and interpretation. *Marine Mammal Science*, Vol. 22 (4), 759-801.

Choquet M., Kosobokova K., Kwaśniewski S., Hatlebakk M., Dhanasiri A. K. S., Melle W., Daase M., Svensen C., Søreide J. E., Hoarau G. (2018) Can morphology reliably distinguish between the copepods *Calanus finmarchicus* and *C. glacialis*, or is DNA the only way? *Limnology and Oceanography Methods*, Volume 16, Issue 4 April 2018 Pages 237-252

Clarkson T. W., Magos L., and Myers G. J. (2003) The Toxicology of Mercury — Current Exposures and Clinical Manifestations. *The New England Journal of Medicine*, Vol. 349 (18), 1731-7.

Coquery M., Cossa D., Martin J. M. (1995) The distribution of dissolved and particulate mercury in three Siberian estuaries and adjacent Arctic coastal waters. *Water, Air, and Soil Pollution*, Vol. 80 (1–4), 653–664.

Daase M., Eiane K. (2007) Mesozooplankton distribution in northern Svalbard waters in relation to hydrography. *Polar Biology*, Vol. 30, 969–981.

Dalsgaard J., St John M., Kattner G., Muller-Navarra D., Hagen W. (2003). Fatty acid trophic markers in the pelagic marine environment. In *Advances in Marine Biology*, Vol. 46, 225-340.

Del Giorgio P. A., France R. L. (1996) Ecosystem-specific patterns in the relationship between zooplankton and POM or microplankton $\delta^{13}\text{C}$. *Limnology and Oceanography*, Vol 41(2), 359-365.

DeMott W. R. (1988) Discrimination Between Algae and Detritus by Freshwater and Marine Zooplankton. *Bulletin of Marine Science*, Vol. 43 (3), 486-499.

Dewailly E., Ayotte P., Bruneau S., Lebel G., Levallois P., Weber J.P. (2001) Exposure of the Inuit Population of Nunavik (Arctic Québec) to Lead and Mercury. *Archives of Environmental Health: An International Journal*, Vol. 56 (4), 350-357.

DiMento B. P., Mason R. P. (2017) Factors controlling the photochemical degradation of methylmercury in coastal and oceanic waters. *Marine Chemistry*, Vol. 196 (20), 116-125

Dittmar T., Kattner G. (2003), The biogeochemistry of the river and shelf ecosystem of the Arctic Ocean: A review, *Marine Chemistry*, Vol. 83, 103–120.

Dommergue A., Ferrari C. P., Gauchard P. A., Boutron C. F., Poissant L., Pilote M., Jitaru P., and Adams F. C. (2003). The fate of mercury species in a sub-arctic snowpack during snowmelt. *Geophysical Research Letters*, Vol. 30 (12 Art. No. 1621).

- Douglas T. A., Sturm M., Simpson W. R., Blum J. D., Alvarez-Aviles L., Keeler G. J., Perovich D. K., Biswas A., Johnson K. (2008) Influence of Snow and Ice Crystal Formation and Accumulation on Mercury Deposition to the Arctic. *Environmental Science and Technology*, Vol. 42 (5), 1542–1551.
- Douglas T. A., Loseto L. L., Macdonald R. W., Outridge P., Dommergue A., Poulain A., Amyot M., Barkay T., Berg T., Chetelat J., Constant P., Evans M., Ferrari C., Gantner N., Johnson M. S., Kirk J., Kroer N., Larose C., Lean D., Nielsen T. G., Poissant L., Rognerud S., Skov H., Sørensen S., Wang F., Wilson S., Zdanowic C. M. (2012) The fate of mercury in Arctic terrestrial and aquatic ecosystems, a review. *Environmental Chemistry*, Vol 9, 321–355.
- Dunton K. H., Weingartner T., Carmack E. C. (2006) The nearshore western Beaufort Sea ecosystem: Circulation and importance of terrestrial carbon in arctic coastal food webs. *Progress in Oceanography*, Vol. 71 (2–4), 362-378.
- Dunton K. H., Schonberg S. V., Cooper L. W. (2012) Food web structure of the Alaskan nearshore shelf and estuarine lagoons of the Beaufort Sea. *Estuaries and Coasts*, Vol. 35 (2), 416–435.
- Durnford D., Dastoor A., Figueras-Nieto D., Ryjkov A. (2010) Long range transport of mercury to the Arctic and across Canada. *Atmospheric Chemistry and Physics*, Vol 10, 6063–6086.
- Emmerton C. A., Graydon J. A., Gareis J. A. L., St. Louis V. L., Lesack L. F. W., Janelle K. Banack A., Hicks F., Nafziger J. (2013) Mercury Export to the Arctic Ocean from the Mackenzie River, Canada. *Environmental Science & Technology*, Vol. 47 (14), 7644–7654.
- Falk-Petersen S., Hopkins C. C. E., Sargent J. R. (1990) Trophic relationships in the pelagic, Arctic food web. In: *Trophic Relationships in Marine Environments. Proceedings of the 24th European Marine Biology Symposium*, Oban, Scotland (eds Barnes M, Gibson RN), 315–333.
- Falk-Petersen S., Sargent J. R., Kwasniewski S., Gulliksen B., Millar R-M. (2001) Lipids and fatty acids in *Clione limacina* and *Limacina helicina* in Svalbard waters and the Arctic Ocean: trophic implications. *Polar Biology*, Vol. 24 (3), 163–170.
- Falk-Petersen S., Dahl T. M., Scott C. L., Sargent J. R., Gulliksen B., Kwasniewski S., Hop H., Millar R-M. (2002) Lipid biomarkers and trophic linkages between ctenophores and copepods in Svalbard waters. *Marine Ecology Progress Series*, Vol. 227, 187-194.
- Fisher J. A., Jacob D. J., Soerensen A. L., Amos H. M., Steffen A., Sunderland E. M. (2012) Riverine source of Arctic Ocean mercury inferred from atmospheric observations. *Nature Geoscience*, Vol. 5, 499–504.
- Focken U., Becker K. (1998) Metabolic fractionation of stable carbon isotopes: implications of different proximate compositions for studies of the aquatic food webs using $\delta^{13}\text{C}$ data. *Oecologia*, Vol. 115, 337–343.
- Foster K. L., Stern G. A., Pazerniuk M. A., Hickie B., Walkusz W., Wang F., Macdonald R. W. (2012) Mercury Biomagnification in Marine Zooplankton Food Webs in Hudson Bay *Environmental Science & Technology*, Vol. 46 (23), 12952–12959.

Fox A. L., Trefry J. H., Trocine R. P., Dunton K. H., Lasorsa B. K., Konar B., Ashjian C. J., Cooper L. W. (2017) Mercury biomagnification in food webs of the northeastern Chukchi Sea, Alaskan Arctic. *Deep Sea Research Part II: Topical Studies in Oceanography*, Vol. 144, 63-77.

Frey K.E., McClelland J.W. (2009) Impacts of permafrost degradation on arctic river biogeochemistry. *Hydrological Processes*, Vol. 23, 169–182.

Fry B., Wainright S. C. (1991) Diatom sources of ^{13}C -rich carbon in marine food webs. *Marine Ecology Progress*, Vol. 76, 149–157.

Fry B. (2006) *Stable Isotope Ecology*.

Gabrielsen T. M. , Merkel B. , Søreide J. E. , Johansson-Karlsson E. , Bailey A. , Vogedes D. , Nygård H. , Varpe Ø. , Berge J. (2012) Potential misidentifications of two climate indicator species of the marine arctic ecosystem: *Calanus glacialis* and *C. finmarchicus*. *Polar Biology*, Vol. 35 (11), 1621–1628.

Gagnon C., Pelletier E., Mucci, A., Fitzgerald F. W. (1996) Diagenetic behavior of methylmercury in organic-rich coastal sediments. *Limnology and Oceanography*, Vol. 41, 428–434.

Gannefors C., Böer M., Kattner G., Graeve M., Eiane K., Gulliksen B., Hop H., Falk-Petersen S. (2005) The Arctic sea butterfly *Limacina helicina*: lipids and life strategy. *Marine Biology*, Vol. 147 (1), 169–177.

Gaye-Siessegger, J., Focken, U., Muetzel, S., Abel, H., Becker, K. (2004) Feeding level and individual metabolic rate affect $\delta^{13}\text{C}$ and $\delta^{15}\text{N}$ values in carp: implications for food web studies. *Oecologia*, Vol. 138, 175–183.

Gilmer R. W., Harbison G. R. (1991) Diet of *Limacina helicina* (Gastropoda: Thecosomata) in Arctic waters in midsummer. *Marine Ecology Progress Series*, Vol. 77, 125-134.

Gordeev V. V., Martin J. M., Sidorov I. S., Sidorova M. V. (1996) A reassessment of the Eurasian river input of water, sediment, major elements, and nutrients to the Arctic Ocean. *American Journal of Science*, Vol. 296, 664–691.

Graeve M., Albers C., Kattner G. (2005) Assimilation and biosynthesis of lipids in Arctic *Calanus* species based on feeding experiments with a ^{13}C labeled diatom. *Journal of Experimental Marine Biology and Ecology*, Vol. 317, 109–125.

Haddock S. H. D. (2007) Comparative feeding behavior of planktonic ctenophores. *Integrative and Comparative Biology*, Vol. 47 (6), 847–853.

Hall B. D., Bodaly R. A., Fudge R.J.P., Rudd J. W. M., Rosenberg D. M. (1997) Food as the dominant pathway of methylmercury uptake by fish. *Water, Air, and Soil Pollution*, Vol. 100 (1–2), 13–24.

Hanssen-Bauer I., Førland E.J., Hisdal H., Mayer S., Sandø A.B., Sorteberg A. (2019) Climate in Svalbard 2100 – a knowledge base for climate adaptation. NCCS report no. 1.

Harrison P. J., Thompson P. A., Calderwood G. S. (1990) Effects of nutrients and light limitation on the biochemical composition of phytoplankton . *Journal of Applied Phycology*, Vol. 2 (1), 45–56.

Heiskanen A.S., Keck A. (1996) Distribution and sinking rates of phytoplankton, detritus, and particulate biogenic silica in the Laptev Sea and Lena River (Arctic Siberia), *Marine Chemistry* Vol 53 (3–4), 229-245.

Hermans C. O., Satterlie R. A. (1992) Fast-Strike Feeding Behavior in a Pteropod Mollusk, *Clione limacina* Phipps. *Biological Bulletin*, Vol.182(1), 1-7.

Hintelmann H., Nguyen H. (2005) Extraction of methylmercury from tissue and plant samples by acid leaching. *Analytical and Bioanalytical Chemistry*, Vol. 381 (2), 360-365.

Hobson K. A., Welch H. E. (1992) Determination of trophic relationships within a high Arctic marine food web using $\delta^{13}\text{C}$ and $\delta^{15}\text{N}$ analysis. *Marine Ecology Progress Series*, Vol. 84 (1), 9-18.

Hoch M. P., Snyder R. A., Cifuentes L. A., Coffin R. B. (1996) Stable isotope dynamics of nitrogen recycled during interactions among marine bacteria and protists. *Marine Ecology Progress Series*, Vol. 132, 229–239.

Holmes R. M. , McClelland J. W , Raymond P. A. , Frazer B. B. , Peterson B. J. , Stieglitz M. (2008) Lability of DOC transported by Alaskan rivers to the Arctic Ocean. *Geophysical Research Letters*, Vol. 35, L03402.

Holmes R. M., McClelland J. W., Peterson B. J., Tank S. E., Bulygina E., Eglinton T. I., Gordeev V. V., Gurtovaya T. Y., Raymond P. A., Repeta D. J., Staples R., Striegl R. G., Zhulidov A. V., Zimov S. A. (2012) Seasonal and Annual Fluxes of Nutrients and Organic Matter from Large Rivers to the Arctic Ocean and Surrounding Seas. *Estuaries and Coasts*, Vol. 35, 369–382.

Jardine T. D., Kidd K. A., Fisk A. T. (2006) Applications, Considerations, and Sources of Uncertainty When Using Stable Isotope Analysis in Ecotoxicology. *Environmental Science & Technology* Vol.40 (24), 7501–7511.

Jones D. A., Kumlu M., Le Vay L. , Fletcher D. J. (1997) The digestive physiology of herbivorous, omnivorous and carnivorous crustacean larvae: a review. *Aquaculture* Vol. 155, 285-295

Juul-Pedersen T., Arendt K. E., Mortensen J., Blicher M. E., Sørensen D. H., Rysgaard S. (2015) Seasonal and interannual phytoplankton production in a sub-Arctic tidewater outlet glacier fjord, SW Greenland. *Marine Ecology Progress Series*, Vol. 524, 27–38.

Kainz M. , Mazunder A. (2004) Relationships between methylmercury and essential fatty acids In planktonic food webs. *RMZ-Mater. Geoenvironment*, Vol. 51, 1095-1098.

Kirk J. L. , Lehnerr I., Andersson M., Braune B. M. , Chan L., Dastoor A. P., Durnford D., Gleason A. L., Loseto L. L., Steffen A., St.Louis V. L. (2012) Mercury in Arctic marine ecosystems: Sources, pathways and exposure. *Environmental Research*, Vol. 119, 64–87.

- Kubiszyn A. M., Wiktor J. M., Wiktor Jr. J. M., Griffiths C., Kristiansen S., Gabrielsen T. M. (2017) The annual planktonic protist community structure in an ice-free high Arctic fjord (Adventfjorden, West Spitsbergen). *Journal of Marine Systems*, Vol. 169, 61-72.
- Kuhnlein H. , Chan H. (2000) Environment and contaminants in traditional food systems of northern indigenous Peoples. *Annual Review of Nutrition*, Vol. 20, 595-626.
- Kuzyk Z. Z. A., Macdonald R. W., Tremblay J-E., Stern G. A. (2010) Elemental and stable isotopic constraints on river influence and patterns of nitrogen cycling and biological productivity in Hudson Bay. *Continental Shelf Research*, Vol. 30 (2), 163-176.
- Loseto L. L., Stern G. A., Deibel D., Connelly T. L., Prokopowicz A., Lean D. R. S., Fortier L., Ferguson S. H. (2008) Linking mercury exposure to habitat and feeding behaviour in Beaufort Sea beluga whales. *Journal of Marine Systems*, Vol. 74 (3-4), 1012-1024.
- Lavoie R. A., Hebert C. E., Rail J.-F., Braune B. M., Yumvihoze E, Hill L. G., Lean D. R.S. (2010) Trophic structure and mercury distribution in a Gulf of St. Lawrence (Canada) food web using stable isotope analysis. *Science of The Total Environment*, Vol. 408 (22), 5529-5539.
- Lawson N. M., Mason R. P. (1998). Accumulation of mercury in estuarine food chains. *Biogeochemistry*, Vol 40, 235-247.
- Lee C.-S., Fisher N. S. (2017) Bioaccumulation of methylmercury in a marine copepod. *Environmental Toxicology and Chemistry*, Vol. 36, 1287- 1293.
- Lehnherr I., St. Louis V. L., Hintelmann H., Kirk J. L. (2011) Methylation of inorganic mercury in polar marine waters *Nature Geoscience*, Vol. 4, 298- 302.
- Leitch D. R. , Carrie J., Lean D., Macdonald R. W. , Stern G. A. , Wang F. (2007) The delivery of mercury to the Beaufort Sea of the Arctic Ocean by the Mackenzie River. *Science of The Total Environment*, Vol 373 (1), 178-195.
- Lindberg S.E. , Brooks S. , Lin C.J. , Scott K.J. , Landis M.S. , Stevens R.K. , Goodsite M. , Richter A. (2002) Dynamic oxidation of gaseous mercury in the Arctic troposphere at polar sunrise. *Environmental Science and Technology*, Vol. 36 (6), 1245-1256.
- Lischka S., Hagen W. (2007) Seasonal lipid dynamics of the copepods *Pseudocalanus minutus* (Calanoida) and *Oithona similis* (Cyclopoida) in the Arctic Kongsfjorden (Svalbard). *Marine Biology*, Vol 150, 443-454.
- Lobbes J. M. , Kattner G., Fitznar H. P. (2000), Biogeochemical characteristics of dissolved and particulate organic matter in Russian rivers entering the Arctic. *Geochimica et Cosmochimica Acta*, Vol 64, 2973-2983.
- Logan J. M., Jardine T. D., Miller T. J., Bunn S. E., Cunjak R. A., Lutcavage M. E. (2008) Lipid corrections in carbon and nitrogen stable isotope analyses: comparison of chemical extraction and modelling methods. *Journal of Animal Ecology*, Vol. 77, 838-846.

Lu J.Y. , Schroeder W.H. , Barrie L.A. , Steffen A., Welch H.E. , Martin K. , Lockhart L. , Hunt R.V. , Boila G. , Richter A. (2001) Magnification of atmospheric mercury deposition to polar regions in springtime: the link to tropospheric ozone depletion chemistry. *Geophysical Research Letters*, Vol. 28 (17), 3219-3222.

Macdonald R. W., Loseto L. L. (2010) Are Arctic Ocean ecosystems exceptionally vulnerable to global emissions of mercury? A call for emphasised research on methylation and the consequences of climate change. *Environmental Chemistry*, Vol. 7, 133.

MacLean R., Oswood M.W., Irons III J.G., McDowell W.H. (1999) The effect of permafrost on stream biogeochemistry: A case study of two streams in the Alaskan (U.S.A) taiga. *Biogeochemistry*, Vol. 47, 239–267.

MacNeil M. A., Drouillard K. G., Fisk A. T. (2006) Variable uptake and elimination of stable nitrogen isotopes between tissues in fish. *Canadian Journal of Fishery and Aquatic Science*, Vol. 63, 345–353.

Mann P. J. , Davydova A. , Zimov N. , Spencer R. G. M., Davydov S. , Bulygina E., Zimov S. , Holmes R. M. (2012) Controls on the composition and lability of dissolved organic matter in Siberia's Kolyma River basin. *Journal of Geophysical Research* Vol. 117, G01028. *Marine Biology*, Vol. 141, 423-434.

Mason R. P., Reinfelder J. R, Morel F. M. M. (1996) Uptake, toxicity, and trophic transfer of mercury in a coastal diatom. *Environmental Science & Technology*, Vol. 30 (6), 1835–1845.

Matthews B., Mazunder A. (2005) Temporal variation in body composition (C:N) helps explain seasonal patterns of zooplankton ¹³C. *Freshwater Biology*, Vol. 50, 502–515.

Mayzaud P., Boutoute M., Gasparini S. (2013) Differential response of fatty acid composition in the different lipid classes from naturally occurring particulate matter during spring and summer in a high arctic fjord (Kongsfjorden, Svalbard). *Marine Chemistry*, Vol. 151, 23-34.

McClelland J. W., Holmes R. M., Dunton K. H., Macdonald R. (2012) The Arctic Ocean estuary. *Estuaries and Coasts* Vol. 35 (2), 353–368.

McClelland J. W., Holmes R. M., Peterson B. J., Raymond P. A., Striegl R. G., Zhulidov A. V., Zimov S. A., Zimov N., Tank S. E., Spencer R. G. M., Staples R., Gurtovaya T. Y., Griffin C. G. (2016), Particulate organic carbon and nitrogen export from major Arctic rivers, *Global Biogeochemical Cycles*, Vol. 30, 629–643.

McConnaughey T. , McRoy C.P. (1979) Food-web structure and the fractionation of carbon isotopes in the Bering Sea. *Marine Biology*, Vol.53 (3), 257-262.

Minagawa M., Wada E. (1984) Stepwise enrichment of ¹⁵N along food chains: further evidence and the relation between $\delta^{15}\text{N}$ and animal age. *Geochimica et Cosmochimica Acta* . Vol. 48, 1135–1140.

Morel M.M. F., Kraepiel A. M. L. , Amyot M. (1998) The chemical cycle and bioaccumulation of mercury. *Annual Review of Ecology and Systematics*, Vol 29:543–66.

- Nriagu J. O. , Pacyna J. M. (1988) Quantitative assessment of worldwide contamination of air, water and soils by trace metals. *Nature*, Vol. 333, 134–139.
- Opsahl S., Benner R., Amon R. M. W. (1999) Major flux of terrigenous dissolved organic matter through the Arctic Ocean. *Limnology and Oceanography*, Vol. 44(8), 2017–2023.
- Overman N., Parrish D. L. (2001) Stable isotope composition of walleye: ^{15}N accumulation with age and area-specific differences in $\delta^{13}\text{C}$. *Canadian Journal of Fishery and Aquatic Science*, Vol. 58, 1253–1260.
- Paffenhöfer G-A. (1988) Feeding Rates and Behavior of Zooplankton. *Bulletin of Marine Science*, Vol. 43 (3)430-445
- Parsons T. R. (1963). Suspended organic matter in sea water. *Progress in Oceanography*, Vol. 1, 205–293.
- Pearre S. Jr. (1981) Feeding by Chaetognatha: Energy Balance and Importance of Various Components of the Diet of *Sagitta elegans* Marine Ecology. *Marine Ecology Progress Series* Vol. 5, 45-54.
- Peterson B. J., Fry B. (1987) Stable isotopes in ecosystem studies. *Annual Review of Ecology and Systematics*, Vol. 18, 293-320.
- Peterson B. J., Holmes R. M, McClelland J. W., Vörösmarty C. J., Lammers R. B., Shiklomanov, Igor A. Shiklomanov A. I., Rahmstorf S. (2002) Increasing River Discharge to the Arctic Ocean. *Science*, Vol. 298 (5601), 2171-2173
- Pickhardt P.C., Fisher N.S. (2007) Accumulation of inorganic and methylmercury by freshwater phytoplankton in two contrasting water bodies. *Environmental Science & Technology*, Vol. 41, 125–131.
- Pomerleau C., Winkler G., Sastri A., Nelson R. J., Williams W. J. (2014) The effect of acidification and the combined effects of acidification/lipid extraction on carbon stable isotope ratios for sub-arctic and arctic marine zooplankton species. *Polar Biology* Vol. 37, 1541–1548.
- Pomerleau C., Stern G. A., Pućko M., Foster K. L., Macdonald R. W., Fortier L. (2016) Pan-Arctic concentrations of mercury and stable isotope ratios of carbon ($\delta^{13}\text{C}$) and nitrogen ($\delta^{15}\text{N}$) in marine zooplankton. *Science of The Total Environment*, Vol. 551–552, 92-100.
- Post D. M. (2002) Using stable isotopes to estimate trophic position: models, methods, and assumptions. *Ecology*, Vol. 83(3), 703–718.
- Poste A. E., Hoel C. S., Andersen T. , Arts M. T., Færøvig P-J., Borgå K. (2019) Terrestrial organic matter increases zooplankton methylmercury accumulation in a brown-water boreal lake. *Science of The Total Environment*, Vol. 674, 9-18.
- Pućko M., Burt A., Walkusz W., Wang F., Macdonald R. W., Rysgaard S., Barber, J.-É. Tremblay D. G., Stern G. A. (2014) Transformation of Mercury at the Bottom of the Arctic Food Web: An Overlooked Puzzle in the Mercury Exposure Narrative. *Environmental Science & Technology*, Vol. 48 (13), 7280–7288.

- Rau G. H., Teyssie J. L., Rassoulzadegan F., Fowler S. W. (1990) $^{13}\text{C}/^{12}\text{C}$ and $^{15}\text{N}/^{14}\text{N}$ variations among size-fractionated marine particles—implications for their origin and trophic relationships. *Marine Ecology Progress Series*, Vol. 59, 33–38.
- Raymond P. A., McClelland J. W., Holmes R. M., Zhulidov A. V., Mull K., Peterson B. J., Striegl R. G., Aiken G. R., Gurtovaya T. Y. (2007) Flux and age of dissolved organic carbon exported to the Arctic Ocean: A carbon isotopic study of the five largest arctic rivers. *Global Biogeochemical Cycles*, Vol. 21, GB4011.
- Renaud P. E., Daase M., Banas N. S., Gabrielsen T. M., Søreide J. E., Varpe Ø., Cottier F., Falk-Petersen S., Halsband C., Vogedes D., Heggland K., Berge J. (2018) Pelagic food-webs in a changing Arctic: a trait-based perspective suggests a mode of resilience. *ICES Journal of Marine Science*, Vol. 75 (6), 1871–1881.
- Reuss N., Poulsen L. (2002) Evaluation of fatty acids as biomarkers for a natural plankton community. A field study of a spring bloom and a post-bloom period off West Greenland. *Marine Biology*, Vol. 141, 423–434.
- Ruus A., Øverjordet I. B., Braaten H. F. V., Evenset A., Chritensen G., Heimstad E. S., Gabrielsen G. W., Borgå K. (2015) Methymercury biomagnification in an arctic pelagic food web. *Environmental Toxicology and Chemistry*, Vol. 34 (11), 2636–2643.
- Rysgaard S., Finster K., Dahlgard H. (1996) Primary production, nutrient dynamics and mineralisation in a northeastern Greenland fjord during the summer thaw. *Polar Biology*, Vol. 16, 497–506.
- Rysgaard S., Nielsen T. G., Hansen B. W. (1999) Seasonal variation in nutrients, pelagic primary production and grazing in a high-Arctic coastal marine ecosystem, Young Sound, Northeast Greenland. *Marine Ecology Progress Series*, Vol. 179, 13–25.
- Rysgaard S., Nielsen T. G. (2006) Carbon cycling in a high-arctic marine ecosystem – Young Sound, NE Greenland. *Progress in Oceanography*, Vol. 71 (2–4), 426–445.
- Saliot A., Laureillard J., Scribeand P., Sicre M.A. (1991) Evolutionary trends in the lipid biomarker approach for investigating the biogeochemistry of organic matter in the marine environment. *Marine Chemistry*, Vol. 36, 233–248.
- Samemoto D. D. (1987) Vertical Distribution and Ecological Significance of Chaetognaths in the Arctic Environment of Baffin Bay. *Polar Biology*, Vol 7, 317–328.
- Sargent J. R., Falk-Petersen S. (1988) The lipid biochemistry of calanoid copepods. *Hydrobiologia*, Vol. 167–168(1), 101–114.
- Schartup A. T., Balcom P. H., Soerensen A. L., Gosnell K. J., Calder R. S. D., Mason R. P., Sunderland E. M. (2015) Freshwater discharges drive high levels of methylmercury in Arctic marine biota. *PNAS*, Vol. 112 (38), 11789–11794.

Schell D. M., Barnett B. A., Vinette K. A. (1998) Carbon and nitrogen isotope ratios in zooplankton of the Bering, Chukchi and Beaufort seas. *Mar. Ecology Progress Series*, Vol. 162, 11–23.

Schuster P. F., Striegl R. G., Aiken G. R., Krabbenhoft D. P., Dewild J. F., Butler K., Kamark B., Dornblaser M. (2011) Mercury Export from the Yukon River Basin and Potential Response to a Changing Climate. *Environmental Science & Technology*, Vol. 45 (21), 9262–9267

Sellers P. , Kelly C.A. , Rudd J., MacHutchon A.R (1996) Photodegradation of methylmercury in lakes. *Nature*, Vol. 380, 694-697.

Søreide J. E., Hop H., Carroll M. L., Falk-Petersen S., Hegseth E. N. (2006) Seasonal food web structures and sympagic-pelagic coupling in the European Arctic revealed by stable isotopes and a two source food web model. *Progress in Oceanography* Vol. 71 (1), 59-87.

Søreide E. J., Falk-Petersen S., Hegseth E., Hop H., Carroll M. L. , Hobson K., Błachowiak-Samołyk K. (2008) Seasonal feeding strategies of *Calanus* in the high-arctic Svalbard region. *Deep Sea Research Part II*, Vol. 55, 2225-2244.

St Louis V. L., Sharp M. J., Steffen A., May A., Barker J., Kirk J. L., Kelly D. J. A., Arnott S. E., Keatley B., Smol J. P. (2005) Some sources and sinks of monomethyl and inorganic mercury on Ellesmere Island in the Canadian High Arctic. *Environmental Science & Technology*, Vol. 39, 2686–2701.

Steffen A., Schroeder W., Macdonald R., Poissant L., Konoplev A. (2005) Mercury in the Arctic atmosphere: An analysis of eight years of measurements of GEM at Alert (Canada) and a comparison with observations at Amderma (Russia) and Kuujjuarapik (Canada). *Science Total Environment*. Vol. 342, 185–198.

Steffen A., Douglas T., Amyot M., Ariya P., Aspmo K., Berg T., Bottenheim J., Brooks S., Cobbett F., Dastoor A., Dommergue A., Ebinghaus R., Ferrari C., Gardfeldt K., Goodsite M. E., Lean D., Poulain A. J., Scherz C., Skov H., Sommar J., Temme C. (2008) A synthesis of atmospheric mercury depletion event chemistry in the atmosphere and snow. *Atmospheric Chemistry and Physics*, Vol. 8, 1445–1482.

Tamelaender T., Kivimäe C., Bellerby R. G. J. , Renaud P. E., Kristiansen S. (2009) Base-line variations in stable isotope values in an Arctic marine ecosystem: effects of carbon and nitrogen uptake by phytoplankton. *Hydrobiologia*, Vol. 630 (1), 63–73.

Tan A., Adam J. C. , Lettenmaier D. P. (2011) Change in spring snowmelt timing in Eurasian Arctic rivers. *Journal of the Geophysical Research*, Vol. 116, D03101.

Thompson P. A., Gou M., Harrison P. J., Whyte J. N. C. (1992) Effects of variation in temperature II. On the fatty acid composition of eight species of marine phytoplankton. *Journal of Phycology*, Vol. 28 (4), 488-497.

Tieszen L. L., Boutton T. W., Tesdahl K. G., Slade N. A. (1983) Fractionation and turnover of stable carbon isotopes in animal tissues: implications for $\delta^{13}\text{C}$ analysis of diet. *Oecologia*, Vol. 57 (1–2), 32–37.

Turner J. T., Levinsen H., Nielsen T. G. , Hansen B. W. (2001) Zooplankton feeding ecology: grazing on phytoplankton and predation on protozoans by copepod and barnacle nauplii in Disko Bay, West Greenland. *Marine Ecology Progress Series*, Vol. 221, 209-219.

Wausmann P., Duarte C. M., Agusti S., Sejor M. K. (2011) Footprints of climate change in the Arctic marine ecosystem. *Global Change Biology*, Vol. 17, 1235–1249.

Walkusz W., Pauli J. E., Williams J. W., Kwasniewski S., Papst M. H. (2011) Distribution and diet of larval and juvenile Arctic cod (*Boreogadus saida*) in the shallow Canadian Beaufort Sea. *Journal of Marine Systems*, Vol. 84 (3–4), 78-84.

Wu P., Kainz M., Åkerblom S., Bravo A. G., Sonesten L., Branfireun B., Deininger A., Bergström A-K., Bishop K. (2019) Terrestrial diet influences mercury bioaccumulation in zooplankton and macroinvertebrates in lakes with differing dissolved organic carbon concentrations. *Science of The Total Environment*, Vol. 669, 821-832.

Ye H., Ladochy S. (2004) The Impact of Climatic Conditions on Seasonal River Discharges in Siberia. *Journal of hydrometeorology*, Vol. 5, 286 – 295.

Zajaczkowski M., Szczuciński W., Bojanowski R. (2004) Recent changes in sediment accumulation rates in Adventfjorden, Svalbard. *Oceanologia*, Vol. 46 (2), 217–231.

Zajaczkowski M., Włodarska-Kowalczyk M. (2007) Dynamic sedimentary environments of an Arctic glacier-fed river estuary (Adventfjorden, Svalbard). I. Flux, deposition, and sediment dynamics *Estuarine, Coastal and Shelf Science*, Vol. 74 (1–2), 285-296.

Zajaczkowski M. (2008) Sediment supply and fluxes in glacial and outwash fjords, Kongsfjorden and Adventfjorden, Svalbard. *Polish Polar Research*, Vol. 29 (1), 59–72.

Zajaczkowski M.; Nygard H. ; Hegseth E. N.; Berge J. (2010) Vertical flux of particulate matter in an Arctic fjord: the case of lack of the sea-ice cover in Adventfjorden 2006-2007. *Polar Biology*, Vol. 33 (2), 223–239.

Zhang Y., Jacob D. J., Dutkiewicz S., Amos H. M., Long M. S., Sunderland E. M. (2015) Biogeochemical drivers of the fate of riverine mercury discharged to the global and Arctic oceans. *Global Biogeochemical Cycles*, Vol. 29, 854–864.

8. APPENDICES

Table A1 Estimation of dry weight (mg/ind) of individuals zooplankton provided by Katarzyna Dmoch from IOPAS - Institute of Oceanology Polish Academy of Science and Janne Søreide

TAXA	mg/ind	TAXA	mg/ind
Copepods		Chaetognatha	
<i>Calanus finmarchicus</i> AM	0,214	<i>E. hamata</i> =>10 mm	0,378
<i>C. finmarchicus</i> AF	0,282	<i>E. hamata</i> =>5 mm	0,052
<i>C. finmarchicus</i> CV	0,214	<i>Sagitta elegans</i> =>20 mm	1,06
<i>C. finmarchicus</i> CIV	0,075	<i>S. elegans</i> =>10 mm	0,23
<i>C. finmarchicus</i> CIII	0,029	<i>S. elegans</i> =>5 mm	0,06
<i>C. finmarchicus</i> CII	0,011	<i>S. elegans</i> <5 mm	0,00
<i>C. finmarchicus</i> CI	0,005	Amphipod	
<i>Calanus glacialis</i> AM	0,620	<i>Themisto abyssorum</i> =>5mm	1,009
<i>C. glacialis</i> AF	1,303	<i>T. abyssorum</i> < 5 mm	0,103
<i>C. glacialis</i> CV	0,620	<i>Themisto libellula</i> =>5mm	3,127
<i>C. glacialis</i> CIV	0,198	Decapod	
<i>C. glacialis</i> CIII	0,062	Euphausiacea furcilia =>5 mm	1,653
<i>C. glacialis</i> CII	0,022	Euphausiacea furcilia <5 mm	0,209
<i>C. glacialis</i> CI	0,009	Cirripedia nauplii	0,021
<i>Calanus hyperboreus</i> AM	1,209	Cirripedia cypris	0,021
<i>C. hyperboreus</i> AF	3,293	Euphausiacea nauplii	0,005
<i>C. hyperboreus</i> CV	1,209	<i>Eupagurus</i> zoea	0,534
<i>C. hyperboreus</i> CIV	0,378	<i>Hyas</i> zoea	0,540
<i>C. hyperboreus</i> CIII	0,112	GASTROPODA	
<i>C. hyperboreus</i> CII	0,029	<i>Clione limacina</i> =>5mm	1,789
<i>C. hyperboreus</i> CI	0,011	<i>C. limacina</i> <5mm	0,303
<i>Microcalanus</i> spp.	0,007	<i>C. limacina</i> veliger	0,018
<i>Pseudocalanus</i> spp. AM	0,012	<i>Limacina helicina</i> =>5 mm	8,062
<i>Pseudocalanus</i> spp. AF	0,014	<i>L. helicina</i> <5mm	1,134
<i>P.</i> spp. CV	0,009	<i>L. helicina</i> veliger	0,008
<i>P.</i> spp. CIV	0,005	Bivalvia veliger	0,012
<i>P.</i> spp. CIII	0,003	Jelly plankton	
<i>P.</i> spp. CII	0,002	<i>Mertensia ovum</i>	0,1317
<i>P.</i> spp. CI	0,001	<i>Beroe cucumis</i>	0,0342
<i>Oithona similis</i>	0,002	<i>Aglantha digitale</i>	2,9
Copepoda nauplii	0,004	Apendicularian	
<i>Oithona atlantica</i>	0,007	<i>Fritillaria borealis</i>	0,018
<i>Metridia longa</i> AM	0,137	<i>Oikopleura</i> spp. =>10 mm	1,531
<i>M. longa</i> AF	0,287	<i>Oikopleura</i> spp. =>5 mm	0,088
<i>M. longa</i> CV	0,120	<i>Oikopleura</i> spp. <5 mm	0,006
<i>M. longa</i> CIV	0,034	Fish larvae	
<i>M. longa</i> CIII	0,016	Fish larvae	0,609
<i>M. longa</i> CII	0,007	Echinodermata	
<i>M. longa</i> CI	0,003	Echinodermata larvae	0,001

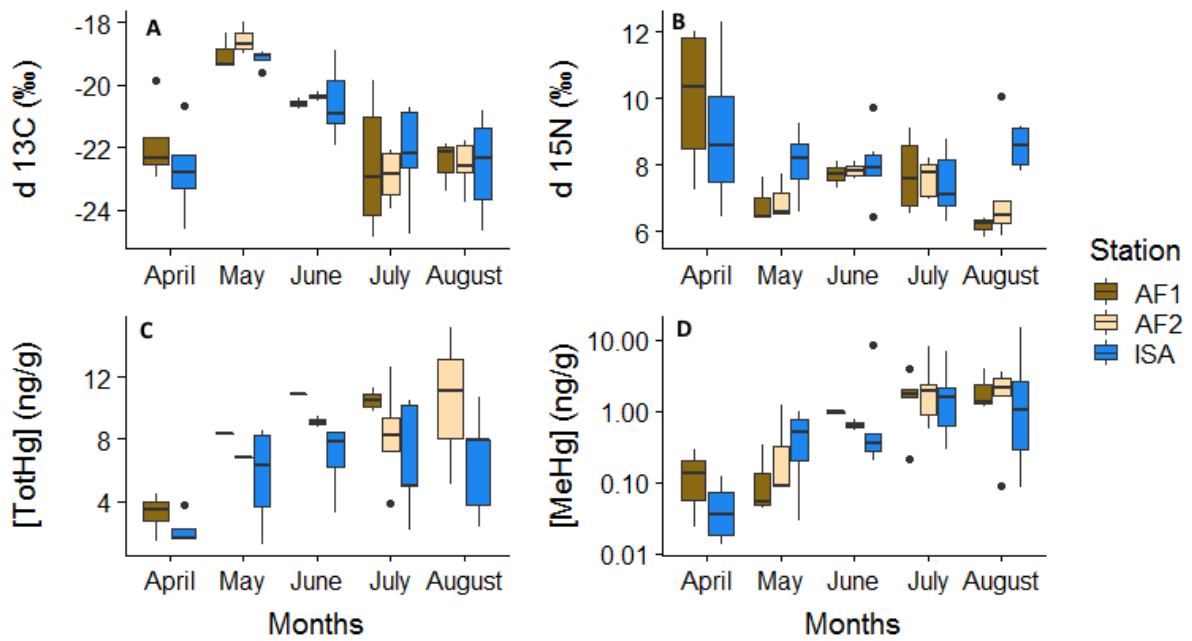


Figure A1 : Boxplots of (A) $\delta^{13}\text{C}$, (B) $\delta^{15}\text{N}$, (C) TotHg, and (D) MeHg concentrations in zooplankton samples collected at the 3 stations from April to August 2018.

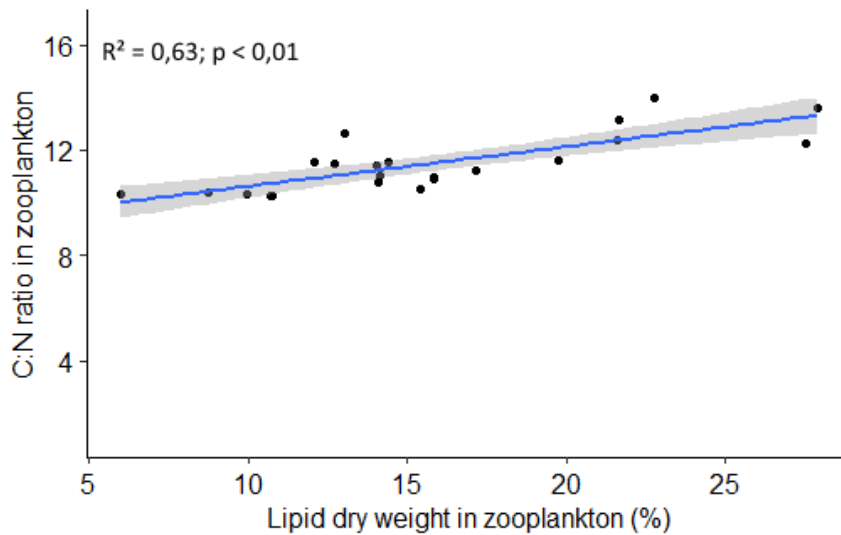


Figure A2 Linear relationship between C :N ratio and lipid dry weight content (%) in a subset of zooplankton size-fractionated samples (n=24 ; 1 outlier Calanus sp. was removed) collected from April to August 2018 at the 3 stations.

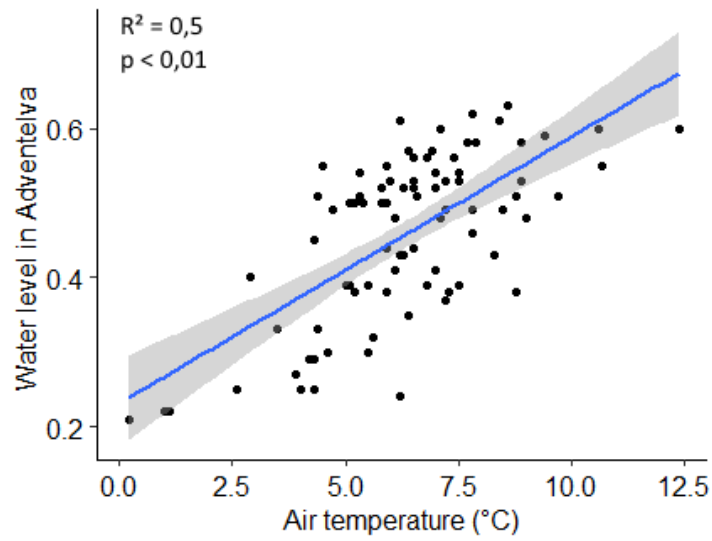


Figure A3 Relationship between air temperatre (°C) and water level in Adventelva between 20/06/2918 and 15/09/18.

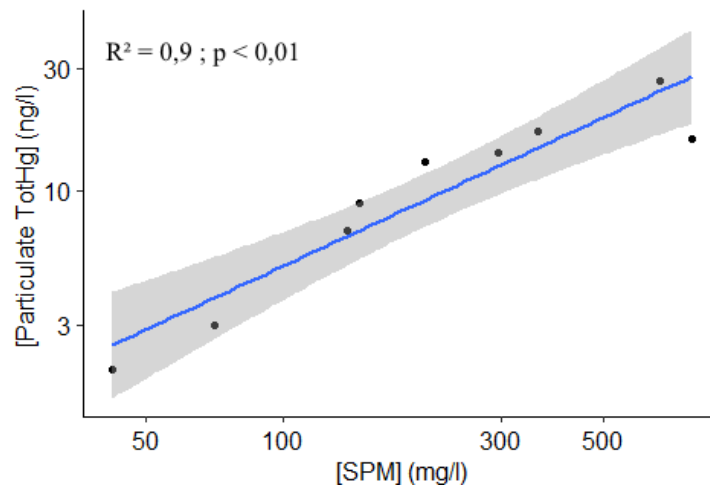


Figure A4 Linear relationship between Suspended Particulate Matter (SPM) and Particulate TotHg concentrations in surface water in Adventelva, Longyearelva and tributaries rivers from May to August. Data presented in Log10 scale

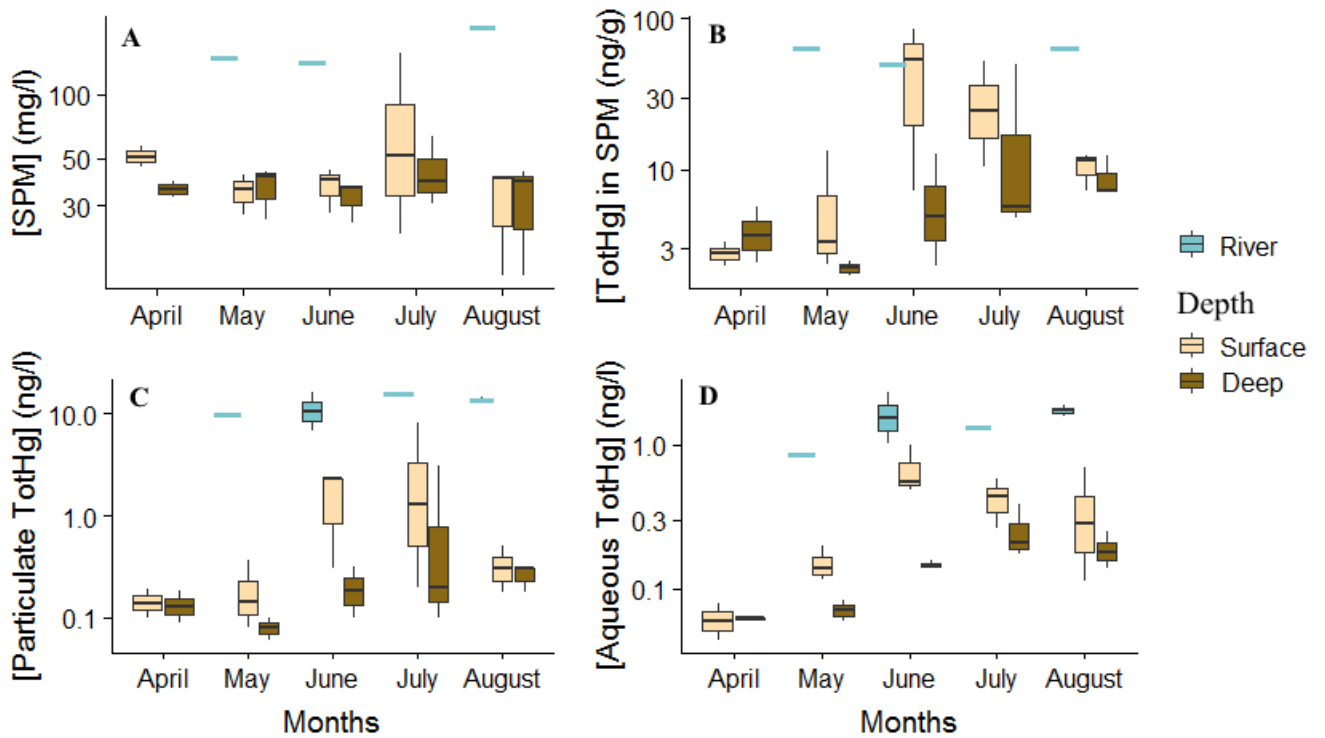


Figure A5 Boxplots of (A) SPM concentration, (B) TotHg concentration in SPM (B), (C) Particulate TotHg concentration, (D) Aqueous TotHg concentration in POM from water samples taken at the surface and 15m deep in the 3 stations (AF1, AF2, ISA) from April to August; and in water samples from Adventelva and Longyearelva (« River ») from May to August 2018. Data presented on a log₁₀ scale.

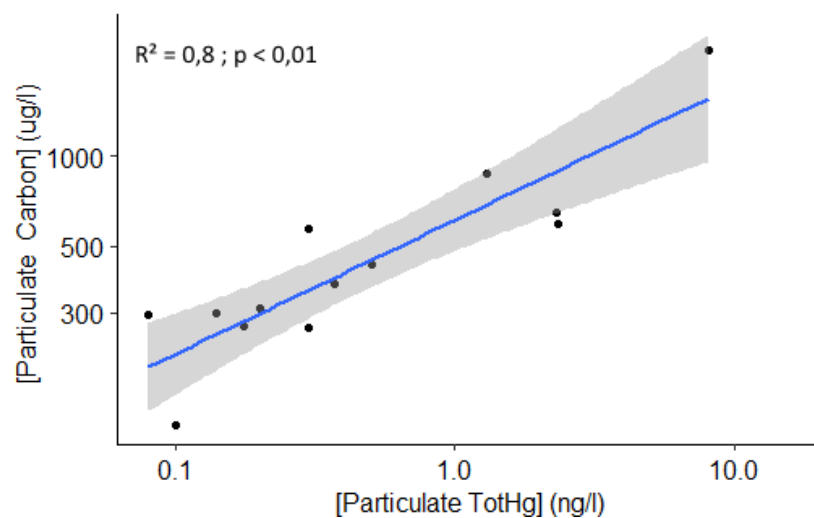


Figure A6 Linear relationship between Particulate TotHg concentration (ng/L) et Particulate Carbon concentration (ug/L) in surface water samples collected from April to August at the 3 stations. Data presented in Log₁₀ scale. (One outlier was removed from ISA in April).

Table A2 Results from Spearman's rank correlation (coefficient and p-value) and linear regression model (R^2 and p-value) on physicochemical parameters in Adventfjord from samples taken at the 3 stations from April to August 2018.

Response variable	Explanatory variable	Spearman's rank Correlation		Linear Regression Model	
		Coefficient	p-value	R^2	p-value
PartTotHg	Turbidity	0.8	< 0.01	0.7	< 0.01
PartTotHg	SPMTotHg	0.9	< 0.01	0.8	< 0.01
PartTotHg	AqueousTotHg	0.8	< 0.01	0.6	< 0.01
PartTotHg	PartC	0.7	< 0.01	0.4	< 0.01
SPMTotHg	Turbidity	0.8	< 0.01	0.6	< 0.01
SPMTotHg	AqueousTotHg	0.6	< 0.02	0.7	< 0.01
SPMTotHg	PartC	0.6	< 0.02	0.4	< 0.01
SPMTotHg	SPMCarbon	0.7	< 0.01	0.3	< 0.01
AqueousTotHg	Turbidity	0.9	< 0.01	0.6	< 0.01
AqueousTotHg	PartC	0.9	< 0.01	0.5	< 0.01
AqueousTotHg	SPMCarbon	0.7	< 0.01	0.3	< 0.01

Table A3 Relative proportion of « Dominant species » in size fractioned samples collected in AF1 from April to August 2018. « Other » included : Copepod nauplii, *Pseudocalanus sp.*, *Microcalanus sp.*, bivalva larvae, *Metridia longa*, Cirripedia cypris, Echinoderm larvae, *Oithona atlantica* , and *Oikopleura spp.*.

AF1 Month	Size fraction	Amhipod Larvae	C. limacina	Calanus sp.	Chaetognatha	Cirripedia nauplii	Decapod zoea	Jelly plankton	L. helicina	O.similis	Other	Total
April	> 1000 um	-	-	97,5	-	-	-	1,93	-	-	0,57	100
April	500 - 1000 um	-	-	98,6	-	-	-	-	-	-	1,4	100
April	200 - 500 um	-	-	-	-	-	-	-	-	59,9	40,1	100
April	50 - 200 um	-	-	-	-	-	-	-	-	100	-	100
May	> 1000 um	2	22,2	-	-	1,2	73,2	-	-	-	1,4	100
May	500 - 1000 um	-	-	-	-	99,3	-	-	-	-	0,7	100
June	> 1000 um	0,3	-	86,4	-	-	11,6	-	-	-	1,7	100
June	500 - 1000 um	1,3	-	93,4	0,8	4,4	-	-	-	-	0,1	100
July	> 1000 um	-	-	98,5	0,8	-	-	-	-	-	0,7	100
July	200 - 500 um	-	-	66,8	-	-	-	-	-	2	31,2	100
August	500 - 1000 um	-	-	96,9	0,7	-	-	-	-	0,1	2,3	100
August	200 - 500 um	-	-	-	-	4,7	-	-	-	50	45,3	100
August	50 - 200 um	-	-	-	-	-	-	-	1	26,5	72,5	100

Table A4 Relative proportion of « Dominant species » in size fractioned samples collected in AF2 from April to August 2018. « Other » included : Copepod nauplii, *Pseudocalanus sp.*, *Microcalanus sp.*, bivalva larvae, *Metridia longa*, Cirripedia cypris, Echinoderm larvae, *Oithona atlantica* , and *Oikopleura spp.*.

AF2 Month	Size fraction	Calanus sp.	Chaetognatha	Cirripedia nauplii	Decapod zoea	L. helicina	O.similis	Other	Total
May	> 1000 um	-	-	-	99,9	-	-	0,1	100
May	500 - 1000 um	-	-	97,2	-	-	-	2,8	100
June	> 1000 um	62,4	-	0,2	30,2	-	-	7,2	100
June	500 - 1000 um	63,4	-	21,2	1,8	-	-	13,6	100
July	> 1000 um	96,2	0,6	-	2	-	-	1,2	100
August	500 - 1000 um	96,5	1,3	-	-	-	0,2	2	100
August	200 - 500 um	10,8	-	-	-	4,3	26,9	58	100
August	50 - 200 um	-	-	-	-	1,1	52	46,9	100

Table A5 Relative proportion of « Dominant species » in size fractioned samples collected in ISA from April to August 2018. « Other » included : Copepod nauplii, *Pseudocalanus sp.*, *Microcalanus sp.*, bivalva larvae, *Metridia longa*, Cirripedia cypris, Echinoderm larvae, *Oithona atlantica* , and *Oikopleura spp.*.

ISA Month	Size fraction	Amhipod Larvae	Calanus sp.	Chaetognatha	Cirripedia nauplii	Decapod zoea	Euphausiacea	Jelly plankton	L. helicina	O.similis	Other	Total
April	> 1000 um	-	99,7	-	-	-	-	-	-	-	0,3	100
April	200 - 500 um	-	-	-	-	-	-	-	-	93,2	6,8	100
April	500 - 1000 um	-	92,1	-	-	-	-	6,9	0,3	0,3	0,4	100
April	50 - 200 um	-	-	-	-	-	-	-	-	100	-	100
May	> 1000 um	-	12,3	-	0,6	65,5	11,4	6,9	-	-	3,3	100
May	500 - 1000 um	1,6	20,5	0,9	65,2	10,2	-	0,2	-	-	1,4	100
May	200 - 500 um	-	3,7	-	89,5	-	-	-	-	-	6,8	100
June	> 1000 um	-	94,5	-	-	0,9	4,3	-	-	-	0,3	100
July	> 1000 um	-	98,4	-	-	-	-	-	-	0,2	1,4	100
July	200 - 500 um	-	54,7	-	-	-	-	-	1,2	18,2	25,9	100
August	> 1000 um	-	89,2	4,2	-	-	6,6	-	-	-	0	100

Table A6 Hand -picked macrozooplankton from zooplankton samples collected at the 3 stations in Adventfjord from April to August 2018 (NI = Non Identified).

Month	Station	Macrozooplankton
June	ISA	NI cnidarians
June	ISA	NI cnidarians
June	ISA	<i>Clione limacina</i>
July	AF1	Fish larvae
July	AF1	Krill
July	AF1	Chaetognatha
July	AF1	Amphipod
July	AF2	<i>Clione limacina</i>
July	AF2	NI cnidarian
July	AF2	Ctenophora
July	AF2	<i>Limacina helicina</i>
July	ISA	NI cnidarians
July	ISA	NI cnidarians
July	ISA	<i>Limacina helicina</i>
July	ISA	<i>Clione limacina</i>
July	ISA	Ctenophora
August	ISA	<i>Mertensia ovum</i>
August	ISA	<i>Beröe cucumis</i>
August	ISA	<i>Clione limacina</i>
August	ISA	<i>Boreogadus saida</i>
August	ISA	<i>Thysanoessa sp.</i>
August	AF2	Chaetognatha
August	AF2	Ctenophora
August	ISA	<i>Clione limacina</i>

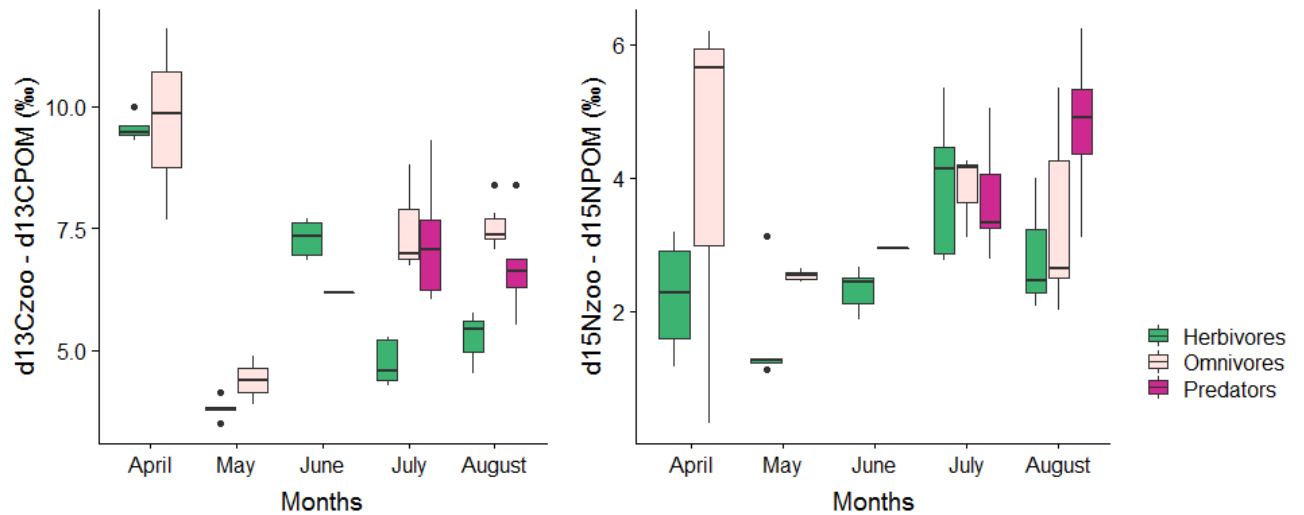


Figure A7 Boxplots of $\delta^{13}\text{C}_{\text{zooplankton}} - \delta^{13}\text{C}_{\text{POM}}$ and $\delta^{15}\text{N}_{\text{zooplankton}} - \delta^{15}\text{N}_{\text{POM}}$ data from zooplankton samples collected at the 3 stations, and POM collected at ISA station at 15m deep from April to August 2018.

Table A7 Results from Spearman's rank correlation (coefficient and p-value) and linear regression model (R^2 and p-value) on TotHg- and MeHg-concentrations in « Herbivores », Aqueous TotHg, FA, and nitrogen and carbon concentrations in « Herbivores » from samples taken at the 3 stations from April to August 2018 (n=15).

Response variable	Explanatory variable	Spearman's rank Correlation		Linear Regression Model	
		Coefficient	p-value	R^2	p-value
TotHg	PUFA	0.8	< 0.01	0.6	< 0.01
TotHg	Carbon	0.6	< 0.02	0.8	< 0.01
TotHg	Nitrogen	0.7	< 0.01	0.8	< 0.01
TotHg	MUFA	-0.8	< 0.01	0.5	< 0.01
TotHg	SFA	-0.7	< 0.01	0.4	< 0.05
MeHg	AqueousTotHg	0.7	< 0.01	0.5	< 0.01
MeHg	MUFA	-0.7	< 0.01	0.5	< 0.01
MeHg	PUFA	0.7	< 0.01	0.4	< 0.02

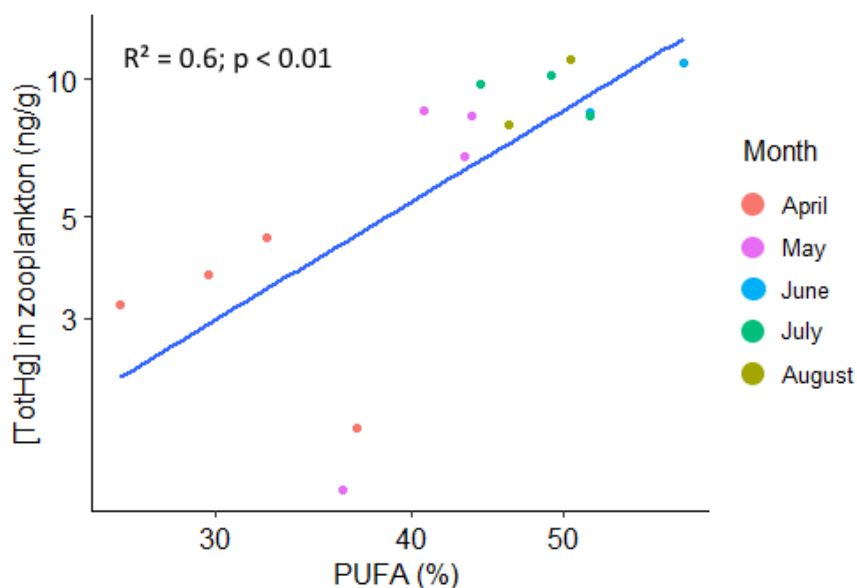


Figure A8 Linear relationship between PUFA (%) and TotHg concentration in « Herbivores » (ng/g) from April to August at the 3 stations (=15). Data presented in Log10 scale.

Table A8 Results from Spearman's rank correlation (coefficient and p-value) and linear regression model (R² and p-value) on TotHg- and MeHg-concentrations in zooplankton, Aqueous TotHg and carbon and nitrogen concentration in zooplankton from samples taken at the 3 stations from April to August 2018 (n =30) .

Response variable	Explanatory variable	Spearman's rank Correlation		Linear Regression Model	
		Coefficient	p-value	R ²	p-value
TotHg	AqueousTotHg	0.5	< 0.01	0.3	< 0.01
TotHg	Carbon	0.8	< 0.01	0.7	< 0.01
TotHg	Nitrogen	0.8	< 0.01	0.8	< 0.01
MeHg	AqueousTotHg	0.8	< 0.01	0.7	< 0.01
MeHg	Carbon	0.6	< 0.01	0.5	< 0.01
MeHg	Nitrogen	0.6	< 0.01	0.5	< 0.01

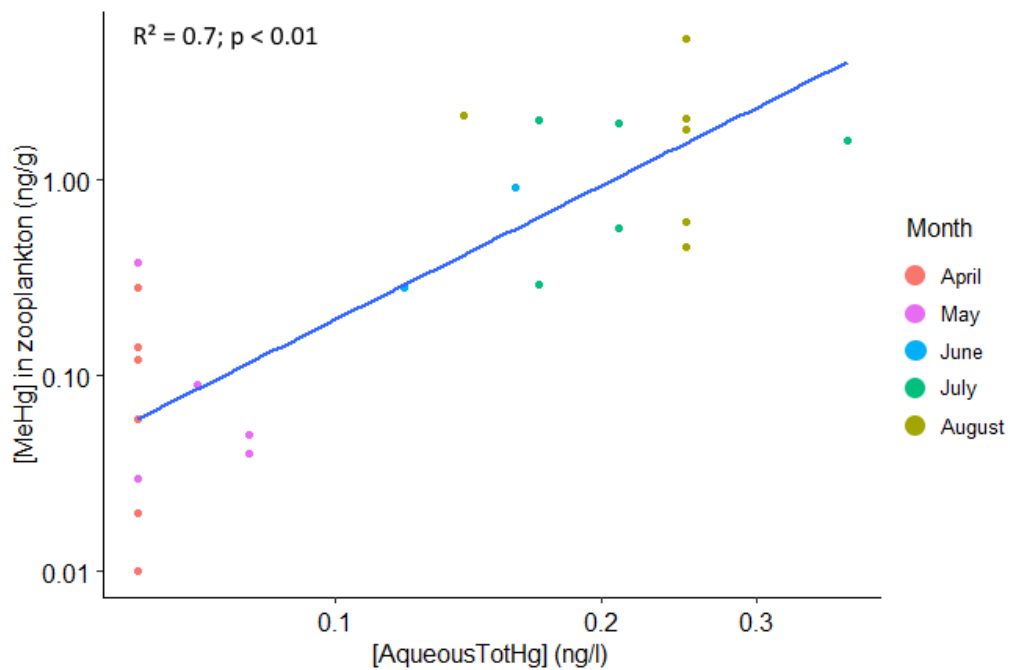


Figure A9 Linear relationship between Aqueous TotHg in water (ng/L) (15m) et MeHg concentration in zooplankton (ng/g) from April to August at the 3 stations (n=28). Data presented in Log10 scale.

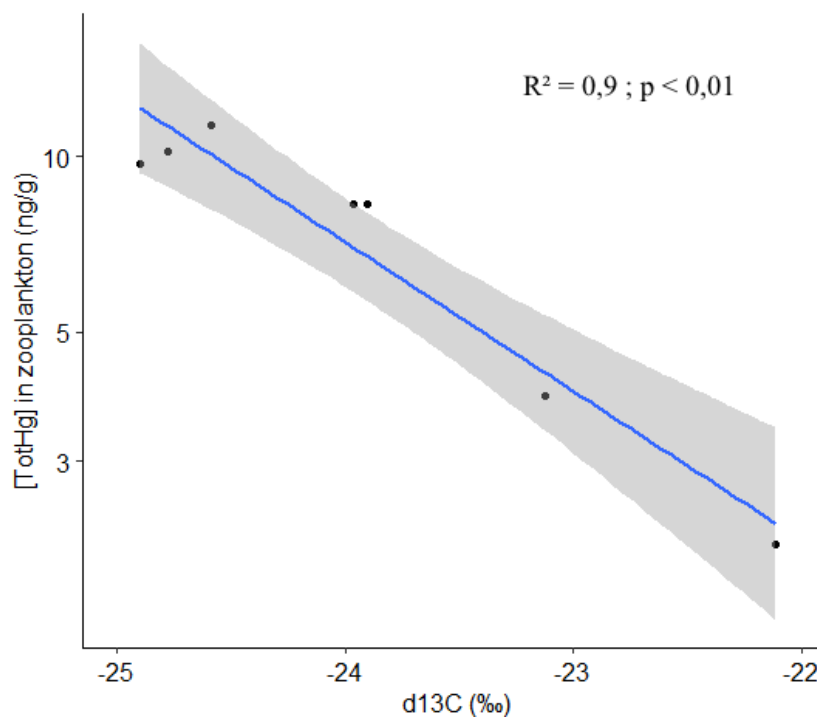


Figure A10 Linear relationship between $\delta^{13}\text{C}$ (‰) and TotHg concentration in zooplankton samples (ng/g) collected in July at the 3 stations (n=7). Data presented in Log10 scale.

Table A9 Results from the linear regression model (R^2 and p-value) in zooplankton samples collected at the 3 stations from April to August 2018 ($\delta^{13}C_{corr} : \delta^{13}C_{zooplankton} - \delta^{13}C_{POM}$ and $\delta^{15}N_{corr} : \delta^{15}N_{zooplankton} - \delta^{15}N_{POM}$).

Response variable	Explanatory variable	Month		Linear Regression Model	
				R^2	p-value
TotHg	$\delta^{15}N_{corr}$	All	n=28	0.02	> 0.05
MeHg	$\delta^{15}N_{corr}$	All	n=47	0.04	> 0.05
TotHg	$\delta^{13}C_{corr}$	All	n=28	0.24	< 0.01
MeHg	$\delta^{13}C_{cor}$	All	n=47	0.04	> 0.05
TotHg	$\delta^{15}N$	April	n=7	0.1	> 0.05
TotHg	$\delta^{15}N$	May	n=5	0.84	< 0.01
TotHg	$\delta^{15}N$	June	n=3	0.34	> 0.05
TotHg	$\delta^{15}N$	July	n=6	0.66	> 0.05
TotHg	$\delta^{15}N$	August	n=7	0.15	> 0.05
TotHg	$\delta^{13}C$	April	n=7	0.001	> 0.05
TotHg	$\delta^{13}C$	May	n=5	0.02	> 0.05
TotHg	$\delta^{13}C$	June	n=3	0.5	> 0.05
TotHg	$\delta^{13}C$	July	n=6	0.92	< 0.01
TotHg	$\delta^{13}C$	August	n=7	0.08	> 0.05
MeHg	$\delta^{15}N$	April	n=7	0.29	> 0.05
MeHg	$\delta^{15}N$	May	n=7	0.02	> 0.05
MeHg	$\delta^{15}N$	June	n=5	0.17	> 0.05
MeHg	$\delta^{15}N$	July	n=13	0.001	> 0.05
MeHg	$\delta^{15}N$	August	n=15	0.001	> 0,05
MeHg	$\delta^{13}C$	April	n=7	0.01	> 0,05
MeHg	$\delta^{13}C$	May	n=7	0.46	> 0,05
MeHg	$\delta^{13}C$	June	n=5	0.2	> 0,05
MeHg	$\delta^{13}C$	July	n=13	0.01	> 0,05
MeHg	$\delta^{13}C$	August	n=15	0.14	> 0,05

Table A10 : Stable Isotopes ($\delta^{13}\text{C}$ and $\delta^{15}\text{N}$), Carbon and Nitrogen concentration, C :N ratio, TotHg and MeHg concentration and MeHg :TotHg ratio (Mean \pm sd (range)) in zooplankton samples with « Dominant species » (representing more than 85% of the biomass of the sample).

Dominant Species		$\delta^{13}\text{C}$ (‰)	$\delta^{15}\text{N}$ (‰)	[Carbon] (ug/mg)	[Nitrogen] (ug/mg)	C :N ratio	[TotHg] (ng/g)	[MeHg] (ng/g)	MeHg:TotHg ratio
Fish larvae	n = 2	-23,0 \pm 0,1 (-23,01; -22,94)	9,1 \pm 0,04 (9,1 - 9,1)	435,9 \pm 14,3 (425,8 - 446)	92,9 \pm 1,9 (91,5 - 94,0)	11,0 \pm 0,6 (10,5 - 11,4)	10,7 (n=1)	4,5 \pm 1,0 (3,8 - 5,2) (n=2)	45,4 (n=1)
Amhipod	n = 1	-19,9	6,5	387,01	71,8	12,6	NA	NA	NA
<i>C. limacina</i>	n = 5	-21,8 \pm 1,2 (-23,7; -20,8)	8,1 \pm 0,7 (6,9 - 8,7)	271,5 \pm 81,5 (176,1 - 375,1)	55,0 \pm 15,6 (43,1 - 78,8)	11,7 \pm 2,8 (9,5 - 16,4)	NA	9,5 \pm 3,6 (7,0 - 15,0) (n=4)	NA
Chaetognatha	n = 2	-22,8 \pm 0,3 (-22,9; -22,6)	9,9 \pm 1,5 (7,9 - 10,0)	342,4 \pm 33,6 (318,6 - 366,2)	84,9 \pm 3,0 (82,8 - 87,0)	9,4 \pm 0,6 (9,0 - 10,0)	NA	NA	NA
Euphausiacea	n = 3	-20,4 \pm 1,04 (-21,4; -19,0)	8,6 \pm 0,5 (8,0 - 9,2)	449,8 \pm 60,8 (376,4 - 524,4)	89,9 \pm 11,6 (74,1 - 100,7)	12,0 \pm 3,3 (8,7 - 16,5)	4,42 (n=1)	0,2 \pm 0,1 (0,08 - 0,04) (n=3)	8,0 (n=1)
<i>L. helicina</i>	n = 2	-22,31 \pm 0,2 (-22,43; -22,19)	6,8 \pm 0,4 (6,51 - 7,07)	367,26 \pm 19,59 (353,4 - 381,11)	93,3 \pm 12,7 (84,3 - 102,3)	9,2 \pm 0,8 (8,7 - 9,8)	NA	2,8 \pm 0,2 (2,6 - 3,0)	NA
Jelly plankton	n = 10	-21,6 \pm 1,4 (-23,1; -18,9)	7,8 \pm 1,2 (6,3 - 9,7)	154,4 \pm 59,4 (68,7 - 260,1)	37,68 \pm 14,53 (17,1 - 65,15)	19,6 \pm 0,6 (9,1 - 11,3)	3,41 \pm 1,05 (2,16 - 4,98) (n=6)	0,9 \pm 0,8 (0,2 - 2,9)	13,9 \pm 2,2 (11,5 - 17,7) (n=6)
<i>O. similis</i>	n = 3	-22,6 \pm 2,0 (-24,6; -20,7)	10,2 \pm 3,3 (6,4 - 12,3)	2,5 \pm 2,4 (0,5 - 5,2)	1,4 \pm 0,8 (0,86 - 2,27)	3,7 \pm 2,3 (1,1 - 5,3)	1,5 \pm 0,1 (1,5 - 1,6)	0,02 \pm 0,01 (0,01 - 0,02)	1,2 \pm 0,4 (0,8 - 1,5)
Decapod zoea	n = 1	-18	7,8	269,6	54,6	11,5	NA	1,2	NA
<i>Calanus</i> spp.	n = 15	-22,9 \pm 1,5 (-24,9; -20,4)	7,7 \pm 0,9 (5,9 - 9,3)	291,8 \pm 156,6 (32,6 - 479,6)	56,4 \pm 29,3 (6,2 - 84,9)	12,1 \pm 1,6 (10,2 - 15,5)	7,3 \pm 3,4 (1,7 - 11,1) (n=11)	1,3 \pm 1,1 (0,1 - 4,0) (n=13)	12,2 \pm 8,2 (1,5 - 24,0) (n=11)
Cirripedia nauplii	n = 3	-19,0 \pm 0,3 (-19,3; -18,7)	7,0 \pm 1,0 (6,4 - 8,4)	297,2 \pm 185,6 (24,3 - 440,5)	60,8 \pm 36,7 (5,9 - 83,0)	11,0 \pm 1,1 (10,0 - 12,3)	5,5 \pm 3,7 (1,3 - 8,3) (n=3)	0,06 \pm 0,02 (0,03 - 0,09) (n=3)	1,1 \pm 0,7 (0,5 - 2,1) (n=3)

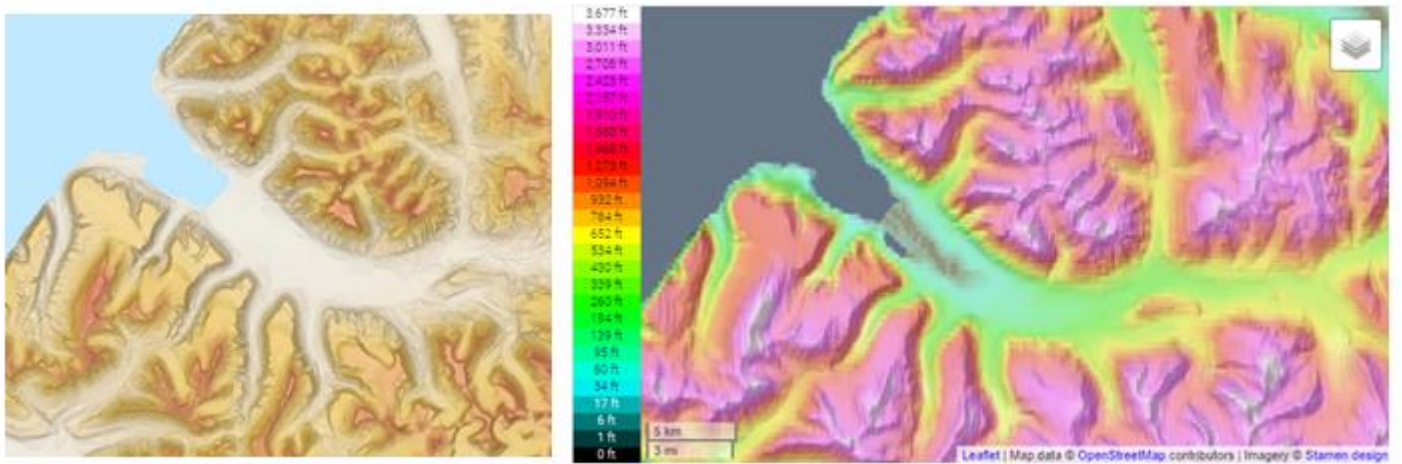


Figure A11 (A) Topografy maps of Adventelva and tributaries rivers from <http://toposvalbard.npolar.no> and (B) <http://en-gb.topographic-map.com>

Table A11 $\delta^{13}\text{C}$, $\delta^{15}\text{N}$ (‰), TotHg and MeHg concentrations (ng/g dw) and MeHg:TotHg ratio (%) in zooplankton taxonomic groups. (RI : River Influenced area; MI : Marine Influenced area)

Dominant Species	$\delta^{13}\text{C}$	$\delta^{15}\text{N}$	[TotHg] (ng/g)	[MeHg] (ng/g)	MeHg:TotHg ratio (%)	Location	Area	References
<i>Calanus spp.</i>	-22,9 ± 1,5	7,7 ± 0,9	7,3 ± 3,4	1,3 ± 1,1	12,2 ± 8,2	Adventdjord	RI	This study
	-22,91 ± 0,26	18 ± 0,31	13,09 ± 1,13	No data	24,2 ± 6,23	Hudson Bay	RI	Foster et al. 2012
	- 23,7 ± 1,9	10,9 ± 2,5	7,0 ± 2,0	No data	No data	Laptev Sea	RI	Pomerleau et al. 2016
	-23,4 ± 1,1	9,4 ± 1,7	22,0 ± 9,0	9,0 ± 4,0	No data	Southern Beaufort Sea	RI	Pomerleau et al. 2016
	-19,6 ± 1,3	7,2 ± 1,8	13,0 ± 7,0	3,0 ± 3,0	No data	Hudson Bay	RI	Pomerleau et al. 2016
	- 25,6 ± 0,2	9,6 ± 0,6	25,0 ± 3,0	7,0 ± 1,0	28	Beaufort Sea	RI	Loseto et al. 2009
	- 25,1 ± 0,2	9,4 ± 0,2	32,0 ± 2,0	11,0 ± 1,0	34,3	Beaufort Sea	MI	Loseto et al. 2009
	-20,7 ± 0,6	10,0 ± 0,7	41,0 ± 21,0	11,0 ± 5,0	No data	Chukchi Sea	MI	Pomerleau et al. 2016
-22,2 ± 1,3	7,5 ± 1,2	14,0 ± 3,0	5,0 ± 1,0	No data	Northern Baffin Bay	MI	Pomerleau et al. 2016	
Euphausiacea	-20,4 ± 1,4	8,6 ± 0,5	4,42	0,2 ± 0,1	NA	Adventdjord	RI	This study
	-22,54 ± 0,35	8,02 ± 0,24	23,82 ± 3,98	No data	34,0 ± 8,4	Hudson Bay	RI	Foster et al. 2012
	-21,9 ± 1,1	11,2 ± 0,7	22,0 ± 13,0	16,0 ± 9,0	No data	Southern Beaufort Sea	RI	Pomerleau et al. 2016
	-19,3 ± 1,9	8,0 ± 1,3	24,0 ± 21,0	10,0 ± 9,0	No data	Hudson Bay	RI	Pomerleau et al. 2016
	-18,5	9,6	22,0	No data	No data	Northern Baffin Bay	MI	Pomerleau et al. 2016
<i>L. helicina</i>	-22,31 ± 0,2	6,8 ± 0,4	NA	2,8 ± 0,2	NA	Adventdjord	RI	This study
	-23,74 ± 0,54	7,36 ± 0,54	83,61 ± 12,38	No data	11,3 ± 3,5	Hudson Bay	RI	Foster et al. 2012
	-21,4 ± 1,2	9,5 ± 0,9	226,0 ± 117,0	19,0 ± 7,0	No data	Southern Beaufort Sea	RI	Pomerleau et al. 2016
	-20,4 ± 1,9	7,4 ± 2,1	84,0 ± 50,0	8,0 ± 5,0	No data	Hudson Bay	RI	Pomerleau et al. 2016
	-19,5 ± 2,0	8,5 ± 1,6	39,0 ± 16,0	9,0 ± 3,0	No data	Northern Baffin Bay	MI	Pomerleau et al. 2016
<i>C. limacina</i>	-21,8 ± 1,2	8,1 ± 0,7	NA	9,5 ± 3,6	NA	Adventdjord	RI	This study
	-24,75 ± 0,28	8,59 ± 0,43	73,48 ± 7,84	No data	44,2 ± 7,2	Hudson Bay	RI	Foster et al. 2012
	-22,6 ± 1,8	10,2 ± 0,9	124,0 ± 71,0	72,0 ± 45,0	No data	Southern Beaufort Sea	RI	Pomerleau et al. 2016
	-21,3 ± 1,2	8,6 ± 2,0	73,0 ± 38,0	24,0 ± 6,0	No data	Hudson Bay	RI	Pomerleau et al. 2016
	-18,4 ± 1,9	8,8 ± 0,5	52,0 ± 10,0	12,0	No data	Northern Baffin Bay	MI	Pomerleau et al. 2016

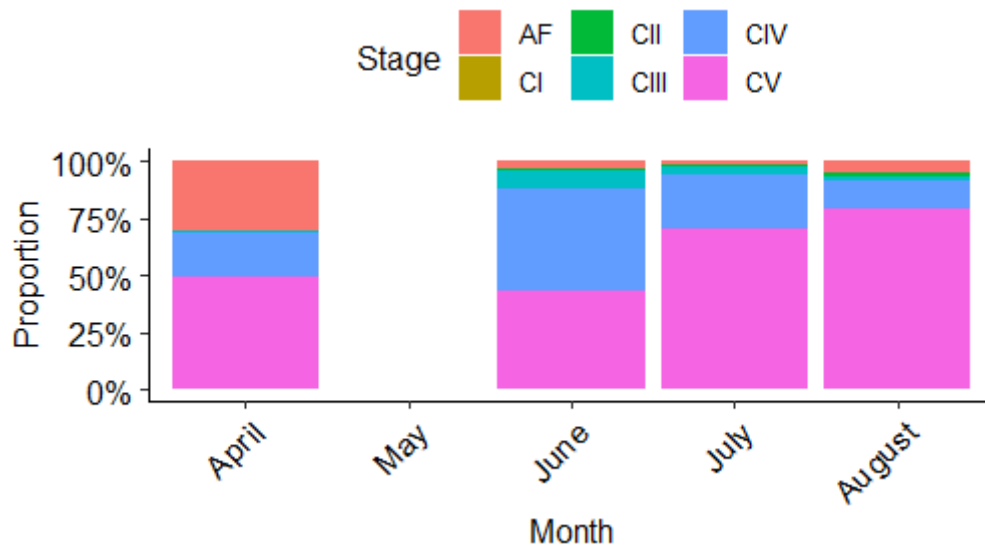


Figure A12 Copepods developmental stages in zooplankton samples dominated by *Calanus* spp. collected at the 3 stations in Adventfjord from April to August 2018.

Table A12 :Water physicochemical parameters (Temperature (°C), pH, Turbidity, Salinity(psu) and particulates parameters (Chla (ug/l), Particulate carbon (ng/l), C :N ratio, $\delta^{13}\text{C}$ and $\delta^{15}\text{N}$ (‰)), from water samples taken at the 3 stations in Adventfjord and at 2 depth (surface and 15m) from April to August 2018.

Station	Depth	Month	Temperature (°C)	pH	Turbidity	Salinity (psu)	Chl a (ug/l)	Particulate Carbon (ng/l)	C:N ratio mol	$\delta^{13}\text{C}$ (‰)	$\delta^{15}\text{N}$ (‰)
AF1	Surface	April	-0,6	7,9	0,9	34,8	0,1	125487,2	11,2	-29,0	4,4
AF1	15m	April	-0,5	8,1	0,9	34,8	0,1	48720,9	22,3	-27,5	6,8
ISA	Surface	April	0,4	7,8	0,4	34,8	0,1	49133,5	26,2	-33,5	5,7
ISA	15m	April	0,5	8,0	0,5	34,8	0,2	50507,7	27,1	-32,3	6,1
AF1	Surface	May	2,9	8,9	2,2	0,2	0,2	373015,4	13,3	-24,8	5,9
AF1	15 m	May	-0,3	8,3	1,2	34,4	0,4	327106,1	9,0	-25,7	5,1
AF2	Surface	May	1,0	8,4	6,6	2,1	0,1	298452,8	4,5	-24,9	2,9
AF2	15 m	May	-0,1	8,4	10,2	34,3	1,0	274337,1	13,0	-24,8	5,3
ISA	Surface	May	-0,8	8,1	0,6	32,2	0,6	294325,3	12,9	-24,0	5,2
ISA	15 m	May	-0,9	8,3	0,6	34,6	0,5	445226,9	8,3	-22,8	5,3
AF1	Surface	June	3,3	7,9	46,3	7,3	0,4	596654,1	25,1	-27,1	4,3
AF1	15 m	June	2,3	8,1	2,7	34,4	1,4	254695,2	14,1	-28,0	5,1
AF2	Surface	June	4,2	8,1	40,4	6,9	0,6	645514,9	25,5	-27,1	4,4
AF2	15 m	June	2,3	8,1	2,5	34,8	1,5	216941,9	15,3	-29,7	5,2
ISA	Surface	June	2,3	8,2	4,3	15,7	3,0	569660,7	7,5	-25,6	3,9
ISA	15 m	June	2,0	8,1	1,8	34,9	0,4	215726,7	13,1	-28,1	5,5
AF1	Surface	July	8,4	8,1	33,3	1,1	0,2	2255615,1	41,0	-26,0	4,0
AF1	15m	July	5,1	8,2	44,7	33,7	0,7	1156247,9	32,6	-26,2	4,2
AF2	Surface	July	8,4	8,2	14,4	3,0	1,9	873534,1	11,4	-27,9	3,6
AF2	15m	July	4,8	8,2	5,6	33,9	0,4	194293,4	17,4	-29,4	4,0
ISA	Surface	July	7,4	8,0	4,3	0,2	1,2	310053,1	16,2	-28,4	4,4
ISA	15m	July	4,3	8,1	1,7	34,1	0,9	205073,7	8,4	-29,2	3,8
AF1	Surface	August	6,9	7,8	4,6	0,2	1,4	267823,5	12,2	-28,0	4,9
AF1	15 m	August	5,3	8,0	4,0	32,2	0,6	266584,6	7,4	-27,6	3,2
AF2	Surface	August	7,7	7,9	7,2	29,1	2,0	434694,1	6,0	-27,2	3,1
AF2	15 m	August	5,1	8,0	3,1	32,1	1,5	332746,6	9,3	-27,5	4,5
ISA	Surface	August	5,6	7,9	1,6	32,8	1,2	269846,3	15,7	-29,1	4,6
ISA	15 m	August	4,4	8,0	1,3	33,6	0,5	205656,8	17,5	-29,2	3,8

Table A13 SPM concentration (mg/l), Aqueous TotHg (ng/l), Particulate TotHg concentration (ng/l) and TotHg concentration in SPM (SPMTotHg ; ng/g) in water samples taken at the 3 stations in Adventfjord and at 2 depth (surface and 15m) from April to August 2018.

Station	Depth	Month	SPM (mg/l)	Aqueous TotHg (ng/l)	Particulate TotHg (ng/l)	SPM TotHg (ng/g)
AF1	Surface	April	45,2	0,1	0,1	2,3
AF1	15m	April	32,5	0,1	0,2	5,7
ISA	Surface	April	56,9	0,0	0,2	3,3
ISA	15m	April	39,3	0,1	0,1	2,4
AF1	Surface	May	27,3	0,1	0,4	13,4
AF1	15 m	May	41,2	0,1	0,1	2,0
AF2	Surface	May	42,0	0,1	0,1	3,3
AF2	15 m	May	43,6	0,1	0,1	2,2
ISA	Surface	May	35,9	0,2	0,1	2,4
ISA	15 m	May	25,6	0,1	0,1	2,5
AF1	Surface	June	27,4	1,0	2,4	85,7
AF1	15 m	June	25,0	0,2	0,3	12,6
AF2	Surface	June	43,7	0,6	2,3	53,1
AF2	15 m	June	37,1	0,1	0,2	4,9
ISA	Surface	June	39,9	0,2	0,3	7,2
ISA	15 m	June	36,6	0,1	0,1	2,3
AF1	Surface	July	155,8	0,6	8,1	52,2
AF1	15m	July	63,2	0,4	3,1	49,6
AF2	Surface	July	51,4	0,4	1,3	24,6
AF2	15m	July	39,2	0,2	0,2	5,7
ISA	Surface	July	22,0	0,3	0,2	10,5
ISA	15m	July	30,5	0,2	0,1	4,8
AF1	Surface	August	41,4	0,3	0,3	7,3
AF1	15 m	August	38,9	0,2	0,3	7,2
AF2	Surface	August	40,6	0,7	0,5	11,5
AF2	15 m	August	43,2	0,1	0,3	7,2
ISA	Surface	August	14,0	0,1	0,2	12,4
ISA	15 m	August	13,9	0,2	0,2	12,5

Table A14 Fatty acid diet markers analyzed (%) in zooplankton samples used in data analysis, including samples dominated by *Calanus* spp. (n = 12), by Cirripedia larvae (n = 3), and belonging to « Herbivores » category (n = 16). Fatty acid diet marker not detected were removed (including : 18:1n-7t ; 19:1n-12 ; 20:1n-15 ; 20:1n-11 ; 24:0)

Sample ID / FA Code	APRIL				MAY				JUNE			JULY			AUGUST	
	Z1	Z2	Z5	Z11	Z8	Z10	Z15	Z16	Z17	Z18	Z21	Z26	Z32	Z38	Z45	Z53
14:0	13,57	19,37	15,52	9,52	5,81	5,56	3,88	4,99	5,31	3,76	6,56	12,24	8,33	9,86	11,11	9,55
14:1n-5	0,23	0,21	0,00	0,00	0,29	0,27	0,00	0,10	0,00	0,00	0,10	0,15	0,10	0,13	0,17	0,11
15:0	0,93	1,44	1,19	0,00	0,36	0,38	0,36	0,47	0,39	0,35	0,41	0,51	0,38	0,43	0,56	0,70
15:1n-5	0,00	0,00	0,00	0,00	0,00	0,00	0,00	0,00	0,00	0,00	0,00	0,00	0,00	0,05	0,00	0,00
16:0	12,28	15,49	13,96	17,38	16,87	17,22	15,94	19,53	14,96	16,76	9,91	13,24	14,32	11,77	13,46	14,95
16:1n-7c	7,28	9,40	8,17	6,51	20,66	20,77	6,95	22,18	3,91	4,29	5,48	3,33	2,92	3,29	4,44	5,29
16:1n-7t	0,29	0,27	0,28	0,00	0,04	0,05	0,18	0,00	0,19	0,24	0,15	0,13	0,16	0,10	0,15	0,26
17:0	0,39	0,55	0,55	0,00	0,12	0,13	0,28	0,21	0,31	0,33	0,18	0,30	0,28	0,26	0,33	0,48
17:1n-7	0,21	0,37	0,36	0,00	0,05	0,07	0,11	0,00	0,00	0,00	0,09	0,15	0,11	0,13	0,15	0,15
18:0	0,82	0,87	1,02	1,93	1,54	1,52	1,03	2,84	1,23	1,53	0,78	0,72	1,16	0,72	1,14	1,15
18:1n-9c	6,05	7,08	8,13	9,24	3,54	3,58	15,07	4,57	3,70	3,56	3,84	10,36	8,84	9,24	7,70	7,32
18:1n-9t	0,00	0,00	0,00	0,00	0,04	0,05	0,00	0,00	0,00	0,00	0,00	0,07	0,00	0,00	0,07	0,08
18:1n-12c	0,12	0,00	0,00	0,00	1,82	1,83	0,65	1,82	0,26	0,27	0,49	0,05	0,11	0,06	0,24	0,34
18:1n-7c	1,07	0,75	0,86	0,00	4,42	4,48	1,69	4,79	1,57	1,67	1,20	0,53	0,59	0,51	0,59	0,72
19:0	0,18	0,19	0,23	0,00	0,00	0,00	0,07	0,00	0,15	0,18	0,11	0,10	0,14	0,11	0,14	0,17
18:2n-6c	1,36	1,69	1,71	2,11	0,00	0,61	2,18	0,75	1,05	0,95	1,56	1,30	1,23	1,35	1,49	1,28
20:0	0,13	0,00	0,00	0,00	0,00	0,04	0,08	0,00	0,13	0,00	0,13	0,08	0,08	0,08	0,08	0,00
18:3n-6	0,00	0,00	0,00	0,00	0,18	0,20	0,22	0,18	0,00	0,09	0,13	0,22	0,15	0,21	0,16	0,11
20:1	0,66	0,79	0,79	0,00	0,05	0,04	0,81	0,00	0,24	0,00	0,60	0,45	0,29	0,38	0,44	0,34
20:1n-9	11,40	6,66	8,57	8,78	0,34	0,35	7,08	0,86	4,14	2,05	9,53	5,55	4,31	6,73	5,99	2,53
18:3n-3	1,13	1,87	1,74	2,45	1,28	1,31	1,71	1,49	1,29	1,33	1,66	2,28	2,23	2,45	2,79	2,26
18:2n-6t	0,00	0,00	0,00	0,00	0,09	0,08	0,13	0,00	0,13	0,00	0,24	0,32	0,27	0,36	0,41	0,32
18:4n-3	0,73	1,47	1,40	0,00	4,13	4,19	3,01	4,13	6,99	5,59	15,78	14,89	11,59	16,85	13,09	8,03
20:2n-6	0,23	0,31	0,32	0,00	0,17	0,17	0,37	0,00	0,16	0,15	0,24	0,15	0,13	0,14	0,18	0,25
22:3n-3	0,00	0,00	0,00	0,00	0,05	0,07	0,00	0,00	0,00	0,00	0,08	0,09	0,10	0,11	0,00	0,15
22:0	0,00	0,00	0,00	0,00	0,04	0,00	0,13	0,59	0,00	0,00	0,00	0,07	0,00	0,03	0,00	0,08
20:3n-6	0,00	0,00	0,00	0,00	0,32	0,04	0,10	0,00	0,17	0,09	0,61	0,26	0,30	0,28	0,36	0,16
22:1n-11	9,08	8,00	7,97	7,86	0,00	0,04	6,60	0,34	2,48	1,08	6,82	5,70	3,68	5,27	5,14	2,87
22:1n-9	1,55	0,82	0,99	0,00	0,13	0,14	1,00	0,31	0,45	0,34	0,93	0,68	0,59	0,70	0,90	0,37
20:3n-3	0,16	0,00	0,20	0,00	0,50	0,58	0,24	0,59	0,17	0,25	0,20	0,14	0,11	0,14	0,14	0,21
20:4n-6	0,24	0,28	0,35	0,00	0,19	0,19	1,09	0,09	0,23	0,19	0,29	0,21	0,19	0,22	0,26	0,26
22:2n-6	0,69	0,91	0,94	0,00	0,49	0,04	0,11	0,00	0,86	0,79	0,07	0,05	1,03	1,11	1,32	1,18
20:5n-3	11,49	8,20	9,82	13,27	27,69	26,89	14,98	22,90	19,66	21,76	14,57	10,14	13,18	10,94	10,99	15,92
24:1n-9	1,45	1,71	1,75	1,89	0,12	0,20	0,49	0,26	1,10	1,41	0,69	1,27	1,56	0,97	1,07	1,87
22:4n-6	0,00	0,00	0,00	0,00	0,00	0,00	0,12	0,00	0,00	0,00	0,00	0,06	0,00	0,06	0,06	0,09
22:5n-3	0,21	0,23	0,30	0,00	0,15	0,16	0,62	0,00	0,69	0,61	0,79	0,77	0,78	0,83	0,81	0,64
22:6n-3	16,08	11,11	12,88	19,08	8,53	8,77	12,69	5,99	28,12	30,39	15,78	13,46	20,79	14,11	14,10	19,83

Tableau A15 Sum metrics of Fatty acid diet markers (%) analyzed in zooplankton samples used in data analysis, including samples dominated by *Calanus* spp. (n = 12), by Cirripedia larvae (n = 3), and belonging to « Herbivores » category (n = 16). Fatty acid diet marker not detected were removed (including : 18:1n-7t ; 19:1n-12 ; 20:1n-15 ; 20:1n-11 ; 24:0)

Sample ID / FA Code	APRIL				MAY				JUNE			JULY			AUGUST	
	Z1	Z2	Z5	Z11	Z8	Z10	Z15	Z16	Z17	Z18	Z21	Z26	Z32	Z38	Z45	Z53
Sum SFA	28,29	37,90	32,47	28,82	24,74	24,85	26,39	28,63	22,47	22,91	18,08	27,25	24,69	23,26	26,82	27,08
Sum MUFA	39,39	36,05	37,87	34,27	31,55	31,92	32,85	35,24	18,02	14,90	30,00	28,49	23,36	27,68	27,04	22,38
Sum PUFA	32,32	26,05	29,66	36,90	43,71	43,23	40,76	36,12	59,51	62,19	51,92	44,26	51,95	49,06	46,14	50,54
Sum MUFA ≥18	31,38	25,80	29,06	27,76	10,51	10,76	13,49	12,96	13,93	10,37	24,17	24,73	20,07	23,97	22,14	16,57
Sum MUFA>18	24,14	17,97	20,07	18,53	0,68	0,83	3,36	1,77	8,39	4,88	18,65	13,73	10,53	14,17	13,54	8,12
Sum C18 PUFA	3,22	5,02	4,85	4,56	5,68	6,38	4,96	6,54	9,46	7,96	19,38	19,01	15,46	21,21	17,92	12,01
Sum C20 PUFA	12,13	8,78	10,69	13,27	28,86	27,88	26,20	23,59	20,39	22,44	15,90	10,90	13,90	11,72	11,94	16,79
Sum C22 PUFA	16,97	12,25	14,11	19,08	9,17	8,97	9,60	5,99	29,67	31,79	16,64	14,35	22,59	16,12	16,28	21,74
Sum EPA & DHA	27,57	19,30	22,70	32,35	36,22	35,66	33,72	28,89	47,78	52,15	30,35	23,60	33,96	25,05	25,09	35,74
Sum n-6	2,52	3,18	3,32	2,11	1,44	1,34	1,18	1,02	2,59	2,26	3,14	2,58	3,29	3,74	4,23	3,66
Sum n-3	29,80	22,87	26,33	34,80	42,32	41,96	39,58	35,10	56,91	59,93	48,85	41,78	48,76	45,43	41,91	47,03
Sum Odd chain	1,72	2,55	2,33	0,00	0,53	0,58	0,50	0,68	0,85	0,86	0,79	1,05	0,91	0,98	1,19	1,50
n-3/n-6	11,84	7,19	7,92	16,51	29,49	31,41	33,62	34,43	21,95	26,50	15,55	16,19	14,83	12,16	9,90	12,85

